A STUDY ON DYNAMIC PROPERTIES
OF COMPACTED CLAYS

Thesis by

ALİ AKGÜL GÜNGÖREN

In Partial Fulfillment of the Requirements For the
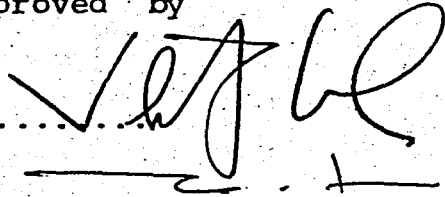
Degree of Master of Science

Boğaziçi University

Bebek - Istanbul
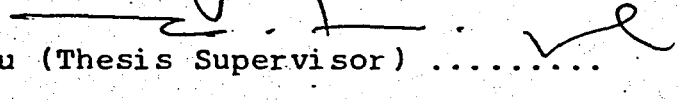
December - 1983

A STUDY ON DYNAMIC PROPERTIES
OF COMPACTED CLAYS

This Thesis has been approved by

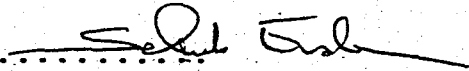Prof. Vahit Kumbasar ....

Doç. Dr. Turan B. Durgunoğlu (Thesis Supervisor) ....

Doç. Dr. Selçuk Erden ....

Boğaziçi University

Bebek - Istanbul

December - 1983

ACKNOWLEDGEMENTS

I would like to express my sincere gratitude to Doç. Dr. Turan H. Durgunoğlu for his invaluable suggestions, guidence and encouragements throughout the course of my study.

I wish to thank Mr. Vedat Yenigün for helping me in preparing the test specimens.

<div align="right">Ali A. GÜNGÖREN</div>

Istanbul, December 1983

ABSTRACT

A STUDY ON DYNAMIC PROPERTIES
OF COMPACTED CLAYS

The dynamic soil properties, shear modulus and damping ratio, are studied on five types of clay samples which have relatively different plasticity characteristics, The resonant column method is conducted on compacted samples. Specimens are compacted by using modified mini proctor compactor. The effect of moisture content,shear strain amplitude and vertical stress on shear modulus and damping ratio of these samples are investigated. The values of shear modulus and damping ratio are tabulated and plotted to understand easyly.

TABLE OF CONTENTS

LIST OF FIGURES

FIGURE

LIST OF TABLES

A (rad/rad) = amplitude of shearing strain

A = damping factor

A_1 (volt) = amplitude of vibration for the first cycle after the power cut off

A_{n+1}(volt) = amplitude for the (n+1)th cycle

AASHTO = american association of state highway officials classification of soils

C = grain characteristcs

C_R (amper) = current flowing through the coils of Hardin Oscillator

$\bar{C}$(PSI, kg/cm^2) = cohesion in terms of effective stress

C_m = mode shape factor

CBR (%) = california bearing ratio

D (%) = damping ratio

D_{free}(%) = damping ratio by free vibration method

D_{steady}(%) = damping ratio by steady state vibration

d (cm) = diameter of specimen

E (PSI, kg/cm^2)= young's modulus

e = void ratio

$\bar{e}$ = volumetric strain. or cubic dilation

F = dimensionless frequency

F (e) = void ratio fucntion

f (H$_z$) = system resonant frequency

$f_o = f_{app}$ (H$_z$) = Apparatus resonant frequency

G (PSI, kg/cm^2) = shear modulus

G_{eq}(PSI, kg/cm^2) = equivalent shear modulus, or average shear modulus

G_{max} (KN/m^2) = maximum shear modulus or initial shear modulus

G_s = specific gravity

g (cm/sec^2) = acceleration due to gravity

H = embient stress history and vibration history

I_p (%) = plasticity index

J ($gr-cm-sec^2$) = inertia of the specimen about its axis

J_o ($gr-cm-sec^2$) = apparatus inertia

J_2'' = second invariant of the stress deviation

K (PSI, kg/cm^2) = modulus of volume compressibility or bulk modulus

K_o = coeffecient of lateral stress at rest

K_o ($gr-cm/rad$) = apparatus spring constant

L = less important (in table 3.1)

L = lime

LFA = lime flay ash

L + S = lime + salt

l (cm) = length of specimen

$N = N_c$ = number of cycles

n = number of cycles after the power cut off

no. 200 (%) = passing from sieve # 200

OCR = overconsolidation ratio

$\bar{P}$ (kg/cm^2) = mean effective stress

R = relatively unimportant (in table 3.1)

R = dimensionless value depending on system factor T

S	= salt
S (%)	= degree of saturation
S	= system energy ratio
S_u (KN/m^2)	= undrained shear strength
T (C^o)	= temperature
T	= the system factor
T_r	= time devided by time to 100 % primary consolidation
t	= secondary effects that are functions of time and magnitude of load increment
U	= relative importance is not clearly known
UC	= unified system
V	= very important
V (cm^3)	= volume of specimen
W (gr)	= total weight of specimen
w (%)	= moisture content
w_L (%)	= liquid limit
w_{opt} (%)	= optimum moisture content
γ	= shear strain
γ_{dry} (t/m^3)	= maximum dry density
γ_r	= reference strain
δ_A	= apparatus damping constant
δ_s	= logarithimic decrement
δ_{ij}	= kronecker delta function
$\overline{\sigma}_o$ (kg/cm^2, PSI)	= effective mean principal stress
σ_{ij} (kg/cm^2)	= total stress tensor
$\overline{\sigma}_v$ (kg/cm^2)	= effective vertical stress

σ_r (kg/cm^2) = radial pressure

σ_z (kg/cm^2) = axial stress

$\overline{\sigma}_{vmax}$ (kg/cm^2) = maximum vertical effective stress

σ_{vc} (kg/cm^2) = vertical effective consolidation stress

τ (kg/cm^2) = shear stress

τ_o (kg/cm^2) = octahedral shearing stress

τ_{max} (kg/cm^2) = maximum shear stress

$\rho \left(\dfrac{gr-sec^2}{cm^4} \right)$ = mass density of specimen

ε_{ij} = total strain tensor

θ = soil structure

θ_R (rad) = amplitude of vibration at the system resonant frequency.

$\overline{\emptyset}$ (deg) = angle of effective shearing resistance

CHAPTER 1 · INTRODUCTION

There are many problems in engineering that require
a knowledge of dynamic soil properties for satisfactory so-
lutions. These problems can be catagorezid into two grops,
according to the loading and response of the soil. One group
involves loading and unloading produced by the wave propaga-
tion of a wave front, where the value of the peak stress is
relatively large, e.g nuclear explosions. The other group
involves relatively small amplitude and repeated loading and
unloading, this type soil vibration may be produced by earth-
quakes, vehicular traffic.

Determination of the dynamic properties of soils,
such as shear modulus and damping, is of foundamental impor-
tance in the analysis of the problems mentioned above.

In the design of earth dams and embankments the dy-
namic properties of soil used has a great importance to pre-
dict the damages under earthquakes.

Compacted clays are often used as a core material in
zoned earth dams, Therefore, their dynamic properties carry
primary importance in predicting behavior during earthquakes.
Many geotechnical properties of compacted clays have been stu-
died systematically in the past. However, there is very limi-
ted information on their dynamic properties. Main purpose of
this study is the investigation of effects of compaction para-

meters such as, moisture content, clay type, compaction ef-
fort on shear modulus and damping ratio under dynamic load-
ing. For this purpose Hardin type resonant column device is
used.

Five types of chosive soils, which have relatively
different plasticity characteristics, are chosen.

In this study, firstly, a critical review and evalu-
tion of previous work is presented. In addition, the methods
to determine the dynamic soil properties are given.

Types of resonant column apparatus are briefly dis-
cussed, and a description of Hardin type resonant column de-
vice is made.

Tests were performed on compacted specimens prepared
by a modified mini Proctor compactor After test set up is
completed, the test is conducted by applying a power to the
Hardin oscillator. The necessary parameters such as, system
resonant frequency, torque volts, and accelerometer out put
voltages are recorded to calculate the shear modulus and
damping. The samples which have optimum moisture content are
tested under various vertical stress and different strain
amplitudes.

The measured values of shear modulus compared with
the calculated values. Test results are tabulated and plot-
ted for practical use.

CHAPTER 2 STRUTURE OF COMPACTED CLAYS AND ITS

EFFECT ON SHEAR MODULUS AND DAMPING

2.1 INTRODUCTION

A knowledge of the behavior of compacted clays under dynamic load is necessary for satisfactory and economical design.

In this chapter, a short summary of existing knowledge on the struture of cohesive soils is given. Changes in structure during compaction are discussed. Effects of structure and compaction type on strength are mentioned. Based on the previous studies the effects of structure and strength of compacted clay on the shear modulus and damping ratio are described.

2.2 STUCTURE OF CLAYS

According to Lambe (1958), the tem "Structure" means the arrangement of soil particles, which is controlled by the electrical forces acting between adjacent particles. Previously, "structure" was limited to the arrangement of soil particles only. The concepts of electrical forces and environmental factors entered into the discussions of structure with the principals of colloid chemistry. The importance of particle arrangements, however, was recognized many years ago by Terzaghi (1925), Casagrande (1932), and Hvorslev (1938).

The concepts of soil structure are concerned primarily

with very small particles - about two micron in size or
smaller. In cohesive soils the structure is explaiend lar-
gely by the clay minerals and the forces acting between
them. There are many forms of clay minerals, with some si-
milarities and wide differences in composition, structure
and behaviour. The most impartant minerals are kaolinite,
montmorillonite, halloysite and illite. All have crystal
structures that include large numbers of atoms arranged in
complex three dimensional patterns. Most clay crystals con-
sist of Silica and Alumina.

Clay particles are usually of small size less than
two microns and most clay minerals are thin flat plates.
All are extremely fine grained, with large surface areas
per unit mass. For this reason, clay particles usually stay
in colloidal range; and, electrical forces acting between
adjacent particles and environmental conditions become im-
portant.

In colloidal range electrical forces between partic-
les may be divided into three groups. Primary valence bonds,
which are the strongest, hold atoms together in the basic
mineral units, and can be grouped as; ionic bonds (an exchan-
ge of electrons by the linked atoms), covalent bonds (shar-
ing of electrons by the linked atoms), and heterpolar bonds
(part ionic and part covalent, since it results from an une-
qual sharing of electrons by the linked atoms). The hydro-
gen bonds happens when an atom of hydrogen is rather strongly
atracted by two other atoms (e.g oxygen, nitrogen atoms).

The primary valence and hydrogen bonds can not be broken by the stresses applied normally to a soil system. The secondary valence forces (also known as Van der Waals forces) arise from electrical moments existing within the units. They are like forces acting between two short bar magnets, in certain positions the magnets repel each other and in others they attract. Because of more attractive position the net force is atractive. Hence, the net effect of secondary valence forces between clay platelets are attraction. Secondary valence forces are much weeker than the other two and decrease with increasing distances between particles. Van der Waals forces are important for soil engineer because they contribute to clay strength most and cause soils to hold water.

Clay particles in the presence of water exhibit greatly different behavior than do other minerals because of the interaction of the electrostatic fields and the diffuse double layers.

Clay mineral faces are generally negative, due to isomorphous substitution, and the edges positive or negative depending on the nature of mineral and the environment with which it is in contact. At low water contents, the cations cluster on negatively charged clay faces to neutralize the particles. When the water content is increased, the cations held at the face of dry clay tend to spread out into the diffuse double layer. Water molecules behave as dipoles although neutral. Therefore water closest to the surface is held,

and the molecules are oriented in the electrostatic field. The water closest to the claysurface appears denser than ordinary water. The thickness of the innermost layer of water is probably 10 $A^O(10^{-6}$ mm) and the total thickness of water that is attracted to the clay may approach 400 A^O. This oriented water zone is called diffuse double layer and is shown in Fig 2.1. The distribution of ions with distance from the clay particles is seen in Fig. 2.1. The concentration of cations in the double layer decreases with the distance from clay faces.

Since the cations are clustered on particle surfaces when the clay is dry, the attractions between the negatively charged edges and the surfaces holding cations result in edge to surface contacts and flocculation of particles. Flocculent soils are light in weight and very compressible but are relatively strong and insensitive to vibration. Because the particles are tightly bound by their edge to face attaction.

When the clay is wetted, the added water helps to the development of double layer. With the development and interaction of these layers, the repulsive forces are created between cations contained in two interacting double layers. If these electrostatic repulsive forces become larger than the attractive forces at edge to surface contacts, the particles reorient themselves into a more dispersed and parallel situation.

In this way, the particle arientation of a clay may be of any arrangement between two different cases:

1. A completely random orientation which is a flocculated structure,

2. A completely parallel orientation which is a dispersed structure.

Pacey (1956) measured particle orientation as a function of molding water content on compacted Boston Blue Clay as shown in Fig. 2.2
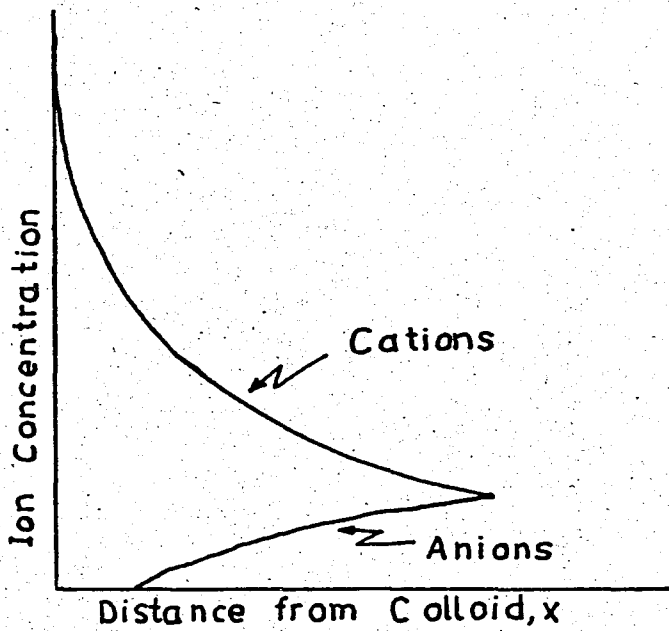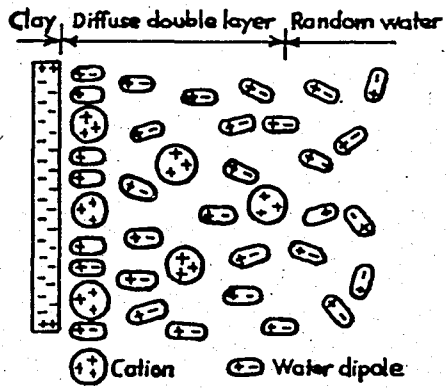
Fig 2.1   Diffuse Double Layer

(After Lambe, 1958)
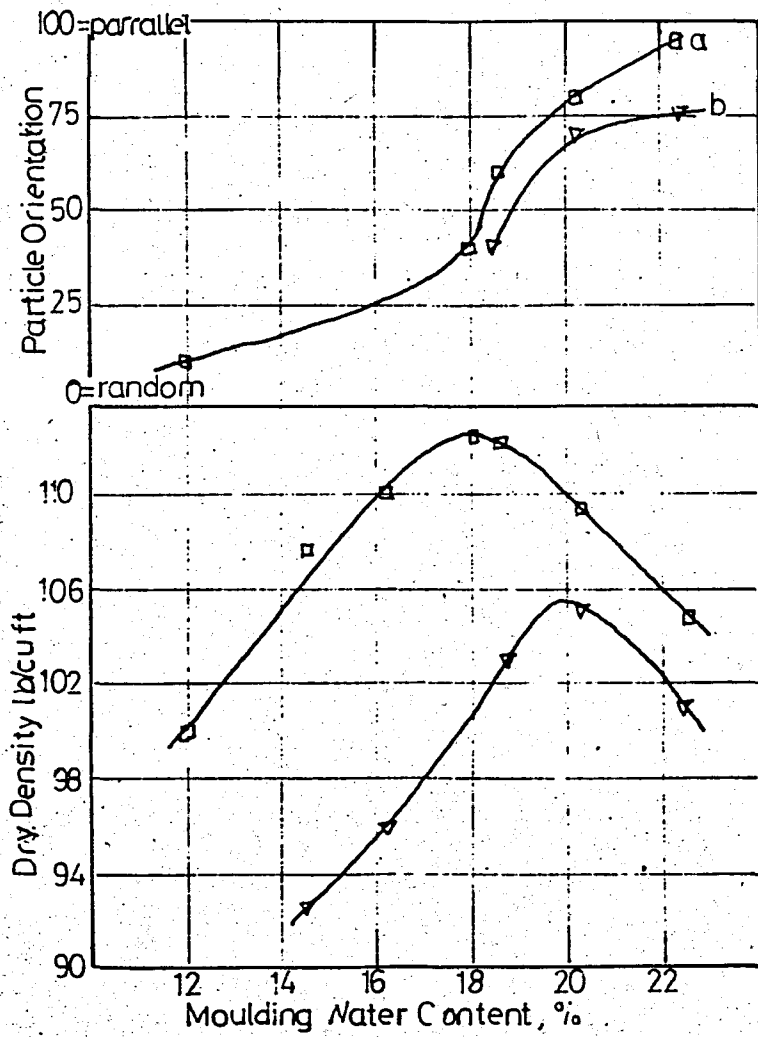
Fig 2.2 Orientation versus Molding Water Content
        for Boston Blue Clay

(After Pacey, 1956)

2.3 STRUCTURE OF COMPACTED CLAYS

Clay particles under a given set of conditions have to have certain amount of water to fully develop their double layers The difference between existing water and needed water is called defficient water which the particles will try to adsorb. Whenever the existing water content of a clay sample is less than the equilibrium water content, the net forces between particles are attractive and the structure is flocculated. If the necessary amount of water is given to the clay, the double layers are fully obtained, the net forces between particles become repulsive and the structure becomes dispersed.

In compacting any particular soil, the main parameters to be concerned are the moisture content, the amount of compaction, and the type of compaction.

By keeping the compaction energy and type constant, only one dry density is obtained for a unique water content. Increasing compactive energy at any given water content increases the orientation of particles and thus gives a higher density. This was first investigated by Lambe (1958) and it is shown on Fig. 2.3

At point A, there is not enough water for the diffuse double layers of the soil particles to develop fully, or clay is water deficient. Hence, the electric repulsive forces between particles are smaller than the attractive forces, resulting in a net attraction between particles,
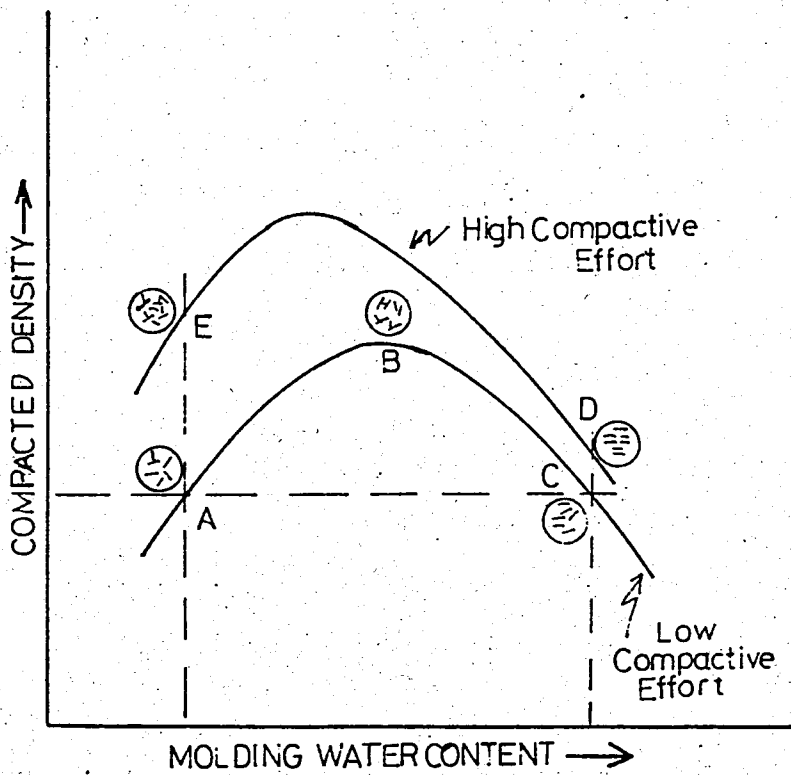
Fig 2.3 Effects of Compaction on Structure

(After Lambe, 1958).

and the particles therefore tend to flocculate in a disorderly array. When the water content is increased toward B, electrolyte concentration decreases, the repulsion between clay particles increases, and double layer around particles becomes larger. Therefore, flocculation decreases. Decreasing degree of flocculation permits a more orderly arrangement of particles. Increasing the order of particles increases the density until the water content of point B is reached.

Beyond point B particle parallelism increases. A further expansion of the double layer causes the repulsion between particles to increase and the attractive force to decrease. Eventhough a more orderly arrangement exist, beyond point B the compacted density begins to decrease because water starts to occupy space which could be filled with soil particles, or dilutes the concentration of soil particles per volume; that means, there is not a marked decrease in air content any more. The changes in structure which are described above can not be seen in all compacted clays, especially in the clays with particles having great tendencies to flocculate.

Seed and Chan (1959) and later Seed (1960) found that different types of compaction methods cause varying amounts of shear strain into the soil and increasing shear strains result in more dispersed structure. So, changes in structure comes from the combined effect of both an increase in water content and induced shear strains. According to

Seed and Chan (1959), there are four basic types of compaction methods; static, vibratory, impact (proctor), and kneading. According to Seed (1960), each method gives different structure and different soil properties for samples compacted at wet of optimum. On the other hand, at dry side of optimum all kinds of compaction methods gives similar structures. This means that none of the compaction type can induce high shear strains below optimum water content. During compaction at wet of optimum, however, the increase in the degree of dispersion is directly related to the increasing shear strains induced by different types of compaction methods. Besides, the "lubrication" of clay particles by water is needed for shear strains to change the particle order into a more parallel arrangement. It should be known that the effects of method of compaction on soil structure can vary with the type of soils compacted.

There are similarities between dry-side and wet-side compacted clays and between undisturbed and remolded clays. The dry-side compacted clay and undisturbed clay both tend to have a flocculated-type structure, while a wet-side compacted clay and a remolded clay both tend to have dispersed types of structures.

2.4 EFFECTS OF STRUCTURE ON SHEAR STRENGTH

According to Lambe (1958), the entire force system between clay particles should be considered for studying

the shear strength of the compacted clays. He explained
that four main horizontal forces act between adjacent par-
ticles, these are: the externally applied intergranular
stress, the electrical attraction forces, the electrical
repulsion forces, and the geometric interaction, i.e, con-
tact pressure.

Main factors which are effecting the strength are
spacing, orientation of particles of clay and the type of
compaction used. When a clay specimen is compacted on the
dry side of optimum, a flocculated structure is formed and
the edge-to-face contact between soil particles provides
high resistance to load. On the other hand, when compacted
on wet of optimum, the specimen has a dispersed structure
with relatively few strong interparticle contacts, result-
ing in a low shear strength. Besides, increased compactive
energy at dry of optimum causes in an increase of strength,
at wet of optimum,however, there is no important change in
strength, as shown in Fig. 2.4

Chae and Chiang (1972) showed the change of the dy-
namic strength (maximum dynamic shear modulus) with the sta-
tic strength, for compacted clay using resonant column tech-
nique. Undrained triaxial compression tests were used to
determine the static strength. The static strength was de-
fined as the deviatoric stress at 1% axial strain. Figure
2.5 shows that a linear relationship exists between the sta-
tic strength and the dynamic shear modulus. This means that
on the dry side of optimum moisture content soil gives hig-
her shear modulus than the wet side of optimum moisture
content.
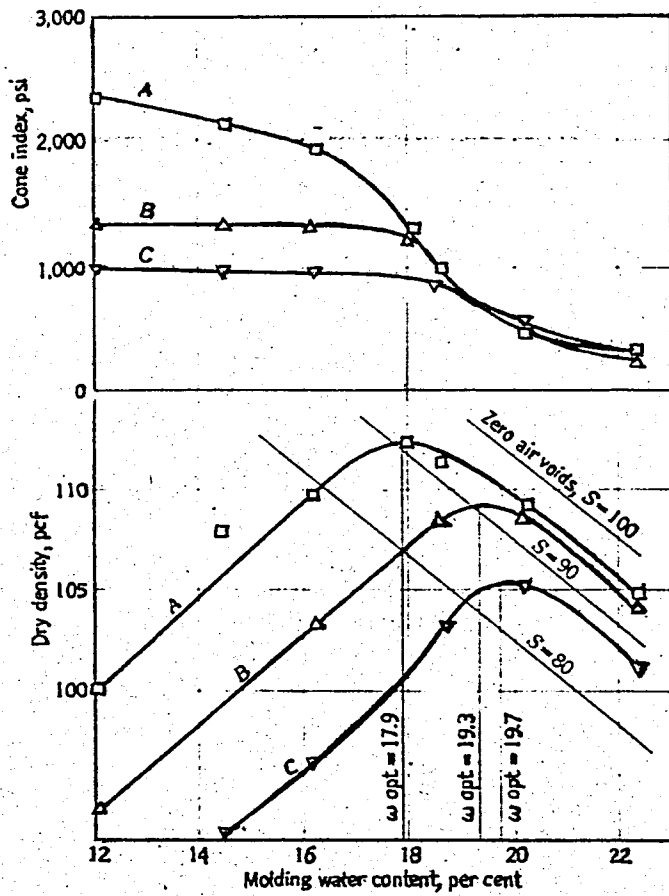
Fig 2.4 Cone Index and Dry Density vs. Molding
        Water Content for Boston Blue Clay.

(After Pacey, 1956)
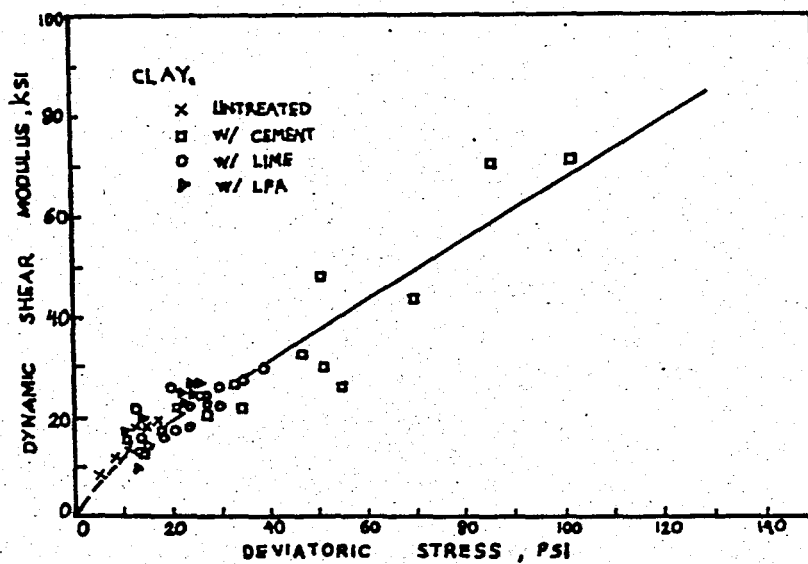
Fig 2.5   Dynamic Shear Modulus vs. Static Shear

Strength for Treated   Untreated Clay

(After Chae and Chiang
1978).

2.5. EFFECTS OF THE STRUCTURE ON SHEAR MODULUS AND DAMPING

As it was previously discussed, the structure of compacted clay changes with increasing moisture content from dry side of optimum to the wet side of optimum.

Theoretically, the effect of water in the soil is to reduce the velocity of weve propagetion. This reduction is brought about by the presence of large diffuse double layers, thus depending on shear wave velocity the shear modulus also decreases. For clays, on the dry side of optimum diffuse double layer is very small, hence the change in shear modulus is small or can be assumed as constant. Beyond the optimum water content diffuse double layer increases, thus, shear modulus decreases.

On the other hand, the variation of damping with moisture is small up to the optimum moisture content. However, beyond the optimum moisture content damping gradually increases. Chae and Chaiang, 1978, showed the effects of moisture content on shear modulus and damping as shown in Fig. 2.6.

2.6. SUMMARY AND CONCLUSIONS

In this chapter, previous studies on particle orientations, fabric of cohesive soils, and structure of compacted clays are summarized. The effects of soil structure on the strength, and shear modulus and damping properties of clays are discussed, and following conclusions are obtained.
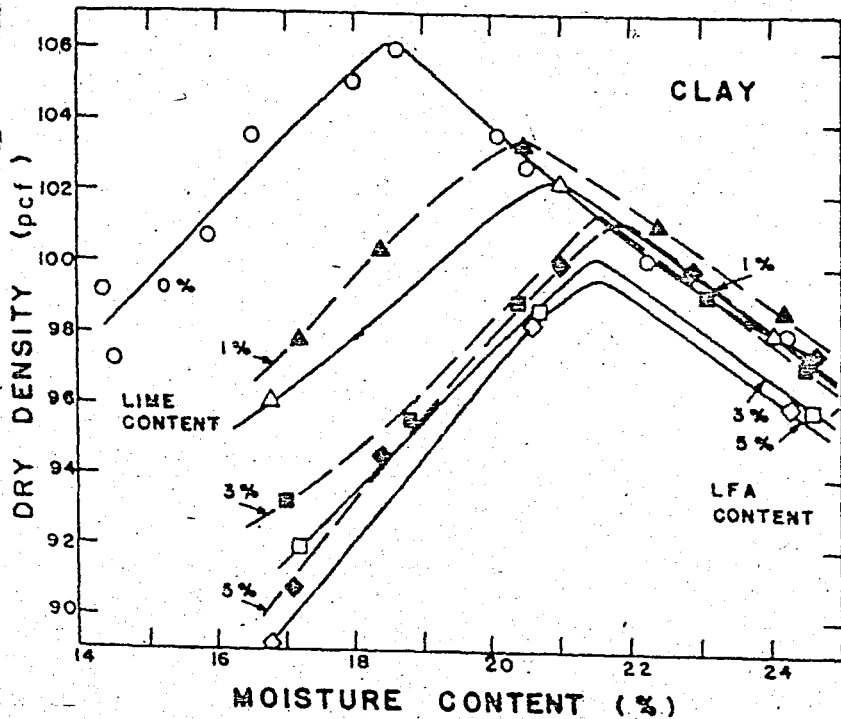
Density vs. Moisture Content for Clay
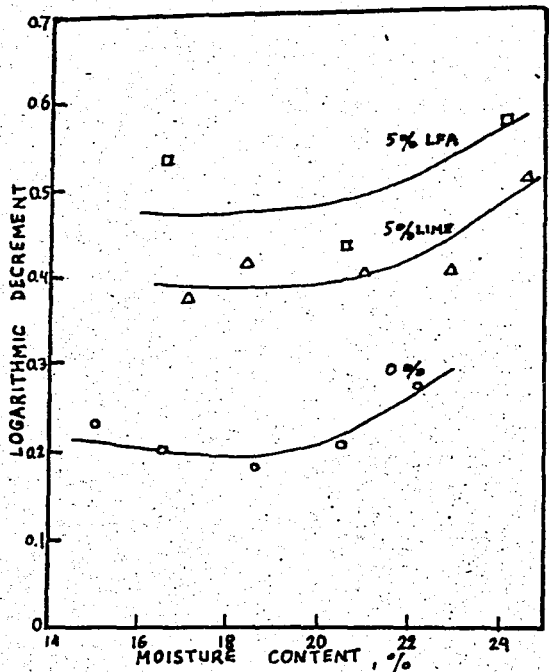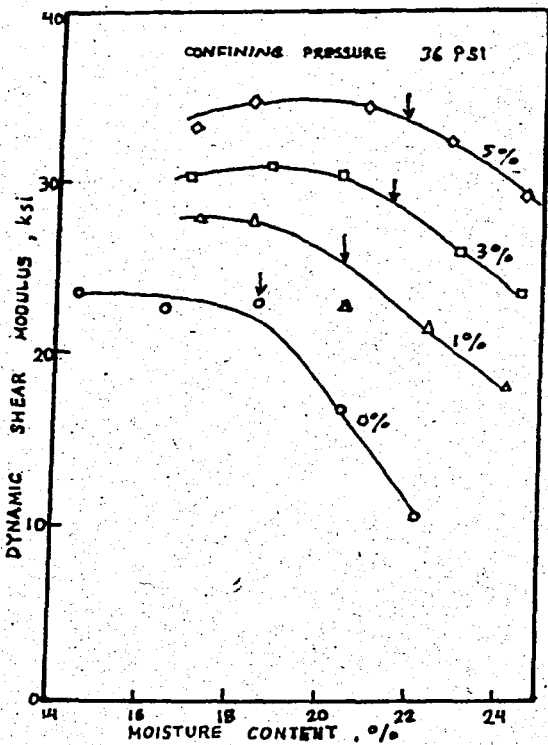
Fig 2.6 Modulus and Damping vs. Moisture Content for Untreated
and Treatet Clay (After ūhea and chaiang, 1978)

1. The particle orientation of a compacted clay can be in a situation between completely flocculated and completely dispersed extreme cases.

2. The structure is flocculated at dry of optimum and dispersed at wet of optimum.

3. The electrical forces acting between clay particles are most responsible for soil strength in compacted clays.

4. Flocculated structures have higher shear modulus than dispersed structures, moreover, opposite is true for damping.

CHAPTER 3 DYNAMIC SOIL PROPERTIES

3.1 INTRODUCTION

The evaluation of the dynamic soil properties such as shear modulus and damping ratio has received increased attention during recent years. This interest has been stated by the need to obtain a better understanding of soil and soil structure interaction behavior during earthquake ground motions.

In this chapter, hyperbolic shear stress-strain relations, shear modulus and damping ratio for undisturbed and remolded soils are discussed in the light of studies previously made.

In addition, the parameters which has effects on shear modulus and damping are analysed. Explanations generally depend on the results previously obtained by various types of resonant column devices.

3.2 DYNAMIC STRESS-STRAIN PROPERTIES OF SOILS

Dynamic loadings develop forces in soils which may change the conventional static stress-strain relationships. These changed relationships are required for dynamic response analyses of soil masses or for dynamic soil structure interaction studies in which time-dependent motions are considered. The shape of the stress-strain relationship for any particular soil depends upon the kind of loading and

boundary restraining conditions. Figure 3.1 shows the behavior of cylindrical somples of cohesionless soil when subjected to an increasing axial stress, σ_z , while a radyol pressure, σ_r acts on its lateral surface.Curve A explains hydrostatic compression ($\sigma_r = \sigma_z$). Curve B shows the condition of constrained compression (no radial expansion permitted). Curve C illustrates the strain softening type of stress-strain curve developed for a constant restraining boundary pressure like developed in a stress-controlled triaxial test.

At very low strain level, the initial part of curves A, B, C may be approximated by a linear elastic stress-strain curve.

Because the different shapes of the stress-strain curves in figure 3.1 are produced by different proportions of volumetric compression and shearing strains, Jackson (1969) has expressed the general stress-strain relations in the form of constitutive equation to describe dynamic behavior of soils under ground shock loadings.

$$\sigma_{ij} = K \, \bar{e} \, \delta_{ij} + 2G \, (\varepsilon_{ij} - \frac{1}{3} \, \bar{e} \, \delta_{ij}) \qquad (3.1)$$

In this equation;

σ_{ij} = total stress tensor

ε_{ij} = total strain tensor

K = Modulus of volume compressibility or bulk modulus.
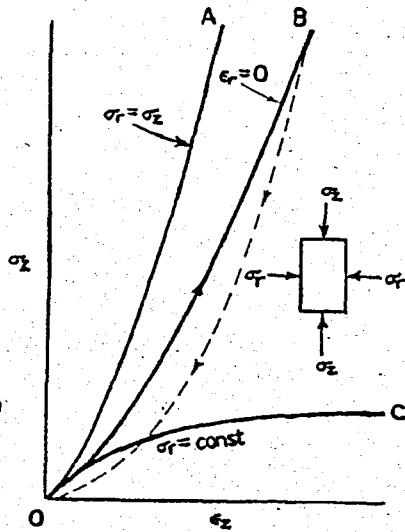
Fig 3.1 Stress-Strain Curves for Triaxial Tests.

(After Yoshimi, 1977).

$$\bar{e} = \varepsilon_x + \varepsilon_y + \varepsilon_z = \text{cubic dilation, or volumetric}$$
$$\text{strain}$$

G = shear modulus

δ_{ij} = kronecker delta function { δ_{ij}=1 when i=j,

δ_{ij}=0, when i≠j)

yield condition $\sqrt{J_2''} = f(\bar{\sigma}_o)$ where;

J_2'' = second invariant of the stress deviation, and

$\bar{\sigma}_o$ = average normal effective stress or octahedral

normal stres.

Soil is considered to deform primarily in one dimen-
sional compression and the general stress strain curve is
similar to curve B in fig. 3.1 . Hadala (1973) found that
for "low stress" level nonlinear curves of the strain soften-
ing type were developed for many soils. This effect depends
upon the type of soil, its initial relative density or degree
of compaction and the degree of saturation.

Theoretically, elastic shearing stress-strain relations
developed by pure shear involve no change of volume, which
couse $\bar{e} = 0$ and Egs. 3.1, becomes a linear form.

$$\tau = G\gamma \tag{3.2}$$

This equation can be used to represent conditions
at any point along a shearing stress-strain curve for the
strain-softening type curve.

On the other hand, pure shear and simple shear differ
only by a rigid body rotation, therefore the stress-strain

relation for the two should be the same. The vibration of horizontal soil layers due to the horizontal component of an earthquake is the best example of simple shear. The simple shear loading produced by an earthquake characterized by stress reversal, with varying amplitude and frequency. The shear stress-strain relation for this general simple shear loading is shown in Fig. 3.3.

Stress reversal is characterized by a loop. The curves through end points of a loop look like ordinary stress-strain curves for a load increasing failure (strain-softening type curve). Hardin and Drnevich (1972) have used a modified hyperbolic stress-strain curve to define the shear stress-strain relationship in Fig. 3.2.

The hyperbolic stress-strain relation curve is asymtotic to the horizontal line defined by $\tau = \tau_{max}$, where τ is shear stress and τ_{max} is the shear stress at failure. The slope of this curve at the origin gives maximum value of shear modulus, G_{max}. The intersection of the line with slope G_{max} and horizontal Line ($\tau = \tau_{max}$) gives reference strain, γ_r.

Where;
$$\gamma_r = \frac{\tau_{max}}{G_{max}} \qquad (3.3)$$

Reference strain is used to normalize the values of shear strain. If a soil exibits truly hyperbolic stress-strain behavior, the curve in Fig. 3.4. can be expressed by either;

$$\frac{\tau}{\tau_{max}} = \frac{\dfrac{\gamma}{\gamma_r}}{1 + \dfrac{\gamma}{\gamma_r}} \qquad \text{or;} \qquad \frac{G}{G_{max}} = \frac{1}{1 + \dfrac{\gamma}{\gamma_r}} \qquad (3.4)$$
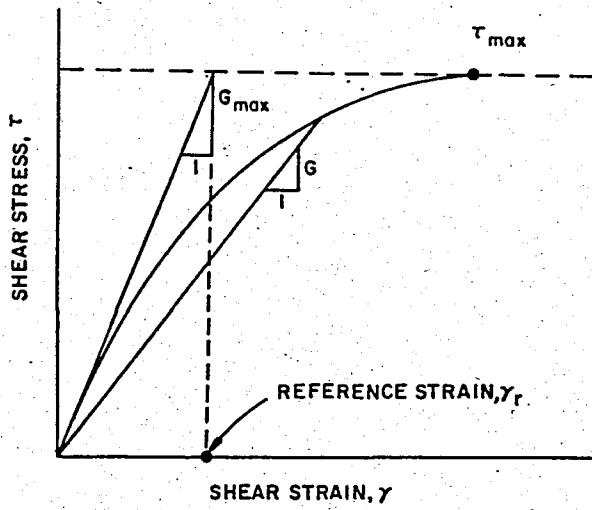
Fig 3.2   Basic Parameters for Hyperbolic stress-
          Strain Curves

                    (After Hardin and Drnevich, 1972)
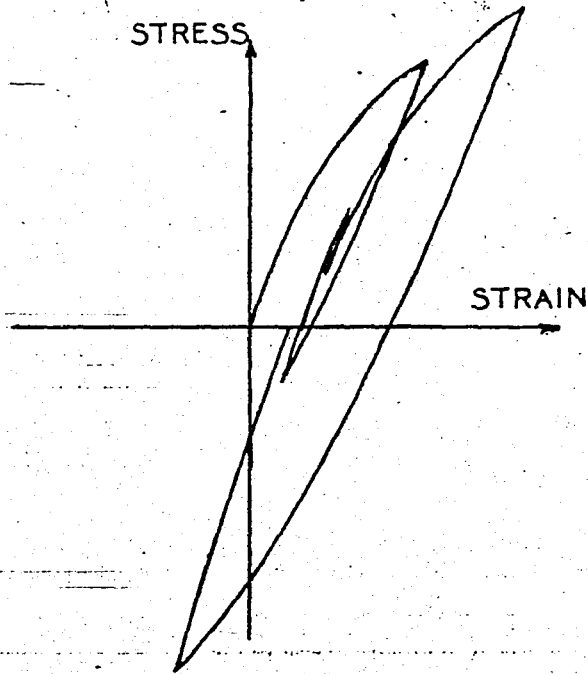
Postulated Generalized Simple Shear Stress-Strain Curve
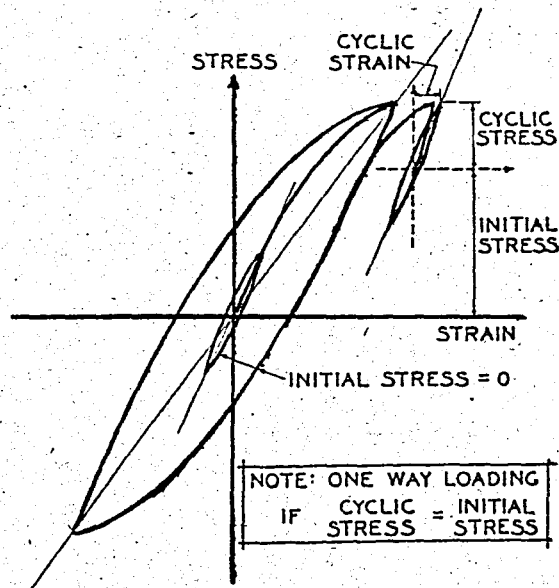
Complete Stress Reversal With and Without Initial
Shear Stress

Fig 3.3 Hysteresis Loops

(After Hardin and Drnevich, 1972)

NORMALIZED SHEAR STRESS, τ/τ_{max}

SAND

CLAY

HYPERBOLIC REPRESENTATION

$$\frac{\tau}{\tau_{max}} = \frac{\gamma/\gamma_f}{1+\gamma/\gamma_f}$$

NORMALIZED SHEAR STRAIN, γ/γ_f
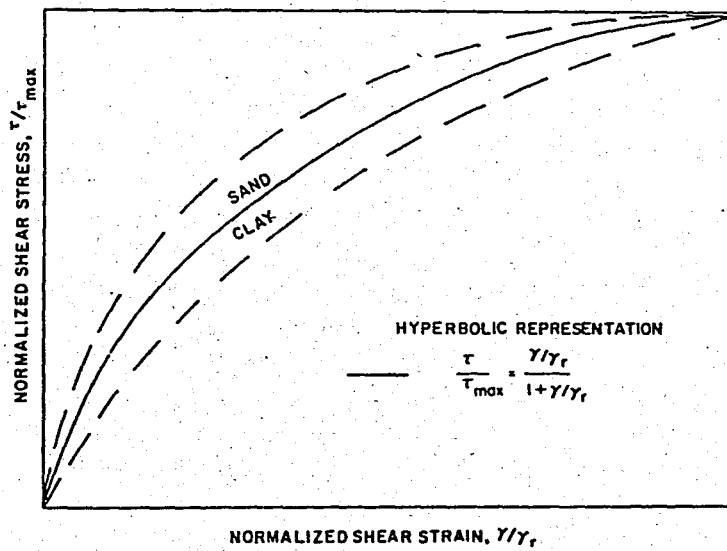
Fig 3.4   Normalized Stress-Strain Relationship for
sands and Clays

(After Drnevich, 1979).

in which G = the secant shear modulus; and G_{max}= the initial
tangent shear modulus. The secant shear modulus is defined
as the slope of the line extending from the origin to any
point on the stress-strain curve. Investigations of a variety
of undisturbed and remolded soils indicate that most soils
do not exactly follow hyperbolic relations. Sands usually
plot above the hyperbolic curve and cohesive soils below.

The concept of reference strain requires the determi-
nation of the maximum shear stress, τ_{max} , and the initial
tangent shear modulus, G_{max}. G_{max} can be calculated directly
in the laboratory using the resonant column method or in the
field using seismic method. The value of τ_{max} depends on the
initial state of stress in the soil and the way in which
the shear stress is applied. For initial geostatic stress
conditions and with the shear stress applied to horizontal
and vertical planes, τ_{max} is related to the strength
envelope of the soil which is shown as in the Fig. 3.5 .
According to Hardin and Drnevich (1972), using the geometry
of Fig. 3.5 it is easily found that for initial geostatic
stress conditions.

$$\tau_{max}= \left\{ \left[\frac{(1+K_o)}{2} \bar{\sigma}_v \; \text{Sin} \; \bar{\emptyset} + \bar{C} \; \text{Cos} \; \bar{\emptyset} \right]^2 - \left[\frac{(1-K_o)}{2} \bar{\sigma}_v \right]^2 \right\}^{1/2} \quad (3.5)$$

in which K_o = coefficient of lateral stress at rest; $\bar{\sigma}_v$ =
effective vertical stress; and $\bar{C}$ and $\bar{\emptyset}$ are the static
strength parameters interms of effective stress.
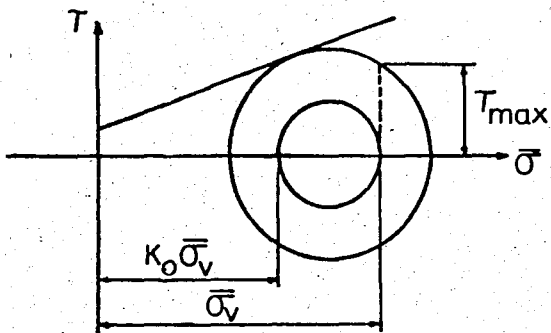
Fig 3.5 Maximum Shearing Stress

(After Hardin and Drnevich, 1972)

The shear stress-strain loop is defined by two parameters; shear modulus and damping ratio, Fig. 3.6 . The slope of the line passing through the end points of the loop is called the average shear modulus, G, and defined as;

$$G = \frac{\overline{AB}}{\overline{OB}} \qquad (3.6)$$

The damping ratio, D, is defined as

$$D = \frac{\text{Area of the loop}}{4 \times \text{Area of } O\overset{\Delta}{A}B} \qquad (3.7)$$

3.3 PARAMETERS WHICH AFFECT THE SHEAR MODULUS AND DAMPING

Hardin and Black (1968) have noted that the parameters which have influences on the shear modulus and damping of soils, and have expressed these as a functional relationship;

$$G , D = f(\overline{\sigma}_o, e , A , t , H , f , C , \theta , \tau_o , S , T , N) \qquad (3.8)$$

Where $\overline{\sigma}_o$ = average effective confining pressure (Mean principal stress)

e = void ratio

A = amplitude of shearing strain

t = secondary effects that are functions of time and magnitude of load increament

H = ambient stress history and vibration history

f = frequency of vibration

C = grain characteristics
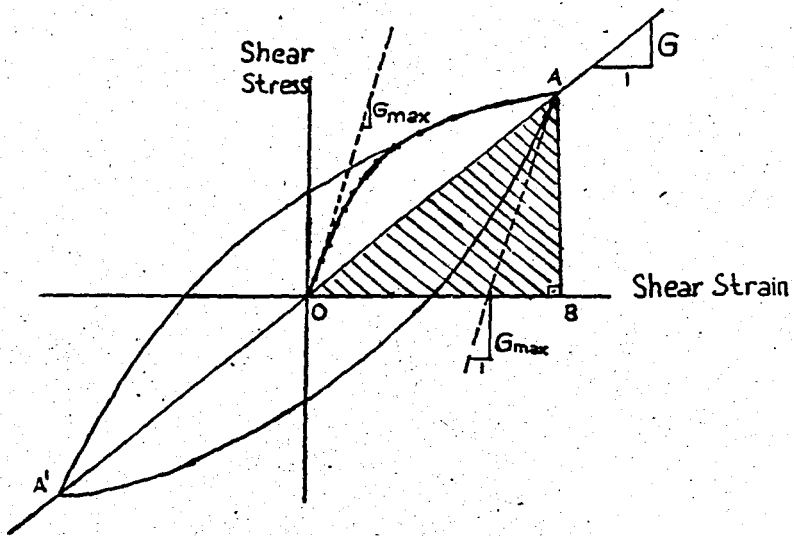
Fig 3.6 Typical Hysteresis Loop

(After Hardin and Drnevich, 1972).

θ = soil structure

τ_O = octahedral shearing stress

S = degree of saturation

T = temperature

N = number of cycles of loading

According to Hardin and Black (1968), for sands, shear modulus is nearly independent of each of the variables except $\bar{\sigma}_o$ and e for shear strain amplitudes of vibration less than about 10^{-4}.

Parameters influencing shear modulus and, damping have been grouped according to their importance by Hardin and Drnevich, 1972, as shown in Table 3.1 for cohesive and cohesionless soils.

Generally, three of parameters have very impartant affect on shear modulus and damping ratio; these are, strain amplitude, effective mean principal stress, and void ratio.

On the other hand, there are some parameters such as grain characteristics; that is relatively unimportant for modulus and damping in all soils, but it affects void ratio which is a very important parameter, and effective strength envelope, a less important parameter.

3.3.1 Strain Amplitude

Shear modulus decreases very rapidly with increasing strain amplitude, while on the other hand damping ratio increases. The form of the shear modulus-strain amplitude

TABLE 3:1 PARAMETERS AFFECTING SHEAR MODULUS AND DAMPING FOR COMPLETE STRESS REVERSAL

(After Hardin and Drenevich, 1972)

| PARAMETERS | IMPORTANCE TO | | | |
| | SHEAR MODULUS | | DAMPING | |
	COHESIVE SOILS	CLEAN SANDS	COHESIVE SOILS	CLEAN SANDS
Strain Amplitude	V	V	V	V
Effective Mean Principal Stress	V	V	V	V
Void ratio	V	V	V	V
Number of Cyclés of Loading	R	R	V	V
Degree of Saturation	V	R	V	L
Over Consoludation Ratio	L	R	L	R
Effective Strength Envelope	L	L	L	L
Octahedral Shear Stress	L	L	L	L
Frequency of Loading	R	R	L	R
Other time effects (Thixotropy)	L	R	L	R
Grain Characteristics	R	R	R	R
Soil Structure	R	R	R	R
Volume Change due to Shear Strain	R	U	R	U

V : very important

L : Less important

R : Relatively unimportant

U : Relative importance is not clearly known

is the same for both cohesive and cohesionless soils, but decreasing rate of modulus is not constant as shown in Fig. 3.7 . This rate depends on the values of maximum shear modulus, G_{max} , and the shear strength of the soil.

According to Drnevich and Massarch (1979), all soils exibit non-linear stress-strain behavior even at very smal strains, but shear modulus can be assumed constant below strain amplitude of 10^{-5}. In a general sense, at shear strains exceeding 10^{-5} the shear modulus decreases rapidly and at 10^{-3} strain level the shear modulus becomes only a fraction of the maximum value, as it is seen in Fig. 's 3.8 and 3.9 .

The damping ratio, D, is appearently equal to zero for zero strain amplitude. The values measured at strain amplitudes on the order of 10^{-6} are very small. At Large strain amplitudes the damping ratio appears to approach to a maximum value.

3.3.2 Mean Princpal Stress

Shear modulus increases with increasing mean principal stress. At large strain amplitudes the modulus depends mainly on the strength of the soil, which is a function of $\bar{\sigma}_o$. For normally consolidated clay, effect of $\bar{\sigma}_o$ is independent of void ratio. Under very low effective mean principal stress, the modulus of cohesive soils decrease rapidly with increasing amplitude.

on the other hand, damping ratio decreases with the
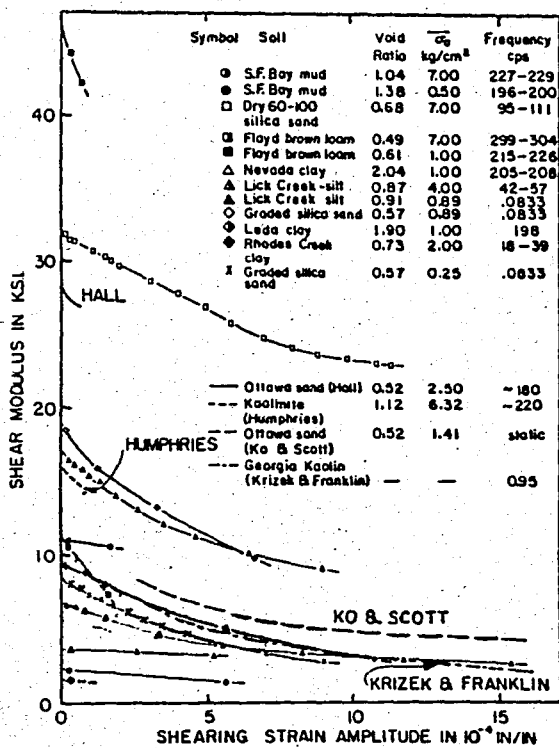
Fig 3.7 Shear Modulus Versus Shearing Strain Amplitude
for Variety of Soils

(After Hardin and Drnevich, 1972)
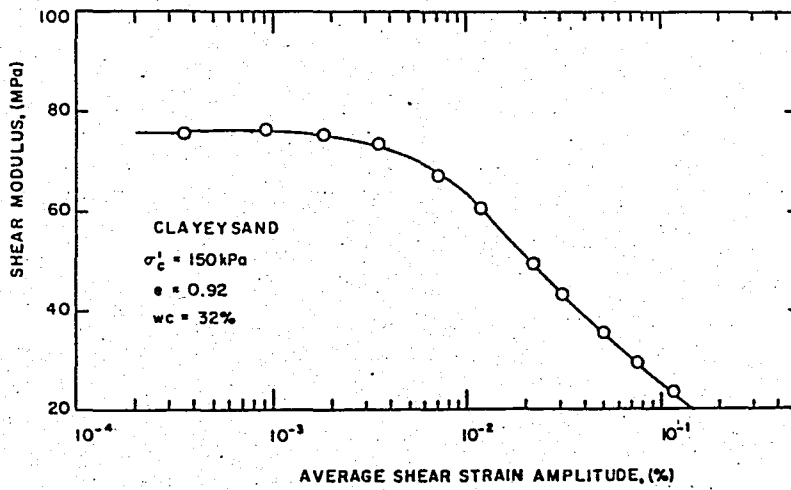
Fig 3.8 Change of Shear Modulus with Shear strain
Determined from Torsional Resonant Column
Test

(After Drnevich and Massarch, 1979)
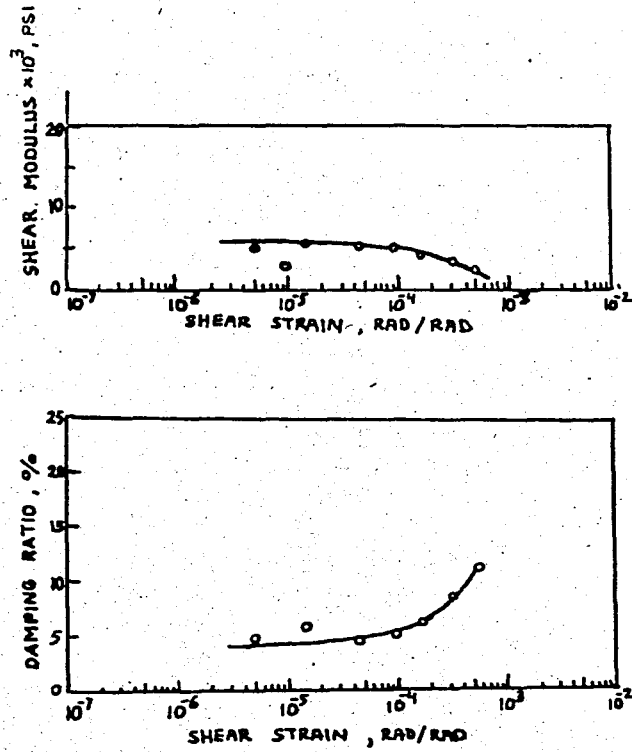
Fig 3.9   Dynamic Shear Modulus and Damping Ratio
versus Shear Strain Amplitude for a Clay

(After William Curro, 1981).
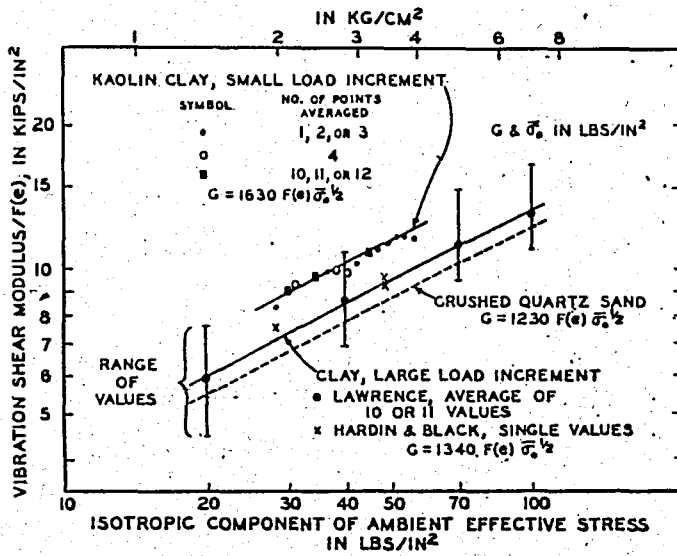
Fig 3.10   Effect of Mean Principal Stress

(After Hardin, 1968)
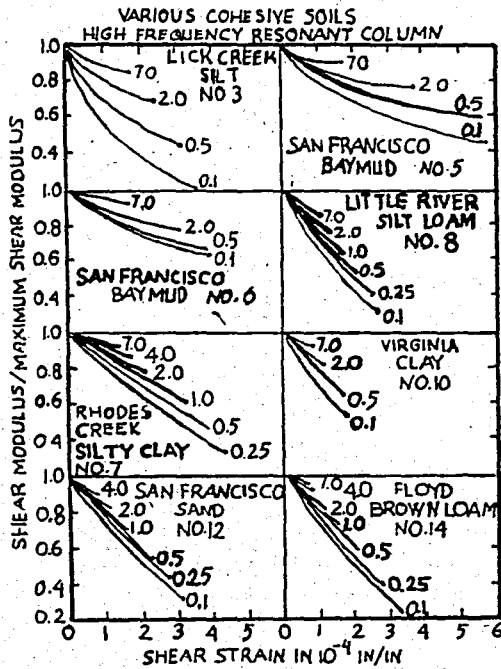
Fig 3.11 Normalized Shear Modulus Versus Shearing
Strain Amplitude.
(After Hardin and Drnevich, 1972)
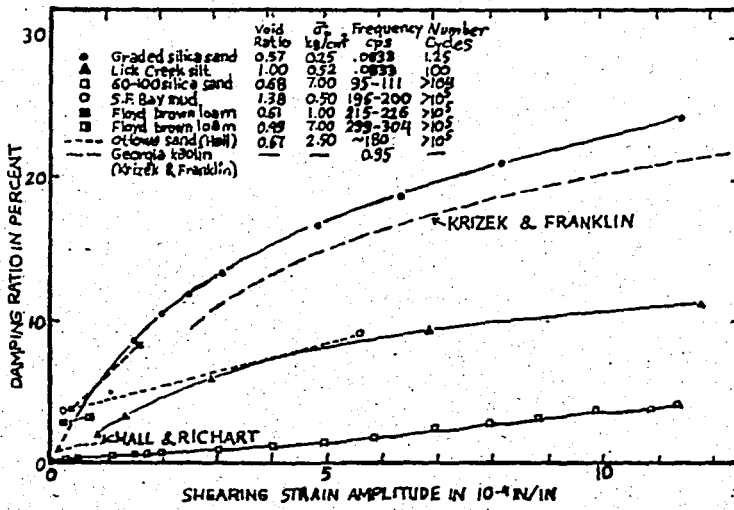
Fig 3.12   Damping Ratio versus Shearing Strain
            Amplitude for variety of soils

                        (After Hardin and Drnevich, 1972)

square root of mean principal effective stress. The affects
of mean principal stress on shear modulus and damping ratio
are shown in Fig. 3.7 and Fig's 3.10 through 3.12 respectively.

3.3.3 Void Ratio

Void ratio has an important affect on shear modulus
and damping ratio for cohesive soils. The void ratio of a
normally consolidated clay is a function of the state of
effective stress. For that reason it is not possible to vary
the void ratio at a constant effective stress without
changing the structure.

Lawrance (1965) have studied on dispersed, flocculated
kaolinite and Boston Blue clay at different confining pressures
as it is seen in Fig. 3.13.. The solid lines are for cohe -
sionless soils and computed using empirical equation proposed
by Hardin and Drnevich (1968)

$$F(e) = \frac{(2.973 - e)^2}{1 + e} \qquad (3.9)$$

Although there is considerable difference, the average
absolute percentage difference of the clay values from the
curves for sand is about 14%. May be a part of this difference
comes from the structure difference.Writers assumes that
Eg. 3.9 is valid to show the effect of void ratio on modulus
for clays with low surface activity. Fig. 3.7 shows that if
the values of $\bar{G}_{max}$ for Lead Clay, Lick Creek silt and Brown
Loam are compared, it's seen that all of these cohesive

soils are at nearly equal effective mean principal stress,
thus modulus differences comes from the different void ratios.
As a result, it is concluded that shear modulus and damping
ratio decreases with increasing void ratio in undisturbed
cohesive soils.

3.3.4 Number of Cycles

For cohesive soils the shear modulus decreases with
the increasing number of cycles. Hardin and Drnevich (1972)
showed that shear modulus decreases with number of cycles
for Lick Greek silt as in Fig. 3.14 . Similarly damping ratio
for the same material decrease with increasing number of
cycles.

In another study, using undrained strain controlled
with the torsional Simple shear device, Ishibashi and Ling
(1974) has showed that for pacific Red Clay the equivalent
shear modulus, Geq, decreases with increasing number of
cycles, but the damping ratio, D, remains almost constant
shown in Fig. 3.15 .

3.3.5 Degree of Saturation

According to Cheong and Chae (1980), the shear modulus
of cohesive soils increases rapidly with decreasing degree
of saturation. Theoretically the existing of water in soil
reduces the velocity of wave propagation, thus the shear
modulus decreases. For compacted clay experiments by using
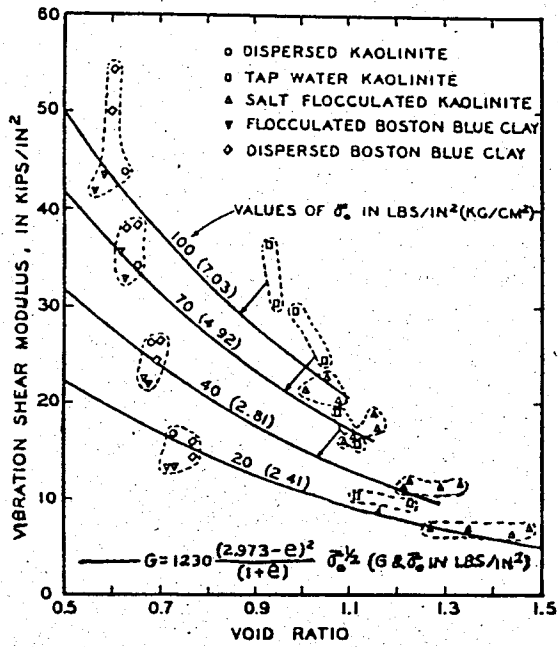
Fig 3.13   Effect of Void Ratio

(After Hardin and Black, 1968)
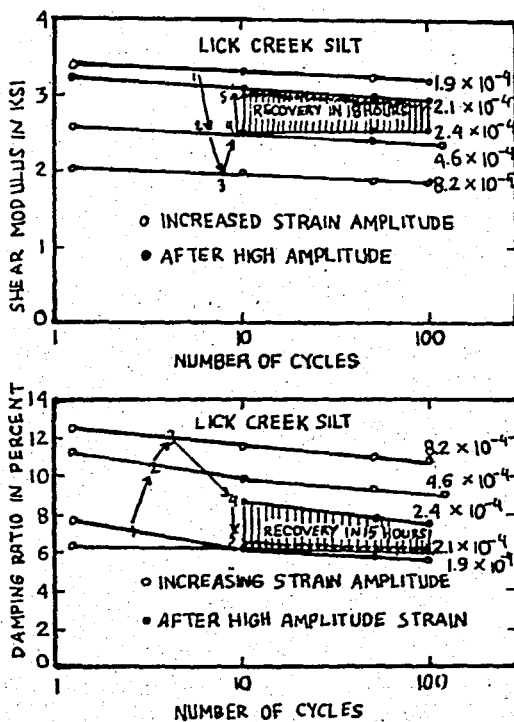
Fig 3.14   Recovery of Shear Modulus and Damping Ratio
with Time After Alteration by high Amplitude
Cylic Loading

(After Hardin and Drnevich)
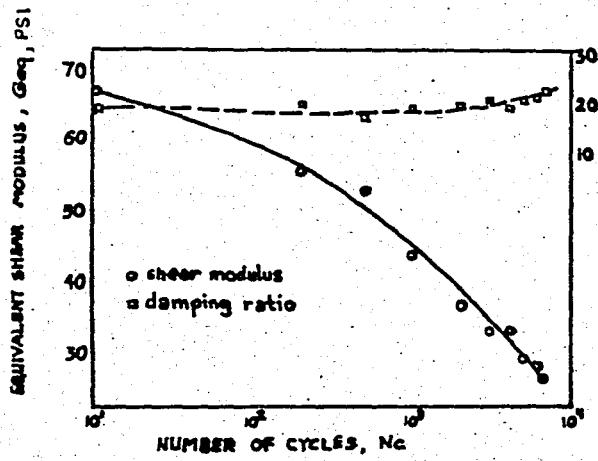
Fig 3.15 Equivalent Shear Moduli and Damping Versus
          Number of Cycles
                              (After Ishibashi and Ling, 1974)

resonant column method shows that shear modulus increases
with increasing degree of saturation up to the optimum -
water content, further increase of saturation degree cause
to decrease the shear modulus. That is shown in Fig. 3.16 .

Damping ratio can be assumed constant for low degree
of saturation, but increases rapidly with increasing degree
of saturation according to the studies of Cheong and Chae
(1980).

Clays treated with lime show higher shear modulus.
When the clay is treated by salt, the shear modulus decreases
with the degree of saturation. According to the opinions of
cheong and chea (1980), this behavior may be explained by
the relationship between salt concentration and Bingham yield
stress shown in Fig. 3.17 .

3.3.6 Overconsolidation Ratio

Test results obtained from Resonant Column and Cyclic
Triaxial tests by Fisher and Koutsoftas at a given consolida-
tion stress have showed that overconsolidated specimens have
higher shear modulus than normally consolidated specimens .
Furthermore, the shearmodulus is strongly influenced by the
magnitude of the maximum past pressure. As an example in
Fig. 3.18, test results on kaolinite indicate that at a
consolidation stress of 25 psi, when the soil is unloaded
from a maximum stress of 100 psi to achieve an OCR of 4, it
has a modulus which is about 17% higher than when unloaded
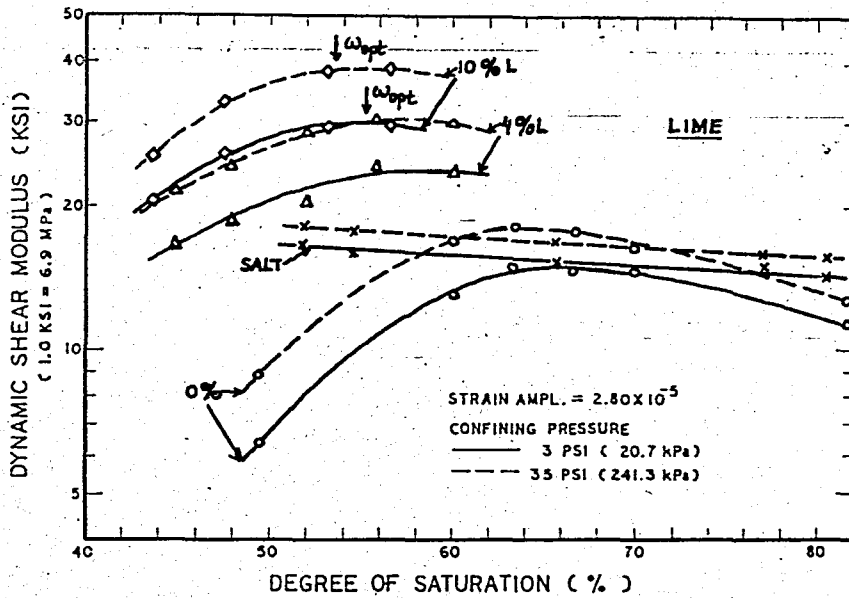
Fig 3.16   Effect of Degree of Saturation on Dynamic
            Shear Modulus of Treated and Untreated
            Clay
                        (After Cheong and Chae, 1980)
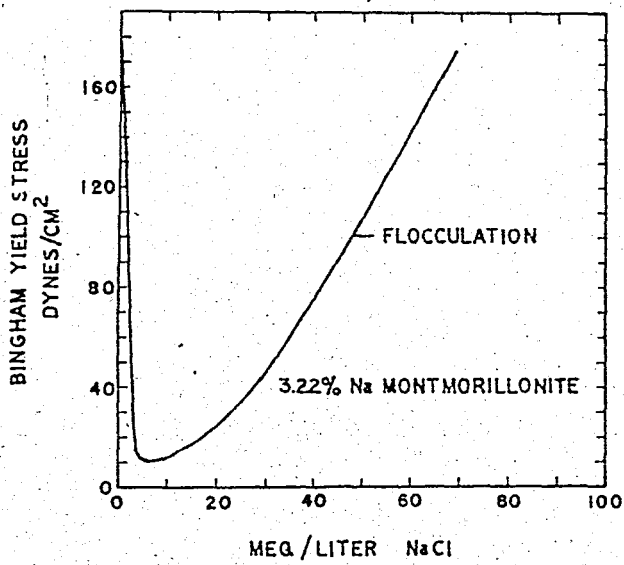
Fig 3.17   Effect of Salt Concentration on Bingham
           Yield Stress
                              (After Olphan, 1963)
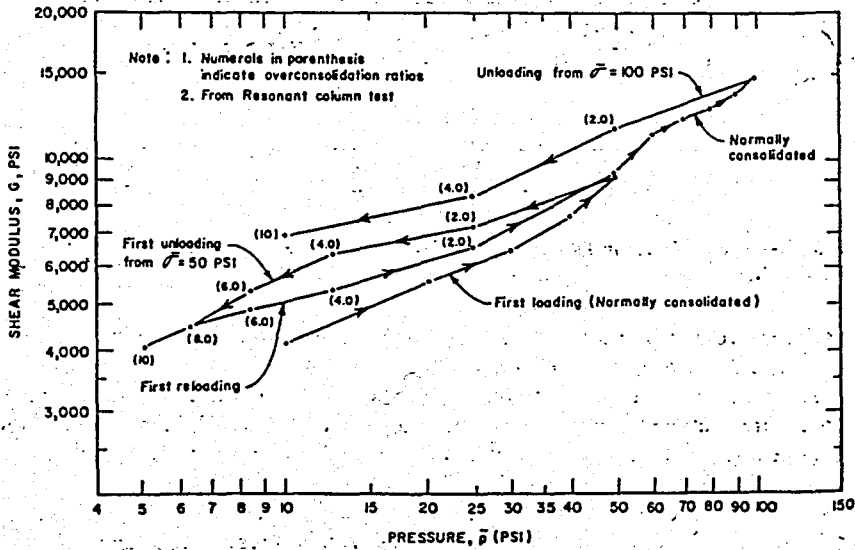
Fig 3.18   Shear Modulus and Functions of Consolidation
Stress and Stress History for Kaolinite

(After Fisher   Koutsoftas, 1980)

from a maximum stress of 50 psi to achieve an OCR of 2.

The normalization of shear modulus with respect to the undrained shear strength is most useful in estimating changes in moduli during consolidation.

Fig. 3.19 shows that normalized shear modulus decreases with increasing Over Consoludation Ratio. However, the damping ratios do not appear to be influenced significantly by over consolidation ratio according to Koutsoftas and Fisher (1980).

3.3.7 Octahedral Shear Stress

Hardin and Black (1968) showed that the shear modulus of a normally consolidated clay is essentially independent of the octahedral shear stress. The effect of relatively high octahedral shear stress on the shear modulus is small after 10 cycles of complete stress reversal when cyclic strain amplitude is measured from the center of the loop. Besides, damping ratios are not influenced by octahedral shear stress for cohesive soils

3.3.8 Time Effects

In order to determine time effect on shear modulus, drained and consolidated-undrained tests have been performed on kaolinite and bentonite by Marcuson and Harvey (1972). As seen in Fig. 3.20, the results for both soils show that shear modulus increases with time at constant effective stress and that the increase in modulus can not be fully attributed
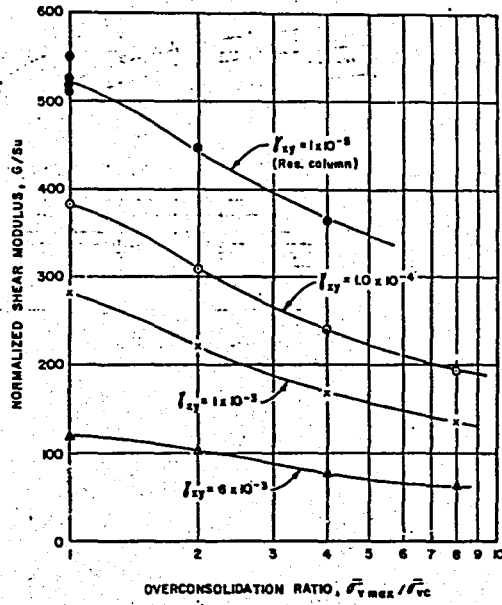
Fig 3.19   Normalized Shear Modulus as Function of
           Shear Strain and OCR for Plastic Clay
                          (After Fisher   Koutsoftos, 1980)
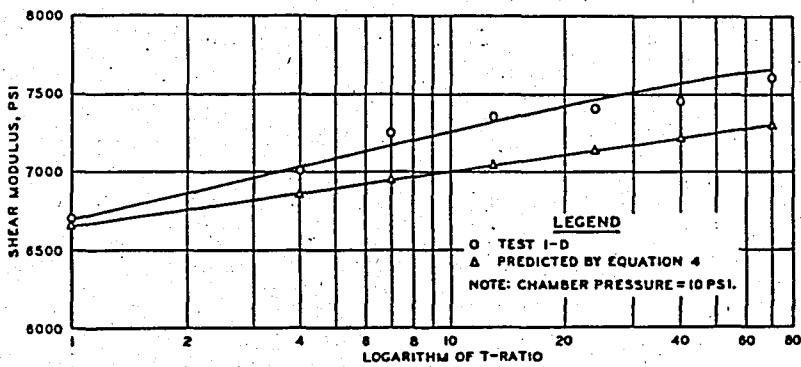
Fig 3.20   Shear Modulus versus Logarithm of Tr for
           Kaolinite
                            (After Marcuson and Harvey, 1972)

to decrease in void ratio. The modulus even increases with
time in undrained tests in which void ratio remain constant
and the effective stress reduced slightly. Shear modulus
continues to increase during secondary consolidation due
to some structural rearrangement.

3.3.9 Thixotropy

According to Hardin and Drnevich (1972), the thixotropic
behavior of soils causes an increase in the modulus and a
decrease in damping with time. Fig. 3.14 shows the recovery
of modulus and damping with time after alteration by high
amplitude cyclic loading. The high strain amplitude loading
causes a decrease in modulus and an increase in damping for
Lick Creak Silt. When the specimen is allowed to rest over-
night and is tested under the same load, almost complete
recovery occurs. The modulus increases and damping ratio
decreases during the rest time to near their original small
starin amplitude values. This behavior shows that during an
earthquake producing low to moderate strains the modulus of
cohesive soils decreases and the damping increases with each
cycle but that the soil will recover very rapidly from the
effect of the earthquake.

3.3.10 Other Factors

Hardin and Drnevich (1972), showed that frequencies
above 0.1 H_z have minor affects on the shear modulus and

damping ratio for cohesive soils.

The effect of temperature, T, during resonant column testing was found to be unimportant by Anderson and Richart (1974), for clays. Tests conducted on seven cohesive soils at $4^{\circ}C$ and $22^{\circ}C$ showed that shear wave velocity, V_s, at $4^{\circ}C$ was equal to or not more than 12% greater than Vs determined at $22^{\circ}C$. However, resonant column test of frozen soils, performed by Stevens (1975), have showed a significant affect of changes in temperature near the freezing point.

Another factor is additives. Test results by Chae and Chiang (1978), using resonant column method, showed that the shear modulus increases with the increase of treatment level at a shear strain of 1.4×10^{-5}, for silty clays. The presence of additives increases the damping capacity of soils. The rate of change of damping ratio is not affected by the strain amplitude, while the effect of additives on damping rate diminishes at higher confining pressures as seen in Fig. 3.21 . Different types of additives have different effects on shear modulus and damping. Lime, alone doubles the shear modulus of the untreated clay. Salt alone changes the soil structure, and increases the shear modulus on the dry side of the optimum moisture content. Addition of salt during lime treatment increases the shear modulus up to five times that of untreated clay, in Fig. 3.22. Moreover, deviatoric stress increases with the increase of treatment level.
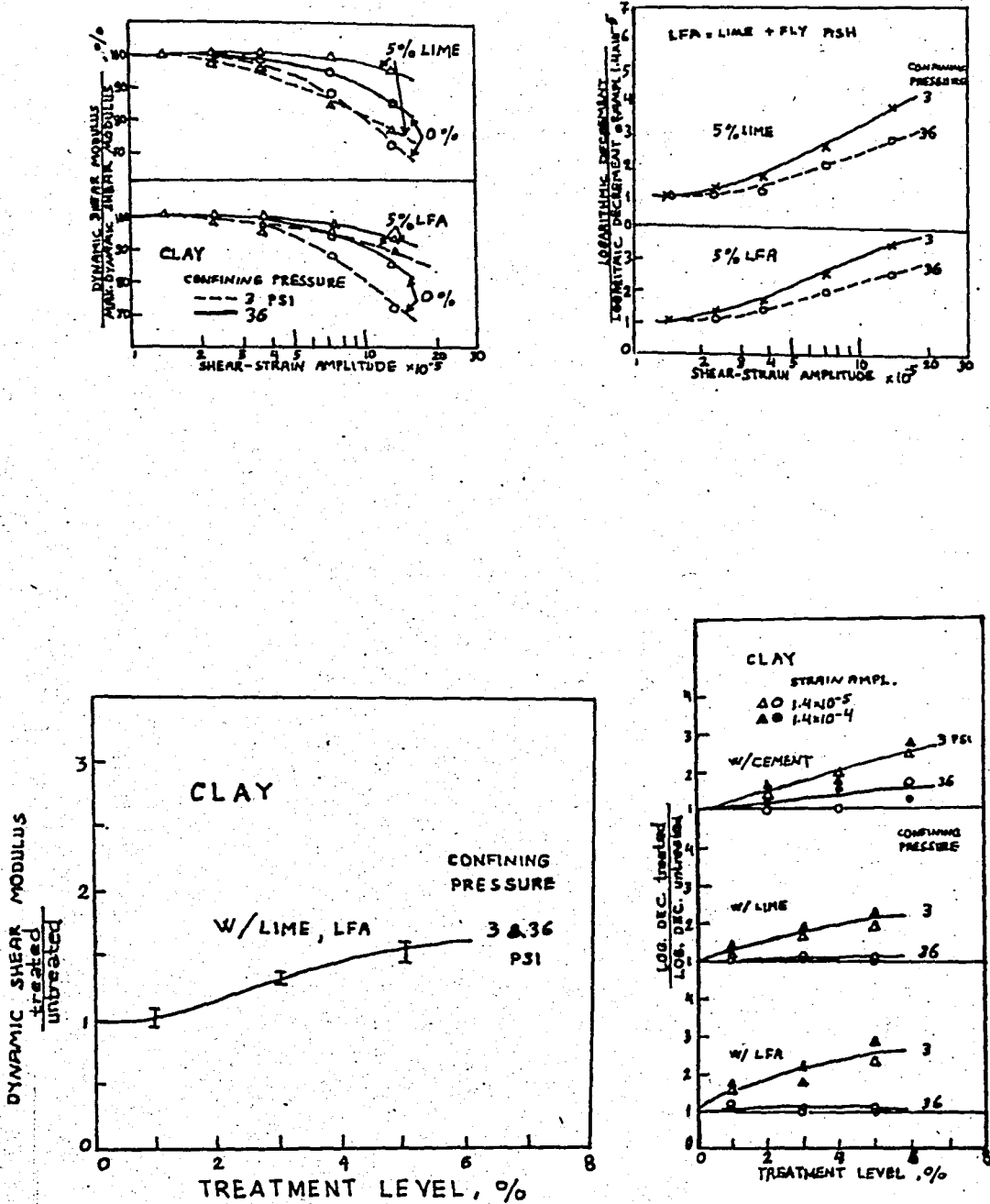
Fig 3.21   Effects of Additives on Shear Modulus and
           Damping.

                    (After Chae and Chaiang 1978)
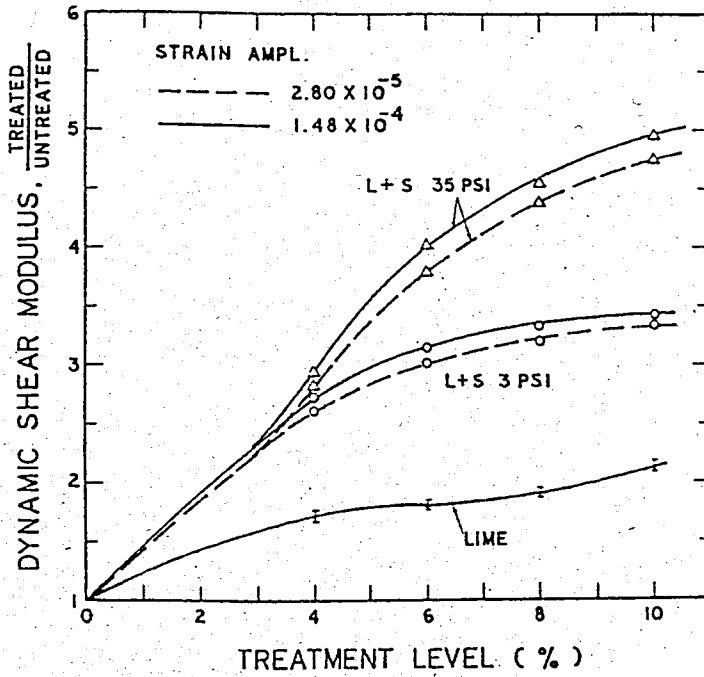
Fig 3.22 Shear Modulus Ratio As Function of Treatment
          Level
                    (After Cheong Au and Chae, 1980)

3.4 SUMMARY AND CONCLUSIONS

In this chapter, shear stress-shear strain relations and the parameters which influence the dynamic properties are discussed. For compacted soils most of the parameters are significant. The main parameters affecting compacted soils are : shear strain amplitude, vertical stress, confining pressure, moisture content, and additives if used.

The folluwing results can be obtained;

1. For undisturbed, remolded and compacted soils, as strain amplitude increases; shear moduli decrease, however, damping ratio increases.

2. As mean principal stress increases, shear modulus increases, and damping ratio decreases.

3. For clays, shear modulus increases with increasing overconsolidation ratio, however, damping ratio is not affected at all.

4. During secondary consolidation of clays shear modulus continues to increase, with a smaller increasing rate.

5. For undisturbed cohesive soils, as void ratio decreases, shear modulus increases, however, damping ratio decreases.

6. In general, additives increase both the shear modulus and damping ratio of soils.

CHAPTER 4 DESCRIPTION OF THE RESONANT COLUMN AND
          SOILS TESTED

4.1 INTRODUCTION

Laboratory and field techniques are used to determine shear modulus. Besides, there are prediction methods which are dependent on the laboratory and field results. Marcuson and Curro (1981), have reported that resonant column method yields better results when compared to the results of other methods.

Although there are several types of resonant çolumn devices, for this study "Hardin" type is used, as represented by the model shown in Fig. 4.1 .

Tests are performed on five different clay samples. The properties of soils are shown on Table 4.1 Samples are compacted by using modified mini proctor compactor with the same energy as for the stardard proctor test.

4.2 MEASUREMENT OF DYNAMIC SOIL PROPERTIES

There are two main technique for evauating dynamic soil properties:

1. Laboratory Techniques,
    a. Strain-Rate Tests
    b. Resonant Column Tests
    c. Ultrasonic Pulse Test

d. Cyclic Tests

    1) Cyclic Triaxial Test

    2) Cyclic Simple Shear Test

    3) Cyclic Torsional Simple Shear Test

    4) Shake Table Test

2. Field Techniques

a. Crosshole method

b. Downhole method

c. Surface vibration Test

d. Cyclic Load Test

e. Rayleigh Wave Test

Moreover, emprical equations may be used to calculate maximum shear modulus, G_{max} . Most widely used formula was derived by Hardin and Black (1968).

$$G_{max} = 1230 \frac{(2.973 - e)^2}{1 + e} (OCR)^k (\bar{\sigma}_o)^{1/2} \qquad (4.1)$$

    e : void ratio

OCR : overconsolidation ratio = $\sigma_{vmax} / \sigma_{vc}$

    k : parameter that depends soil plasticity.

    $\bar{\sigma}_o$: mean principal effective stress (psi)

G_{max} : shear modulus (psi)

Marcuson and Curro (1981), have found that for clays, values determined using field techniques were very close to those determined by resonant column tests, which proves the accuracy of the resonant column method.
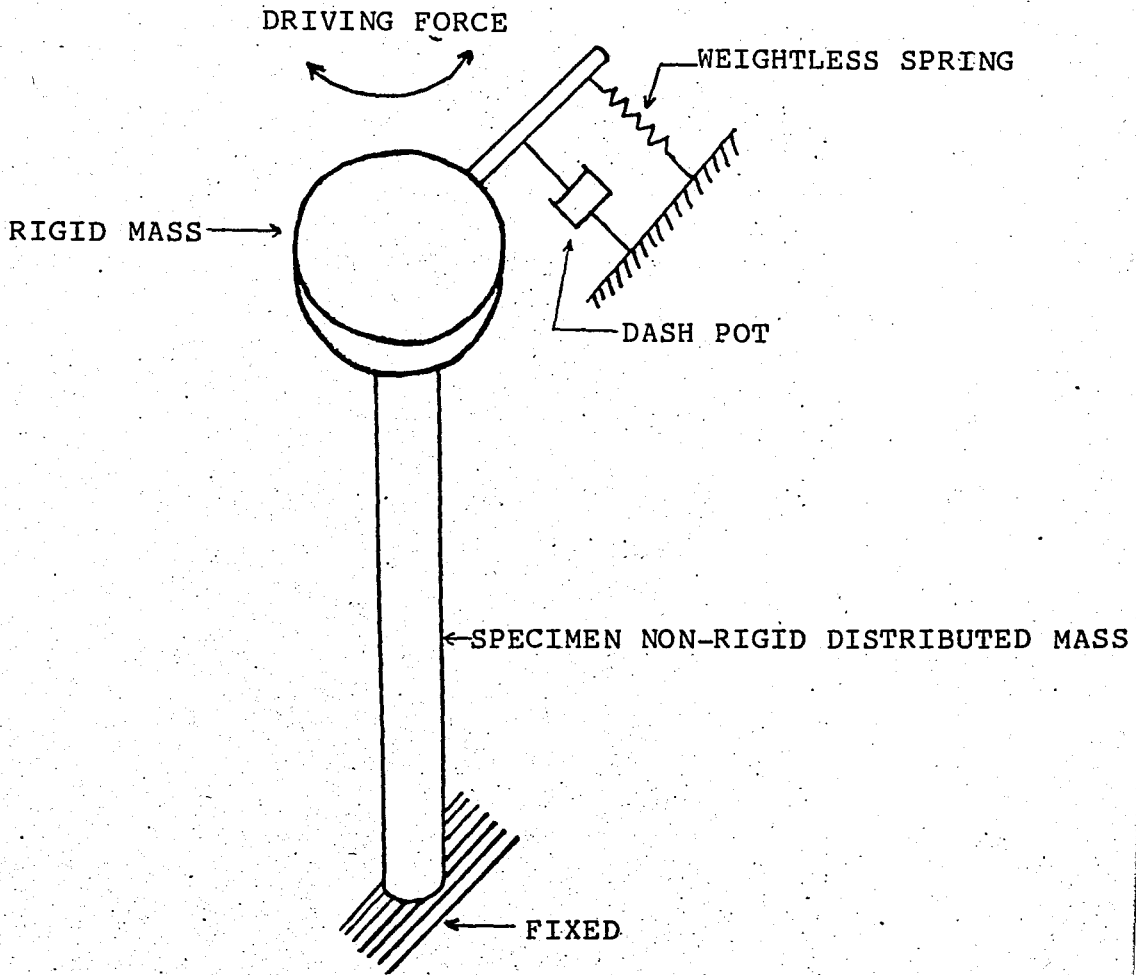
Fig 4.1 Hardin Type Resonant Column Model
(After Hardin 1970)
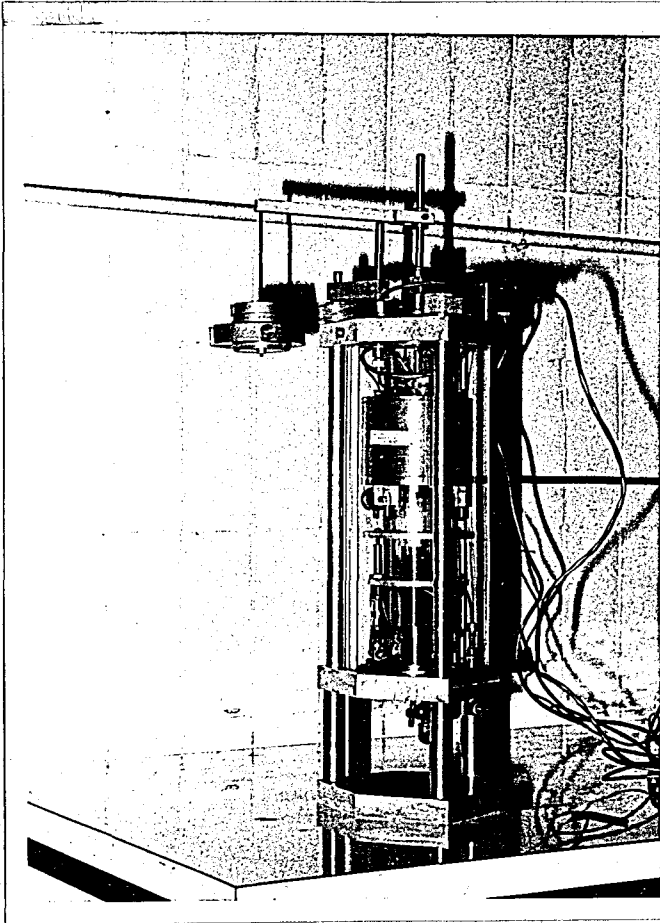
Fig 4.2   Hardin's   Resonant Column Apparatus

4.3   RESONANT COLUMN TEST DEVICES

The resonant column test for determining shear modulus and damping capacity of soils is based on the theory of wave propagation in prizmatic rod.

Either shear waves or compression waves can be applied to the soil specimen from which either shear modulus or Young's modulus can be determined.

The resonant column technique was first used to find soil moduli by Japanese engineers Ishimoto and Iida (1937), and Iida (1938 , 1940). Shannon, Yamane and Dietrich (1959), and Wilson and Dietrich (1960) described a new resonant column apparatus.

Depending on the end conditions, several types of resonant column tests are possible.Early versions of resonant column apparatus were only capable of applying isotropic confining stress conditions to the specimens.

To learn the influence of anisotropic stress conditions on shear modulus and damping, Hardin and Music (1965) developed the apparatus shown in Fig. 4.2 . This apparatus, also shown shematically in Fig. 4.1, has a fixed base and a top cap that is partially restrained by a spring which in turn reacts against an inertial mass, which is balanced by a counter weight,but by changing the counter weight axial load can be applied to the specimen.

To study the influence of shearing strain amplitude

on shear modulus and damping, Drenevich (1967,1972) developed an hallow cylindrical apparatus. To test clays at shearing strain amplitude up to 1% Anderson (1974) used a modified "Drenevich" apparatus.

Drenevich (1978) have developed a special resonant column device. Using that apparatus both shear modulus, G, and Young's modulus, E, can be measured in the same sample. The various types of apparatus that have been used in the resonant column test all give similar results.

Most of the resonant column devices were designed to operate at small strain amplitudes less than 10^{-4}. Good results can be taken at strain amplitudes 10^{-5} or less.

Resonant column tests should not be considered to be tools only for soil dynamics. In sofar as many static soil-mechanic problems deal with small elastic-strain conditions, the resonant-column test can provide informations. For that reasons resonant column test become a common laboratory procedure. Because of small strain amplitude disturbance decreases in this test.

The device which was used in this study is "Hardin" type resonant column apparatus shown in Fig. 4.2 . According to Hardin, resonant column means a cylindrical specimen or column of soil attached to a rigid pedestal of sufficient inertia to make the motion of the attached end of the specimen essentially zero during vibration of the specimen. This motionless end of the specimen is called the fixed end and

the rigid pedestal of large inertia is called the fixed

base. At the opposite end of the specimen, apparatus is

attached to produce sinusoidal excitation, and to measure

the vibration amplitude of the end of the specimen. This

end of the specimen is called the vibration end. The frequency

of excitation will be adjusted to produce resonance of the

system, composed of the specimen and its attached apparatus.

This system is the resonant column.

Resonant column apparatus consists of several components;

Vibration Excitation Device; The Hardin Oscillator,

a device for applying a forcing torque to the vibration end

of the specimen about its axis, that varies sinusoidally

with time, and for which the frequency is variable, shall

be rigidly coupled to the specimen cap. It's shown in Fig.

4.3. The force is produced electromagnetically with coil and

permanent magnet current-to-force transducers. The rigidity

and mass distribution of the vibration excitation device

and specimen cap shall be such that it can be accurately

represented a rigid mass attached to weightless springs and

a dashpot. That is, the vibration excitation device by itself

is essentially a single degree of freedom system.

Specimen Cap and Base; The cap and base have a circular

cross section and plane surface of contact with the specimen.

To provide for coupling with the ends of the specimen plane

surface can be roughaned. The diameter of the specimen base

and cap shall be equal to the diameter of the specimen.

During a test the specimen cap shall be rigidly coupled to
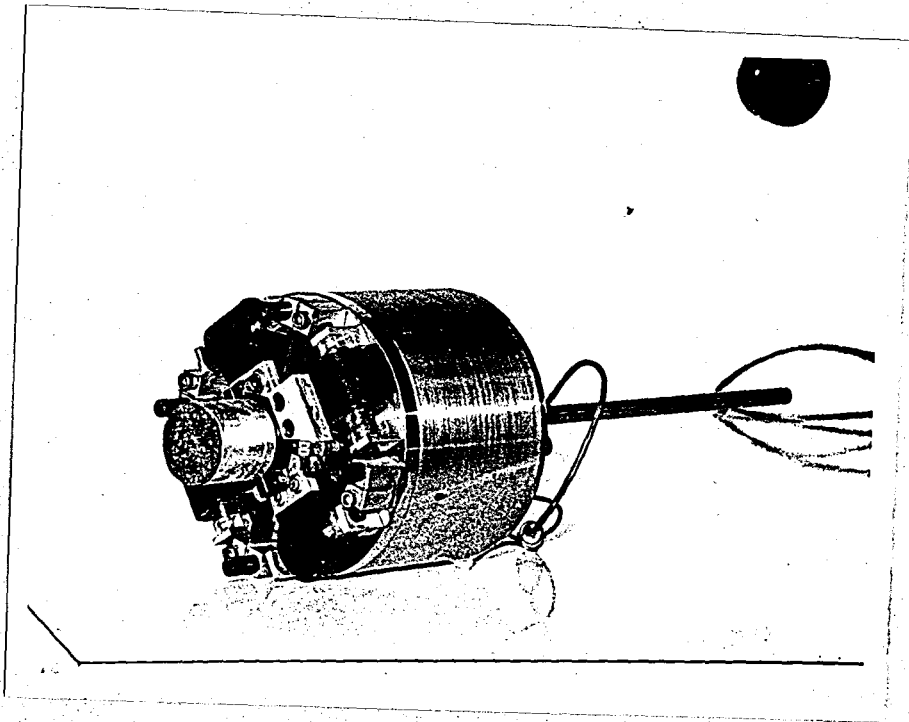
Fig 4.3   The Hardin Oscillaton

the vibration excitation device. The material and construction of the specimen cap and base shall be such that they're essentially rigid with respect to the specimen.

Sine wave generator: An electronic instrument which is producing a sinusoidal voltage. This device provides sufficient power to produce the required vibration amplitude.

Vibration Measuring Device;   Which is an accelerometer that have been attached to and become a part of the rigid mass of the Hardin oscillator. Accelerometer produces a calibrated output that is a measure of the angular acceleration of the vibration end of the specimen. The Readout instrument is capable of measuring the voltage from the vibration measuring device. In this study the read out device is an oscilloscope (Tektronix 214 Storage Oscilloscope). Other devices are charge amplifier (Columbia Research Laboratories 4102 Charge amplifier), which amplifies the signal that comes from vibration measuring device. Bridge Amplifier; which amplifies the signal that comes from load Cell. Load Cell is a device that measures axial load that acts on sample. Fluce Multimeter ; is a device which is capable of measuring voltage, resistance and current digitally. Switch box with cables; is a controlling box which permits connections from Hardin Oscillator to oscillascope, and from amplifiers to the oscillascope and multimeter.

Support for Vibration Excitation Device;   Hardin Oscillator is too heavy to be supported by an unconfined

specimen without causing an axial compression failure. Hence the device must be supported during test set up. This support is consists of suspending the apparatus from above using a frame support, or pneumatic cylinder support. After test set up the counter balance is used.

4.4 PREPARATION OF SPECIMENS

Five types of silty clays are tested in this study. One of them was taken from the "BOGAZİCİ University" Campus, the other from the construction site of "DENİZCİLİK BANKASI T.A.O", İçerenkoy, - İSTANBUL during its geotechnical investigation.

Index properties, specific gravity of particles, compaction properties, and the classification of soils are given in Table 4.1

The samples are compacted using modified mini proctor compactor according to impact procedure. The 0.474 kg hammer is used to compact the samples in three layers applying 25 drops per layer from 15 cm, which delivers a nominal compaction energy equivalent to that of Standard Compaction Test energy.

To obtain the desired moisture content necessary amount of water is added to the specimen. After mixing, soil is placed in the mold, and than sample is compacted in three layers Specimens are 8 cm in length and 3.57cm in diameter. Immediatel following the extrusion, each specimen is wrapped in aluminium foil and placed in a glass container to avoid any changes in

TABLE 4.1 Index and Compaction Properties of Clays Tested

	W_L	W_p	I_p	-No.200	U.C	AASHTO	w_{opt}	γ_{dry}	CBR	G_s
İçerenköy Sample 1	27.7	19.0	8.7	43.4	SC	A-4	13.0	1.885	–	2.86
İçerenköy Sample 2	51.0	26.8	24.2	61.2	CL	A-7-6	22.0	1.630	25	2.78
İçerenköy Sample 3	35.0	24.5	10.5	41.6	SC	A-6	13.3	1.845	31	2.74
İçerenköy Sample 4	34.0	17.5	16.5	35.0	–	A-6	15.4	1.800	29	2.87
Boğaziçi University sample	41.0	26.0	15.0	–	–	–	19.2	1.665	26	2.69

w_1 : Liquid limit, %

w_p : plastic limit, %

I_p : plasticity index, %

-No.200 : passing from # 200, %

U.C. : unified system

AASHTO : American Association of State Highway Officials Classification of soils

w_{opt} : optimum moisture content, %

γ_{dry} : maximum dry density, t/m^3

G_s : specific gravity

CBR : California Bearing Ratio, %
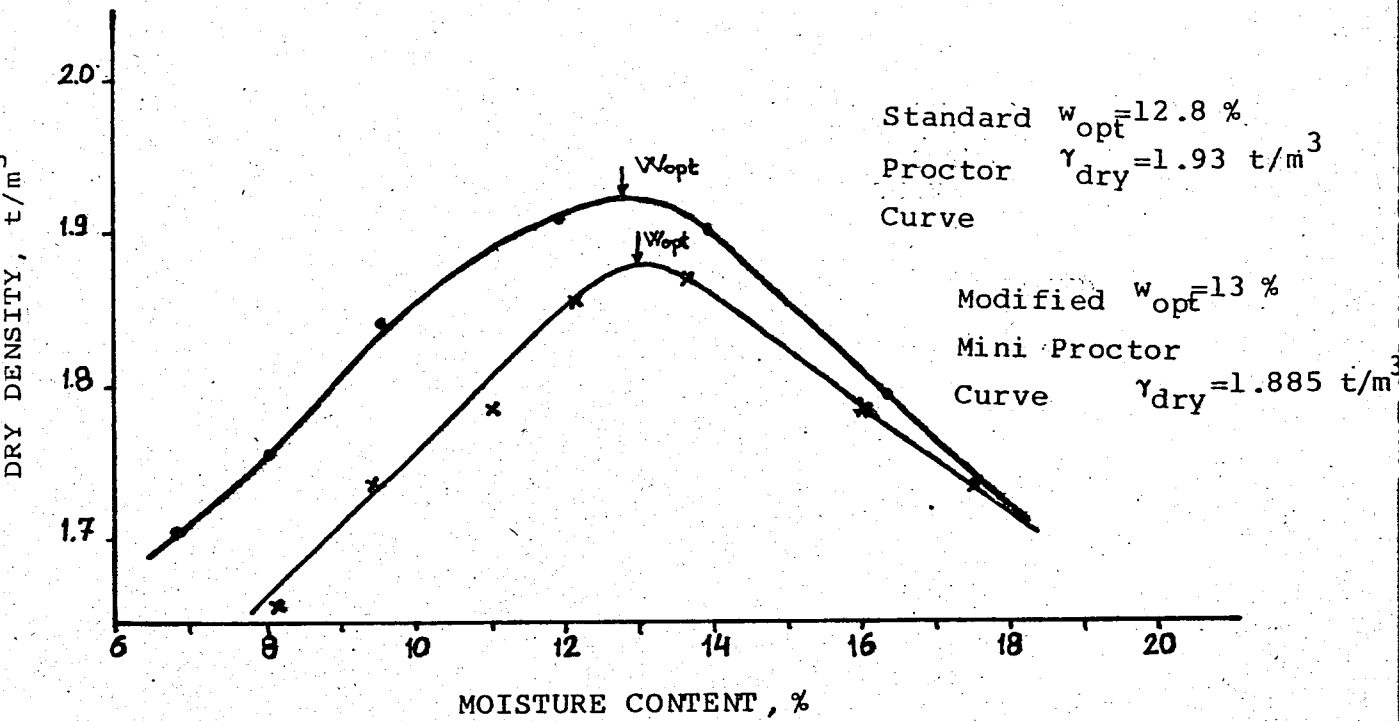
FIG 4.4 Dry Density versus Moisture Content for İçerenköy
Sample 1

$w_{opt}=22$ %

$\gamma_{dry}=1.630$ t/m3

Standard Proctor
curve

w_{opt}

Mini proctor
curve
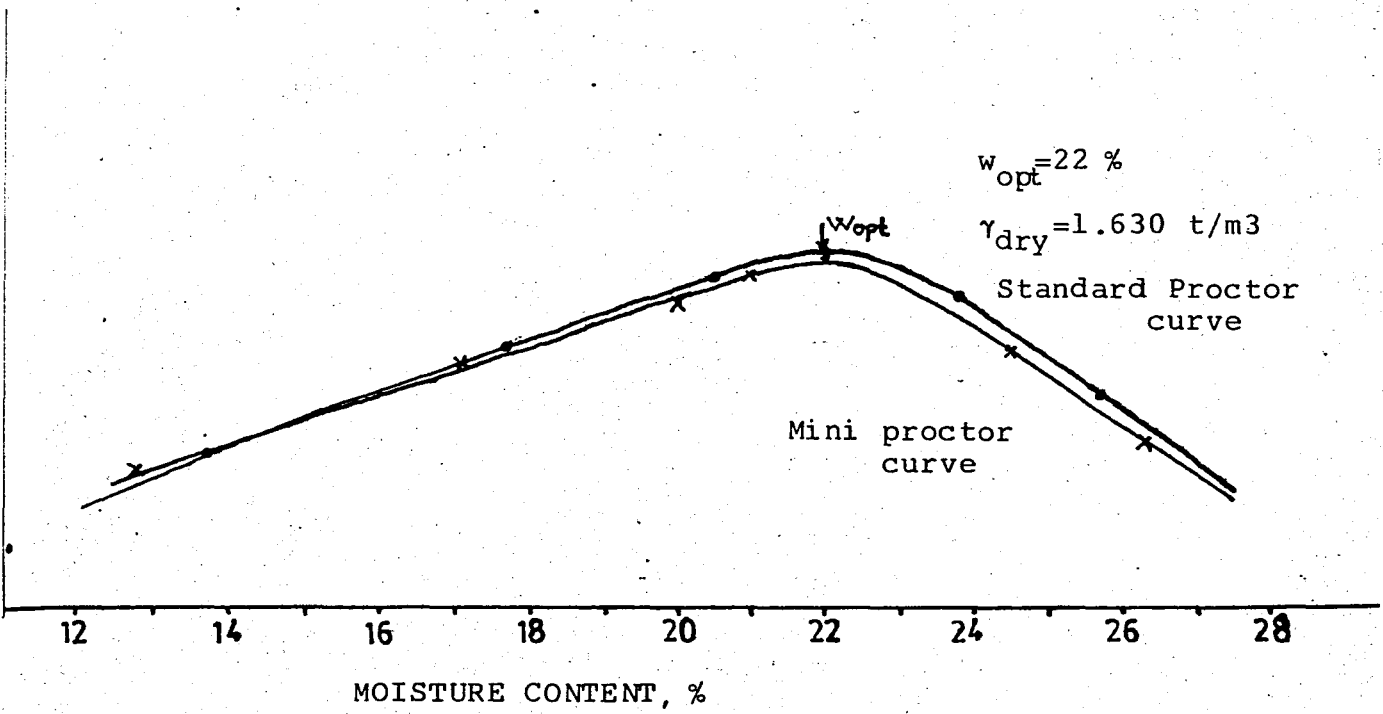
MOISTURE CONTENT, %

RY DENSITY VERSUS MOISTURE CONTENT FOR SAMPLE 2

CBR =25%

PENETRATION, IN
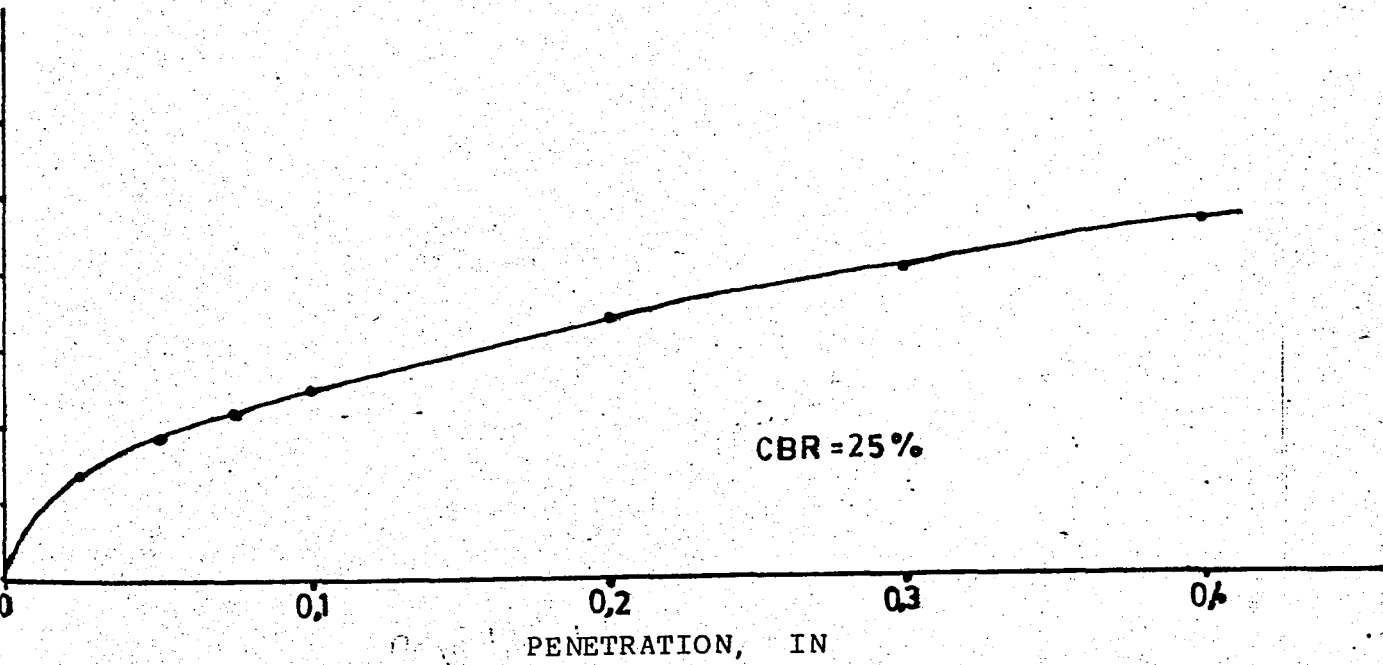
CBR CURVE OF SAMPLE 2

FIG 4.5   Compaction Curve for İçerenköy Sample 2

Standard $w_{opt}=13$ %
Proctor $\gamma_{dry}=1.89$ t/m^3
Curve

Modified
Mini Proctor $w_{opt}=13.3$ %
Curve

$\gamma_{dry}=1.845$ t/m^3
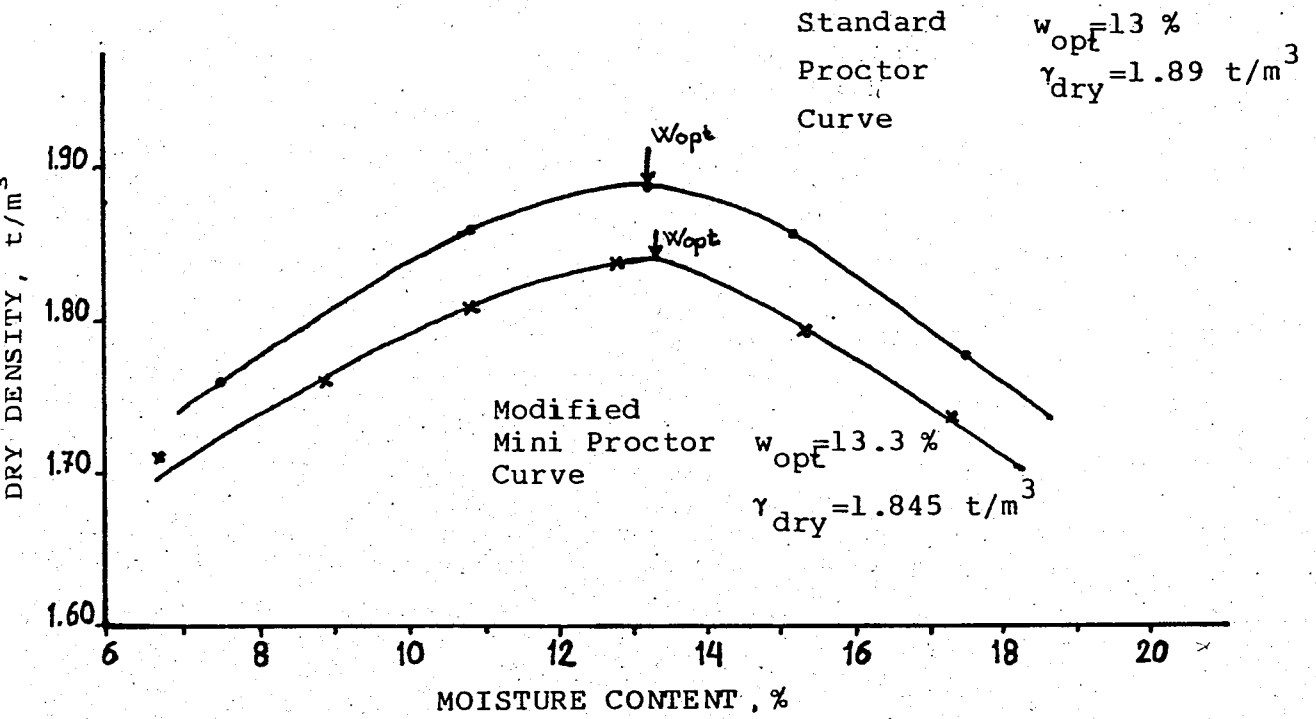
DRY DENSITY VERSUS MOISTURE CONTENT FOR SAMPLE 3

CBR = 31 %
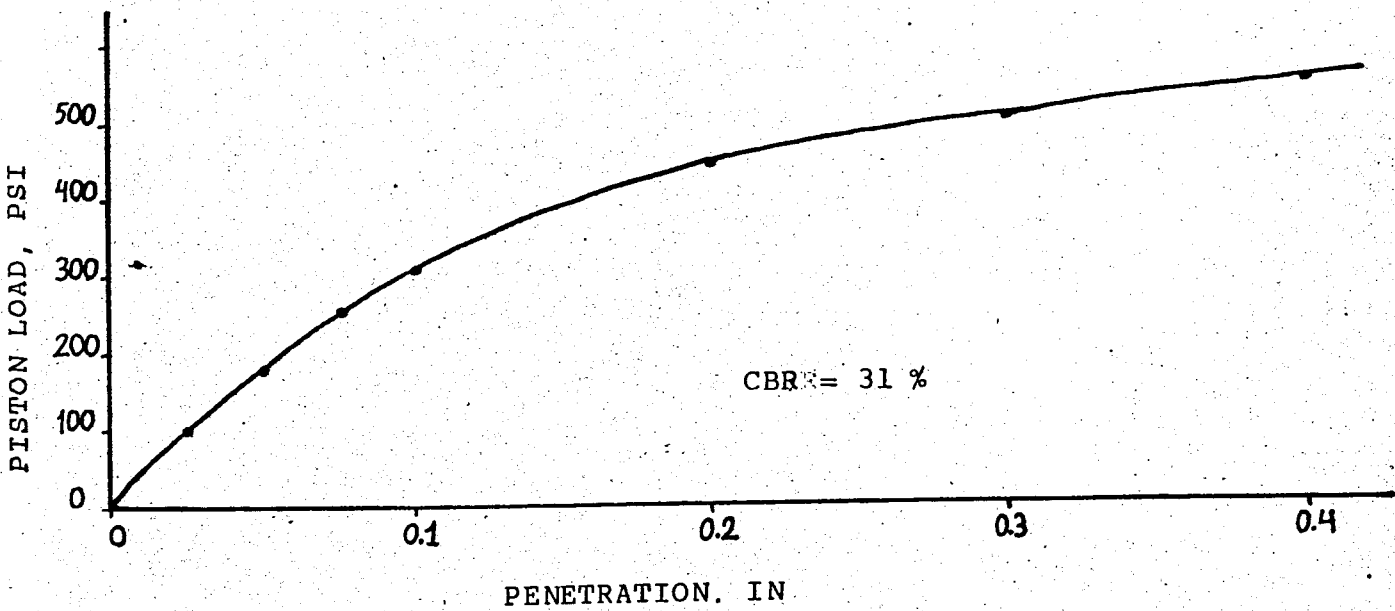
CBR CURVE OF SAMPLE 3

FIG 4.6 Compaction Curves for İçerenköy Sample 3
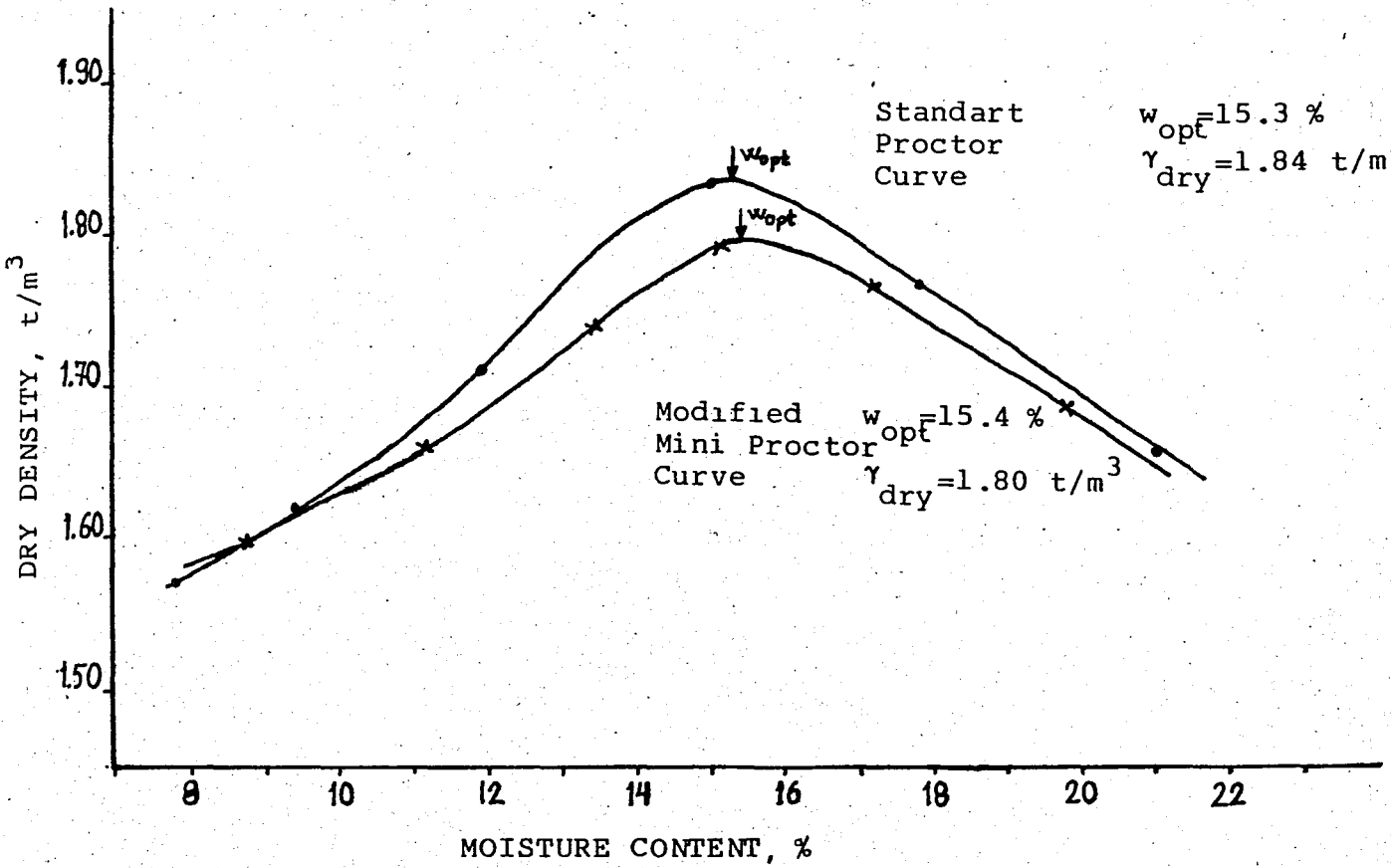
DRY DENSITY VERSUS MOISTURE CONTENT FOR SAMPLE 4
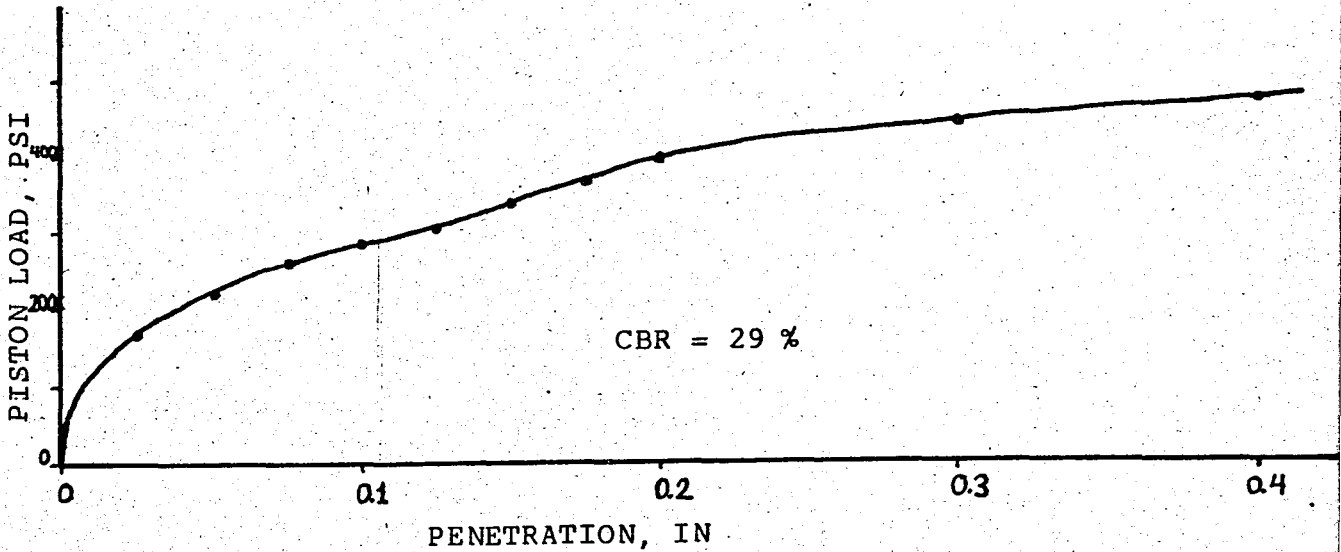
CBR CURVE OF SAMPLE 4

FIG 4.7 Compaction Curves for İçerenköy Sample 4
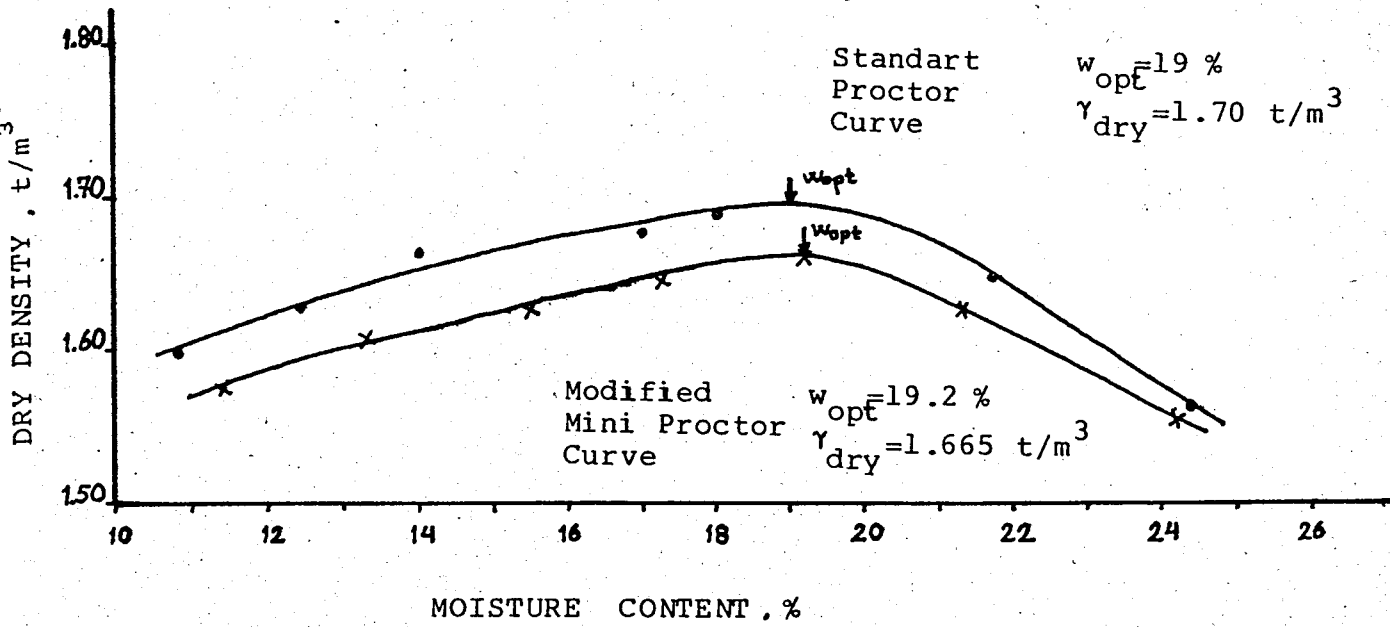
DRY DENSITY VERSUS MOISTURE CONTENT FOR UNIVERSITY SAMPLE
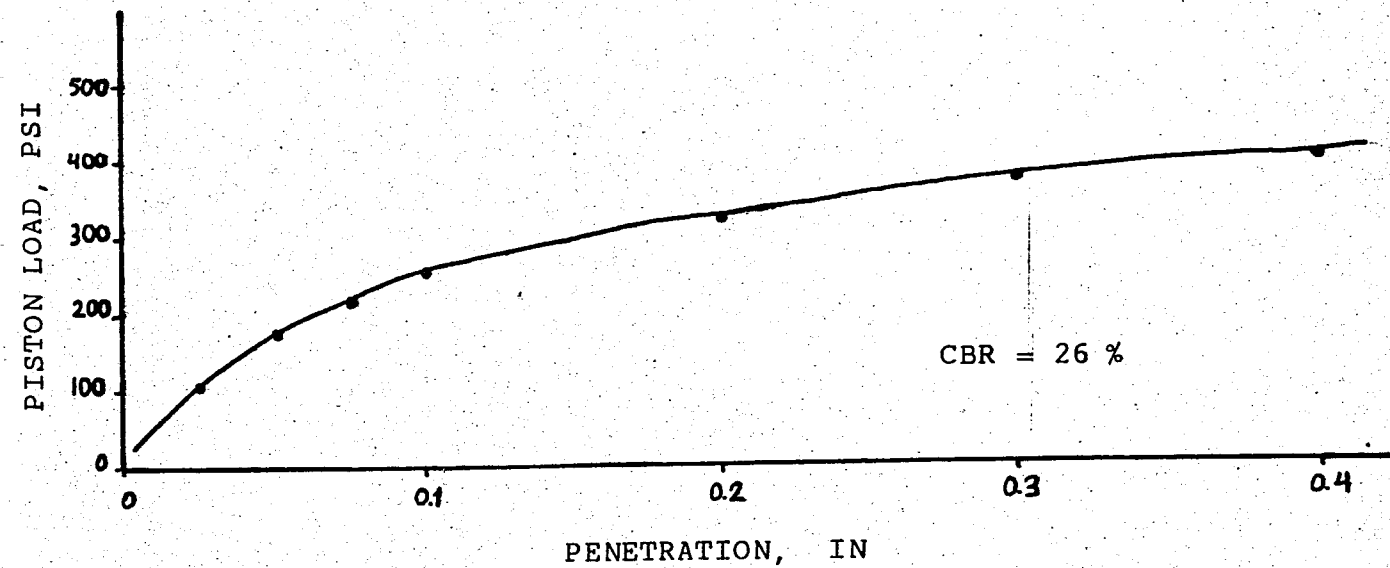
CBR CURVE OF SAMPLE 5

FIG 4.8 Compaction Curves for Boğaziçi University Sample

moisture content. Compaction test results are tabulated in Table 4.1 . Standard proctor, modified mini proctor and CBR curves are plotted as shown in Fig. s 4.4 through 4.8 .

4.5 SUMMARY AND CONCLUSIONS

In this chapter, techniques of test for dynamic soil properties are mentioned, Hardin type resonant column device and its equipment are summarized. The index and compaction properties of soils are analized. First, Standard proctor test is performed and Standard proctor curve is plotted, then, compaction test is performed by using modified mini proctor compactor for each sample. Both the standard proctor and modified mini proctor curves yield aproximately the same optimum water content and maximum dry density for each samples. Maximum difference between maximum dry densities is 2.4 percent.

CHAPTER 5 DETERMINATION OF SHEAR MODULUS BY USING
RESONANT COLUMN APPARATUS

5.1 INTRODUCTION

Previous studies show that the most important dynamic
soil property is shear modulus. According to Hardin, B.O.,
the stress-strain relation for a specimen of soil subjected
to the steady state vibration of the resonant column is a
hysteresis loop. Shear modulus corresponds to the slope of
a line through the end points of the hysteresis loop stress-
strain relation.

In this chapter, test set-up, testing procedure, and
computation of the shear modulus from the measured system
resonant friquency are explaind in the light of the Hardin's
studies. Effects of moisture change, strain amplitude, and
vertical stress, on shear modulus of compacted clays are
observed and plotted.

5.2 TEST SET - UP

The electronic components are interconnected according
to the wiring diagram which is shown in Fig. 5.1 .

Specimen is placed on the base cap, and the lower
half of the pneumatic cylinder support device is placed on
the triaxial chamber base, and pneumatic cylinders are connected
to the outlet in the base. An air pressure is applied to the
pneumatic cylinders to extend the pistons approxmately 1/2 in
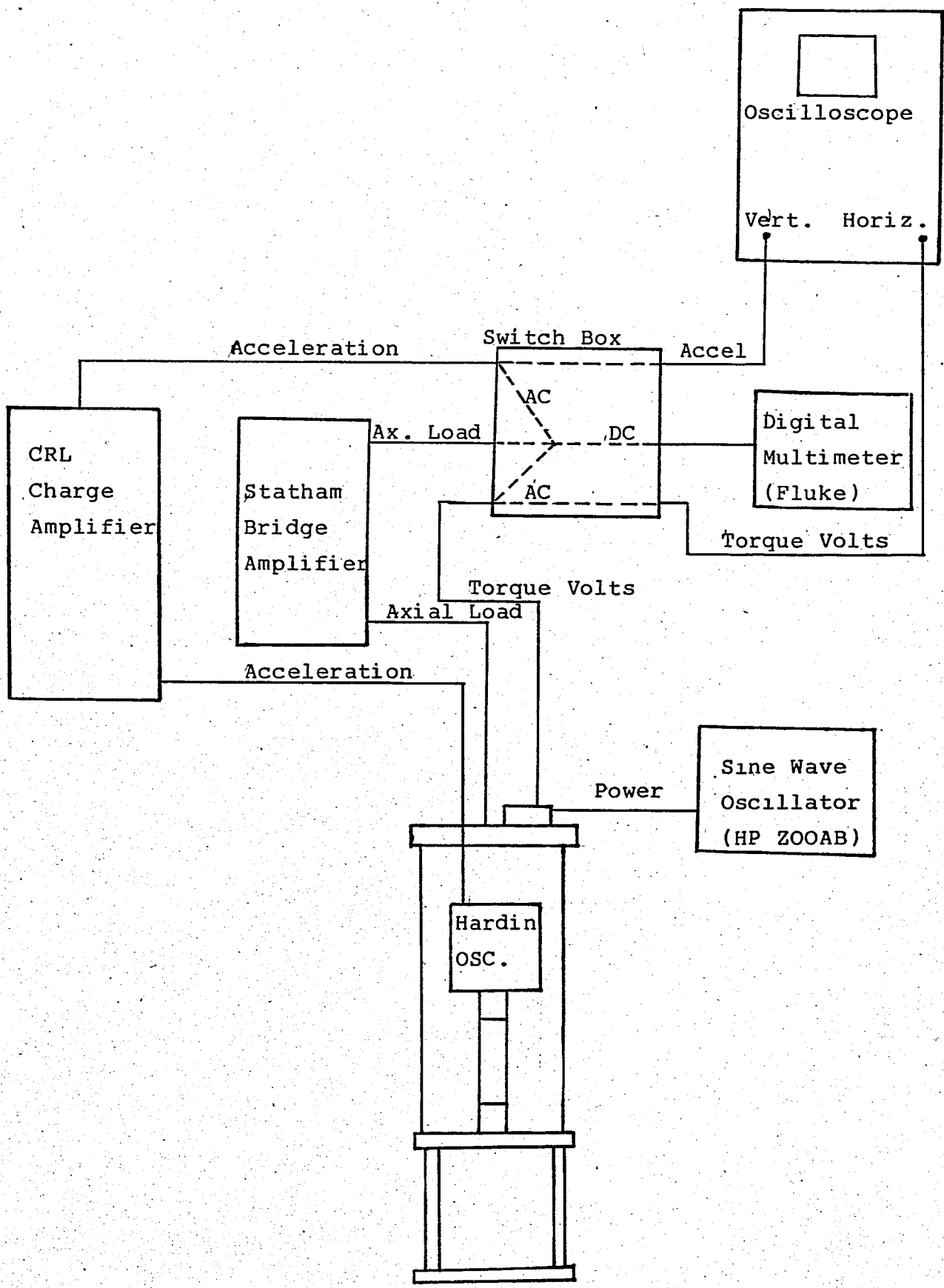
FIG. 5.1. Hardin Oscillator Wiring Diagram

as illustrated in Fig. 5.2 . Top ring plate with the brass
adjusting nuts extended are placed to the top of the pistons.
The vibration excitation device is placed on the pneumatic
cylinder support, and lowered on the specimen with the brass
adjusting nuts, thus the vibration excitation device is attached
to the top of the specimen with the top cap shown in Fig. 5.3 .
The air pressure to the pneumatic cylinders should be great
enough to keep the pistons extended as the weight of the
vibration excitation device is applied. After Hardin Oscillator
is placed, the plastic triaxtial champer is placed over the
Hardin Oscillator to rest on the base. The triaxial chamber
piston is inserted in to the vibration excitation device.
And, holding the top plate of the triaxial chamber above the
plastic cylinder, the power, accelerometer and load cell
cables are plugged in. With the electrical cables connected,
the top plate is carefully lowered onto the piston to rest
on the plastic cylinder. The plugs and cables should not
put a downward force on the vibration excitation device.
Then tie rods are inserted and tightened. After that, the
counter balence device is fastened in place, and enough weights
are applied to balence the weight of the Hardin Oscillator,
and the air pressure is removed to the pneumatic cylinders.
And then connect the sine wave generator, that produces
power, to the power socket of Hardin Oscillator. Now the
set-up is completed. The general view of tha "Hardin" resonant
column apparatus and its equipments are shown in Fig 5.4 ..
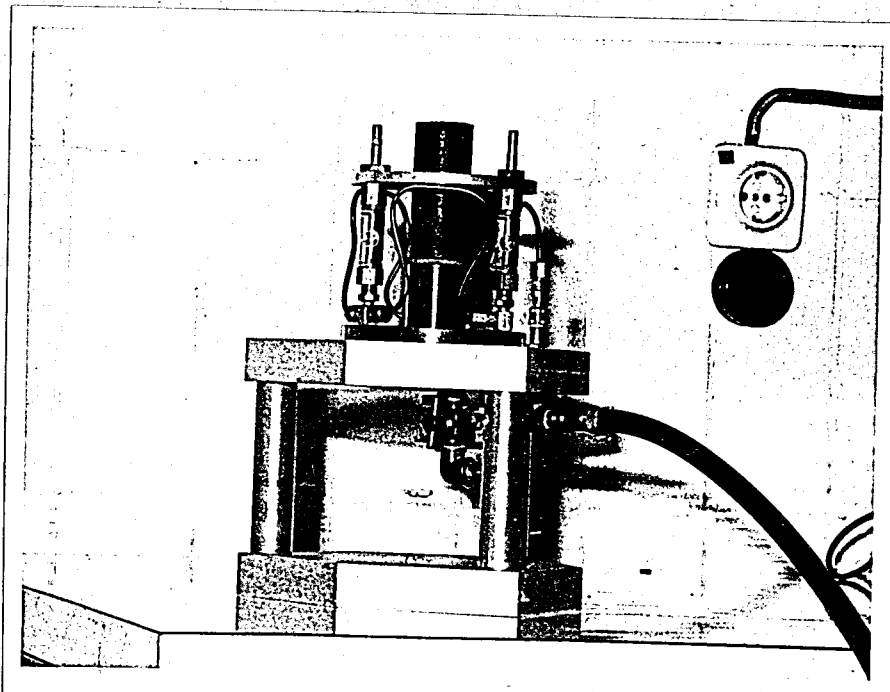
Fig 5.2   A View During Set-up
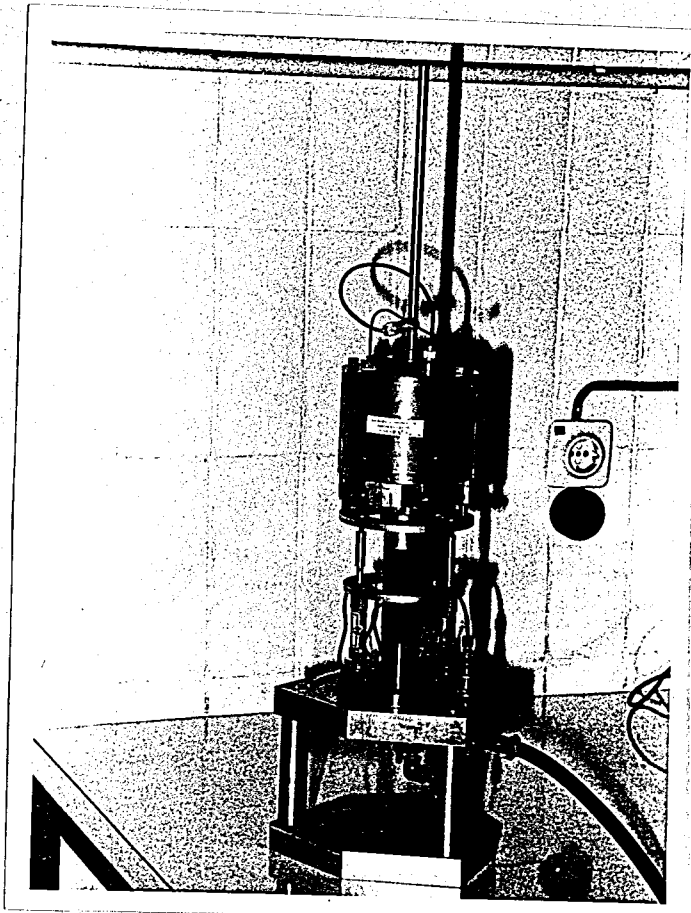
Fig   5.3   The Set-up of Hardin Oscillator
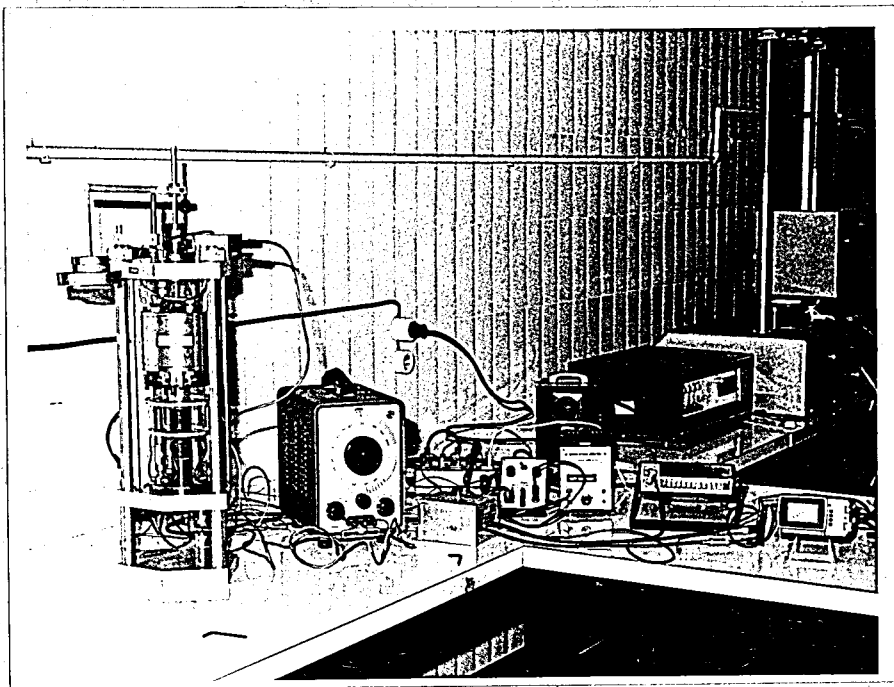
Fig 5.4 The General View of the 'Hardin' Resonant
          Column Apparatus and its Equipment

5.3 DESCRIPTION OF TESTING PROCEDURE

In this study, the readout instrument used is oscilloscope on which the wave form can be obserwed. Oscillascope time swich is held on x-y position. The power applied to the Hardin Oscillator is to be as low as is practical to have low strain amplitude. At the beginning the frequency should be on about 20 H_z.

Now the frequency of excitation is changed until the resonant condition exists. To have this condition, the figure traced on the screen is controlled. The horizontal component of this figure shows the forcing torque applied to the system, and the vertical component of this figure is the output of the vibration measuring device (accelerometer), and the figure traced on the screen is a measure of the phase between the two voltages. To have 90° phase difference the frequency is adjusted until a vertical axis ellipse, or a circle (if the voltage sensitivites are adjusted) shown in Fig. 5.5 , is obtained. And the value of frequency is recorded as resonant frequency

5.4 CALCULATIONS

For determining shear modulus and damping following calculations have to be done.

1. Tha mass density of the specimen is calculated;

$$\rho = \frac{4W}{\pi d^2 lg} = \frac{W}{Vg} \qquad (5.1)$$
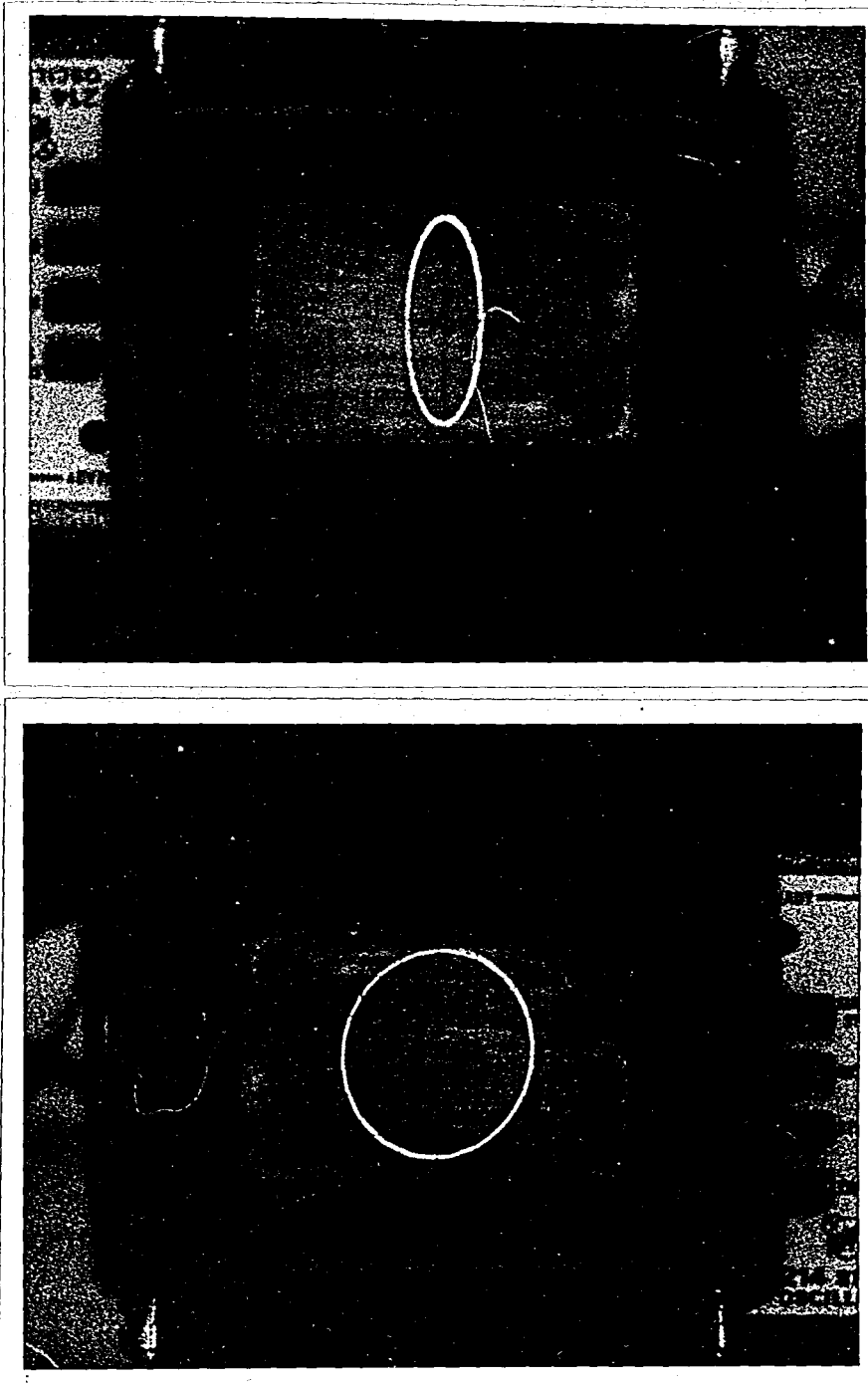
Fig 5.5   Figures Traced on the Screen When the System
           Vibrating at the System Resonant Frequency

where ;

l = length of specimen

d = diameter of specimen

V = volume of specimen

W = total weight of specimen, and

g = acceleration due to gravity

2. The inertia of the specimen about its axis, J,

$$J = \frac{\pi \rho \, d^4 \, l}{32} \qquad (5.2)$$

3. The system factor, T, is calculated

$$T = \frac{J_o}{J} \left[1 - \left(\frac{fapp}{f}\right)^2 \right] \qquad (5.3)$$

where ;

f_o = fapp = apparatus resonant frequency

J_o = apparatus inertia

K_o = apparatus spring constant

f_o , J_o , K_o , are given by apparatus menual

f = system resonant frequency

4. Using the given chart shown in Fig. 5.6, the dimensionless frequency, F, is determined as the abscissa corresponding to the value of T as ordinate.

5. And, the shear modulus, G, can be determined in gr/cm^2

$$G = 4 \pi^2 \rho \left(\frac{fl}{F}\right)^2 \qquad (5.4)$$
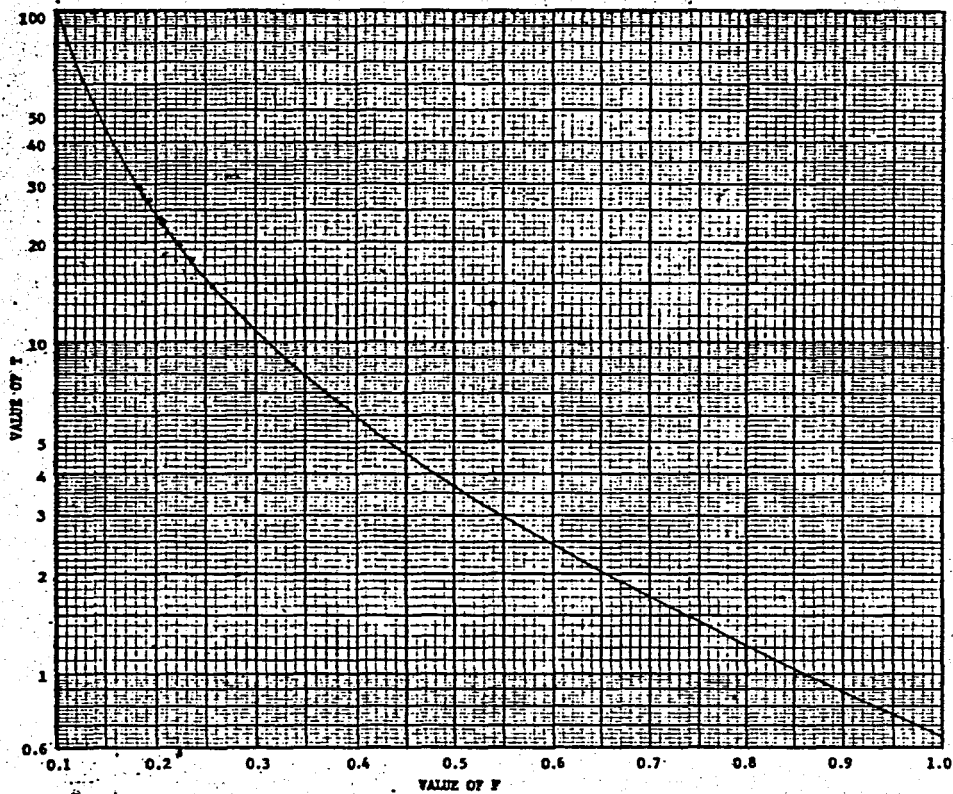
Fig 5.6   System Factor versus F

(After Hardin 1965)

5.5 TEST RESULTS

The results of the calculations are tabulated for each type of soils in different water contents as shown in Tables 5.1 through 5.9 .

In this study, tests were performed under a constant vertical stress of 0.144 kg/cm^2 applied by changing the counter balance load. Specimens have no ambient pressure, so test were performed under unconfined conditions. The lack of confining pressure causes lower values of shear modulus. As it was discussed in chapter 3, the shear modulus increases with increasing confining pressure.

5.5.1 Effects of Moisture Change on Shear Modulus

The change of shear modulus with the moisture content is investigated for compacted samples. The plots of shear modulus versus moisture content are shown in Fig's. 5.7 through 5.11 . As shown in figures, on the dry side of optimum moisture content shear modulus approximately remains close to its maximum value. Shear modulus reaches to its maximum value slightly less than optimum moisture content. Beyond the optimum moisture content, shear modulus drops sharply. This change is due to the structure of compacted clay. On the dry side of optimum moisture content compacted clays have higher shearing resistance, hence, the value of shear modulus is higher. On the wet side of optimum moisture content, the structure is more dispersed, therefore, has lower shearing

TABLE 5.1 Results for İçerenköy Sample 1

w %	W	l	d	ρ	J	T	F	f	G KN/m^2	Strain amp.
10	152.5	8	3.57	0.00194	0.247	25.2	0.195	64	5.28×10^4	1.2×10^{-5}
11.7	159.4	8	3.57	0.00203	0.259	24.0	0.20	63	5.1×10^4	9×10^{-6}
12.9	163.0	8	3.57	0.00208	0.265	23.5	0.202	64	5.28×10^4	7×10^{-6}
13.5	166.0	8	3.57	0.00212	0.270	22.7	0.206	62	4.85×10^4	7.2×10^{-6}
16.0	169.5	8	3.57	0.00215	0.274	21.0	0.215	57	3.82×10^4	6×10^{-6}
17.0	168.0	8	3.57	0.00214	0.273	17.5	0.235	47.5	2.21×10^4	6.2×10^{-6}

w : water conten, %

W : weight of specimen, gr

l : length of specimen, cm

d : diameter of specimen, cm

ρ : mass densitiy, gr-sec^2/cm^4

J : the inertia of the specimen about its axes, gr-cm-sec^2

T : system factor

F : dimension less frequency system

f : resonant frequency, H_z

G : shear modulus, KN/m^2

TABLE 5.2 Results for İçerenköy Sample 2

w, %	W	l	d	ρ	J	T	F	f	$\dfrac{G}{KN/m^2}$	strain amp.
17.0	136.0	8	3.57	0.00173	0.221	29.0	0.185	67	5.73×10^4	7.2×10^{-6}
19.3	153.9	8	3.57	0.00196	0.250	26.0	0.192	69	6.40×10^4	9×10^{-6}
21.1	153.2	8	3.57	0.00195	0.249	26.6	0.190	72	7.08×10^4	8×10^{-6}
22.6	159.5	8	3.57	0.00203	0.259	25.2	0.195	70	6.51×10^4	8.3×10^{-6}
24.6	157.0	8	3.57	0.00200	0.255	23.5	0.202	60	4.46×10^4	1.1×10^{-5}
26.6	154.2	8	3.57	0.00196	0.250	22.4	0.208	55	3.46×10^4	1.04×10^{-5}

TABLE 5.3 Results for İçerenköy Sample 3

w ,%	W	l	d	ρ	J	T	F	f	KN/m^2 G	strain amp.
8.8	157.8	8	3.57	0.00201	0.256	24.2	0.200	63.5	5.12×10^4	7×10^{-6}
11.2	159.1	8	3.57	0.00203	0.259	23.4	0.203	61.0	4.63×10^4	7×10^{-6}
12.8	164.2	8	3.57	0.00209	0.267	23.3	0.203	64.0	5.25×10^4	9.9×10^{-6}
13.45	163.7	8	3.57	0.00208	0.265	23.0	0.205	62.0	4.81×10^4	8.5×10^{-6}
14.4	165.5	8	3.57	0.00211	0.269	23.0	0.205	63.2	4.61×10^4	7.6×10^{-6}
16.9	163.5	8	3.57	0.00208	0.265	20.0	0.220	52.0	2.94×10^4	9×10^{-6}
18.7	162.0	8	3.57	0.00206	0.263	16.4	0.240	44.5	1.80×10^4	1×10^{-5}

TABLE 5.4 Results for İçerenköy Sample 4

w, %	W	l	d	ρ	J	T	F	f	G KN/m^2	strain amplitude
12.4	147.0	8	3.57	0.00187	0.239	29.0	0.182	80	9.13×10^4	7.2×10^{-6}
14.4	157.0	8	3.57	0.00200	0.255	27.5	0.188	85	10.33×10^4	7×10^{-6}
15.2	160.0	8	3.57	0.00204	0.260	27.0	0.190	86	10.56×10^4	7.5×10^{-6}
16.3	168.5	8	3.57	0.00215	0.274	25.0	0.196	82	9.51×10^4	8×10^{-6}
18.2	167.4	8	3.57	0.00212	0.272	24.0	0.190	71	7.52×10^4	9.2×10^{-6}
19.5	164.2	8	3.57	0.00208	0.267	22.4	0.205	60	4.52×10^4	7×10^{-6}

TABLE 5.5   Results for B.U Sample

w , %	W	l	d	ρ	J	T	F	f	KN/m^2 G	strain amp.
13.3	144.0	8	3.57	0.00184	0.235	26	0.192	62.-	4.85×10^4	1.4×10^{-5}
15.4	143.3	7.9	3.57	0.00185	0.233	27	0.190	64.-	5.17×10^4	1.2×10^{-5}
16.3	149.2	8	3.57	0.00190	0.242	26	0.194	66.-	5.56×10^4	1.3×10^{-5}
19.7	152.6	8.1	3.57	0.00192	0.248	25	0.196	64.-	5.30×10^4	1.2×10^{-5}
23.0	155.2	8.1	3.57	0.00195	0.252	22	0.210	54.-	3.34×10^4	1.2×10^{-5}

TABLE 5.6 Results for İçerenköy Sample 1

w,%	W	l	d	ρ	J	T	F	f	G (KN/m^2)	strain amp.
10.0	152.5	8	3.57	0.00194	0.247	17.5	0.235	43.7	1.70×10^4	1.4×10^{-4}
11.7	159.4	8	3.57	0.00203	0.259	15.5	0.250	43.8	1.50×10^4	1.69×10^{-4}
12.9	163.0	8	3.57	0.00208	0.265	15.5	0.250	43.0	1.52×10^4	1.49×10^{-4}
13.5	166.0	8	3.57	0.00212	0.270	14.6	0.258	42.5	1.45×10^4	1.7×10^{-4}
16.0	169.5	8	3.57	0.00215	0.274	12.6	0.275	40.0	1.15×10^4	1.9×10^{-4}
17.0	168.0	8	3.57	0.00213	0.273	8.9	0.328	36.2	0.66×10^4	2×10^{-4}

TABLE 5.7 Results for İçerenköy Sample 2

w,%	W	l	d	ρ	J	T	F	f	G KN/m^2	strain amp.
17.0	136.0	8	3.57	0.00173	0.221	25	0.195	54	3.35×10^4	1.06×10^{-4}
19.3	153.9	8	3.57	0.00196	0.250	22	0.210	54	3.27×10^4	1.01×10^{-4}
21.1	153.2	8	3.57	0.00195	0.249	23	0.205	58	3.94×10^4	1.1×10^{-4}
22.6	159.5	8	3.57	0.00203	0.259	22	0.210	57	3.78×10^4	1.13×10^{-4}
24.6	157.0	8	3.57	0.00200	0.255	21	0.215	52	2.96×10^4	1.13×10^{-4}
26.6	154.2	8	3.57	0.00196	0.250	20	0.220	49	2.46×10^4	1.4×10^{-4}

TABLE 5.8   Results for İçerenköy Sample 3

w,%	W	l	d	ρ	J	T	F	f	G KN/m^2	strain amp.
8.8	157.8	8	3.57	0.00201	0.256	19	0.225	48.0	2.31×10^4	1.08×10^{-4}
11.2	159.1	8	3.57	0.00203	0.259	19	0.225	48.5	2.38×10^4	1.2×10^{-4}
12.8	164.2	8	3.57	0.00209	0.267	18	0.230	47.5	2.25×10^4	1.06×10^{-4}
13.45	163.7	8	3.57	0.00208	0.265	19	0.225	49.5	2.54×10^4	1.16×10^{-4}
14.4	165.5	8	3.57	0.00211	0.269	17	0.238	46.5	2.04×10^4	1.12×10^{-4}
16.9	163.5	8	3.57	0.00206	0.263	16	0.245	44.0	1.70×10^4	1.15×10^{-4}

TABLE 5.9   Results for İçerenköy Sample 4

w, %	W	l	d	ρ	J	T	F	$\dot{\epsilon}$	$\dfrac{KN/m^2}{G}$	strain ampl.
12.4	147.0	8	3.57	0.00187	0.239	21.0	0.215	49.0	2.45×10^4	$1.9 \times 10^{\bar{2}}$
14.4	157.0	8	3.57	–	–	–	–	–	–	–
15.2	160.0	8	3.57	0.00204	0.260	19.6	0.222	50.0	2.62×10^4	$2 \times 10^{\bar{4}}$
16.3	168.5	8	3.57	0.00215	0.274	18.0	0.230	49.1	2.48×10^4	$1.9 \times 10^{\bar{4}}$
18.2	167.4	8	3.57	0.00212	0.272	17.0	0.240	46.9	2.05×10^4	$2.2 \times 10^{\bar{4}}$
19.5	164.2	8	3.57	0.00208	0.267	13.7	0.265	41.0	1.26×10^4	$2.3 \times 10^{\bar{2}}$

resistance, hence, yields lower values of shear modulus. General shape of shear modulus varsus moisture content curves are similar but the rates of change are different for each type of soil sample.

Narmalized shear modulus is plotted against moisture content shown in Fig's 5.7 through 5.11 The shear modulus obtained at a moisture content of 17 % is approximately around 80 % of maximum shear modulus for sample number 2 as seen in Fig. 5.8. The shear modulus reaches to its maximum value just below the optimum moisture content. For sample 2 optimum moisture content is 22 %, and maximum shear modulus is attained at a moistrure content of 21.4 %. Beyond this point the shear modulus decreases sharply. At a moisture content of 26.5 % the shear modulus drops to 50 % of its maximum value for sample 2. For sample 4 in Fig. 5.10 similar behavior is observed at different moisture contents. On the dry side of optimum moisture content shear modulus remain aproximately constant for samples 1 and 3.

5.5.2 Effect of Strain Amplitude on Shear Modulus

The variation of shear modulus with shear strain amplitude are plotted and presented in Fig's 5.12 through 5.15. Tests are performed only for samples compacted at optimum moisture content. Vertical stress applied during test is 0.54 kg/cm^2. Shear modulus versus strain amplitude curves imply that; under small shear strain amplitudes shear modulus has very high values, but as shear strain amplitude increases, shear modulus diminishes.

FIG 5.7 Variation of Shear Modulus and Normalized
Shear Modulus with Moisture Content for
İçerenköy Sample 1

İçerenköy Sample No 2
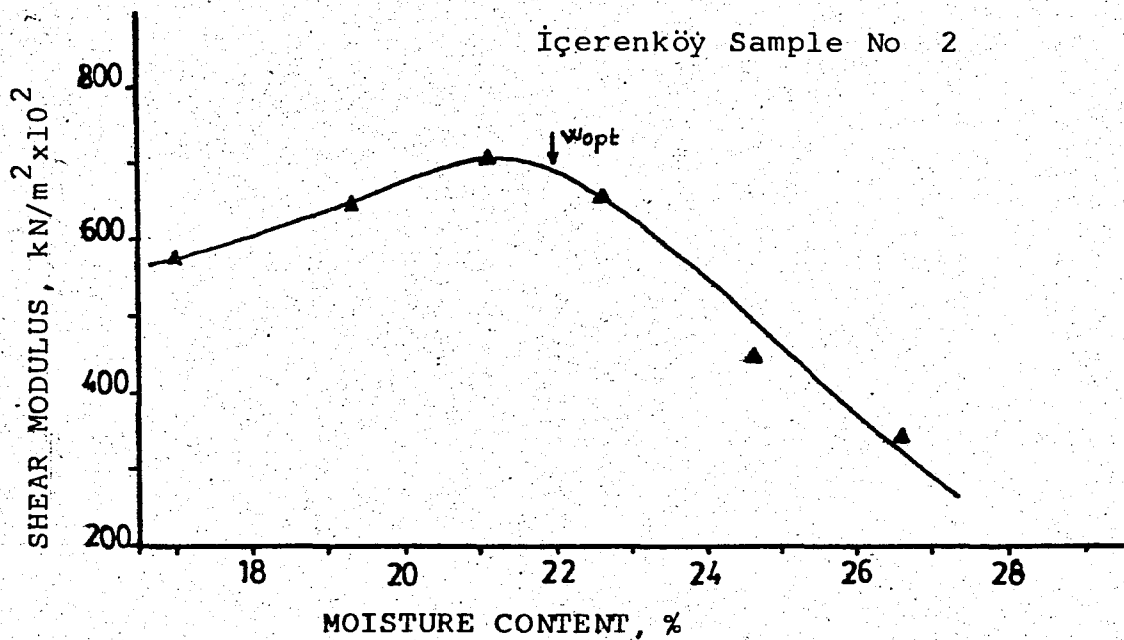
FIG 5.8   Variation of Shear Modulus and Normalized
           Shear Modulus with Moisture Content for
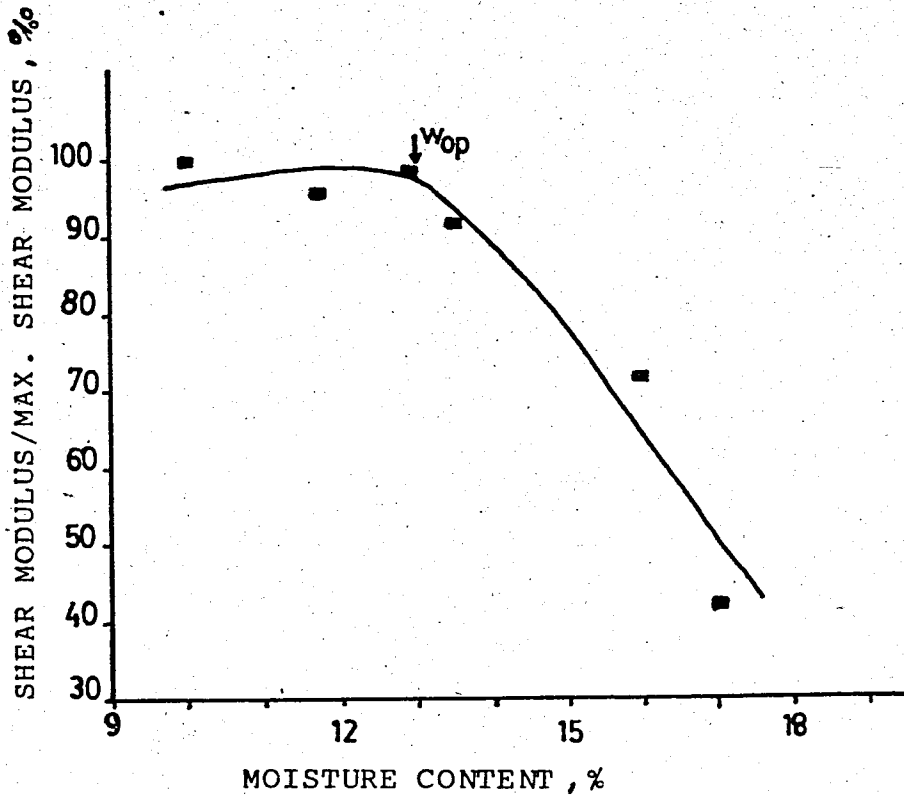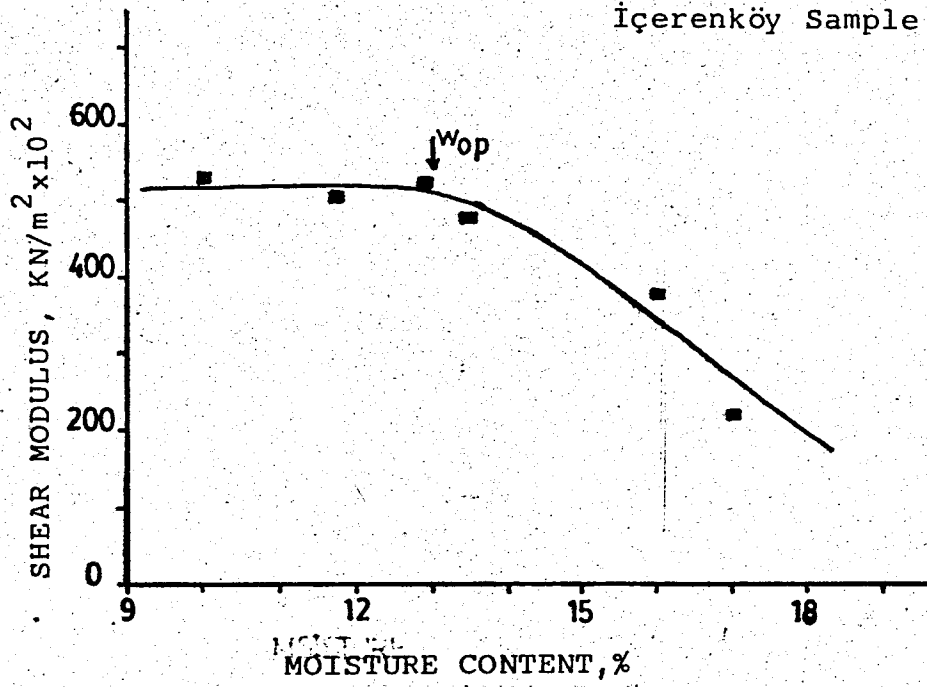   İçerenköy Sample 2
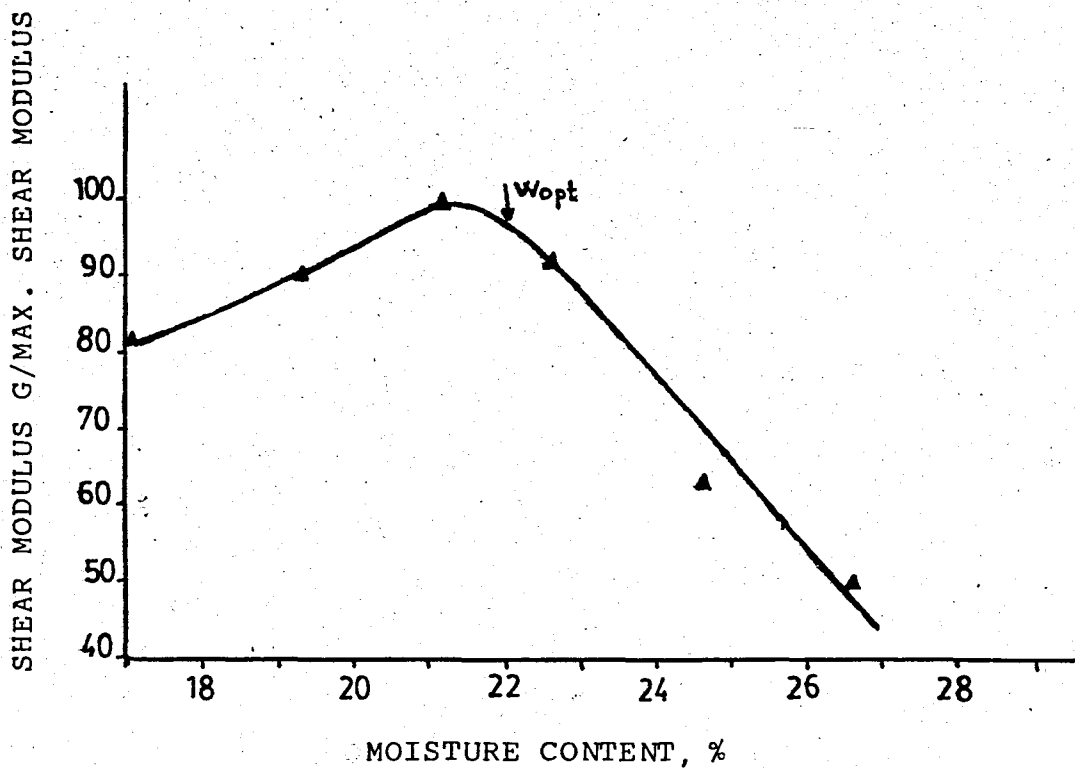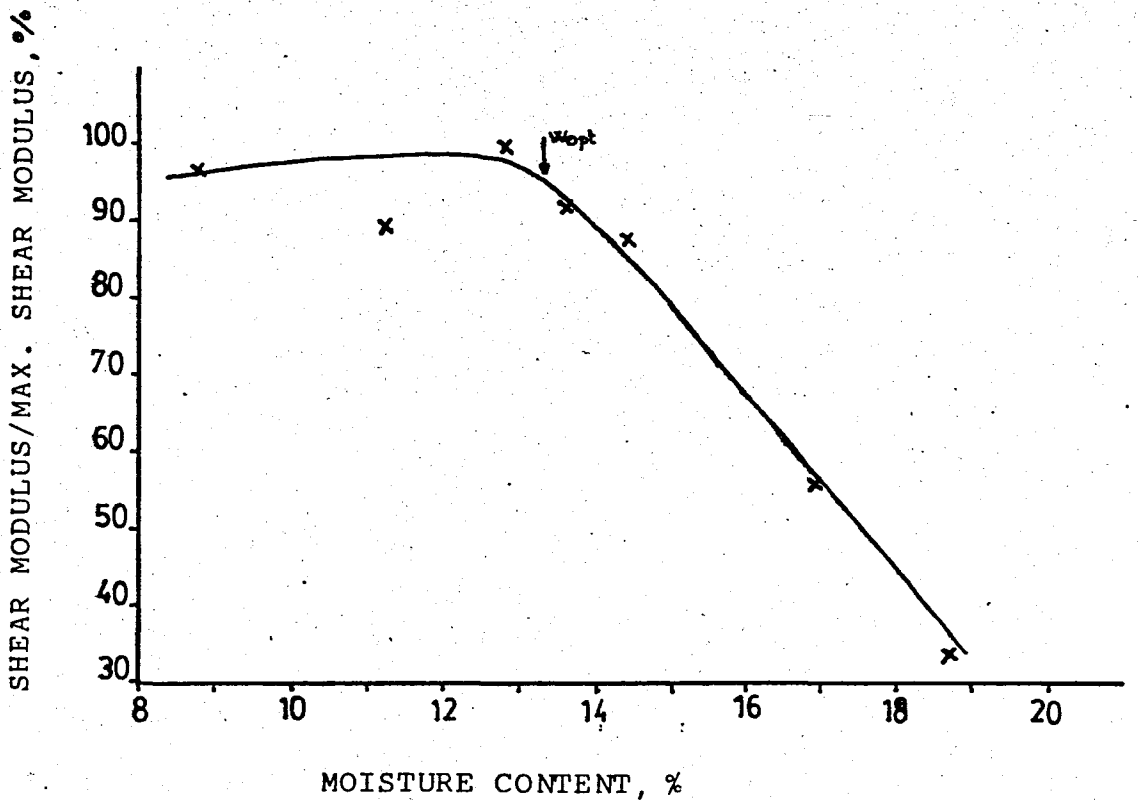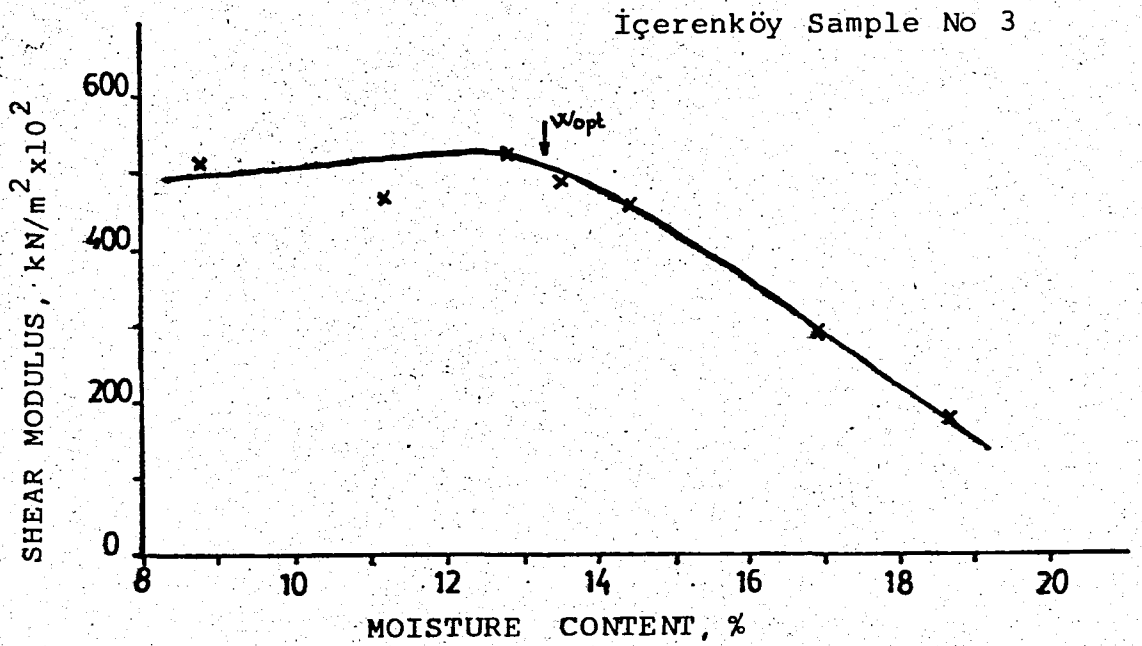
FIG 5.9 Variation of Shear Modulus and Normalized
Shear Modulus with Moisture Content for
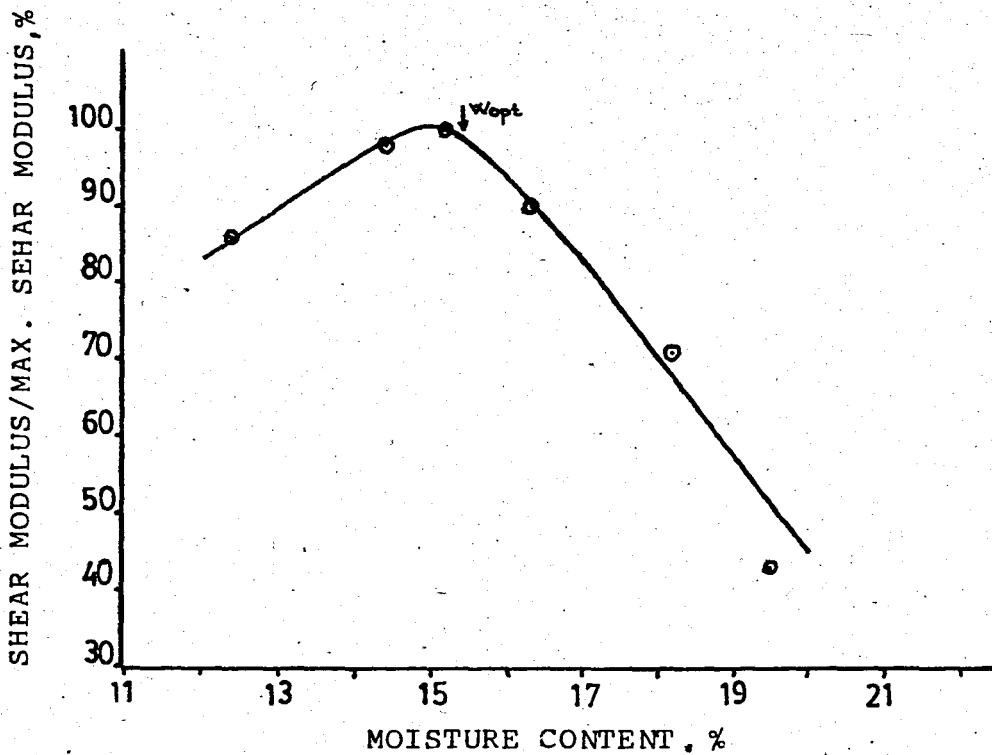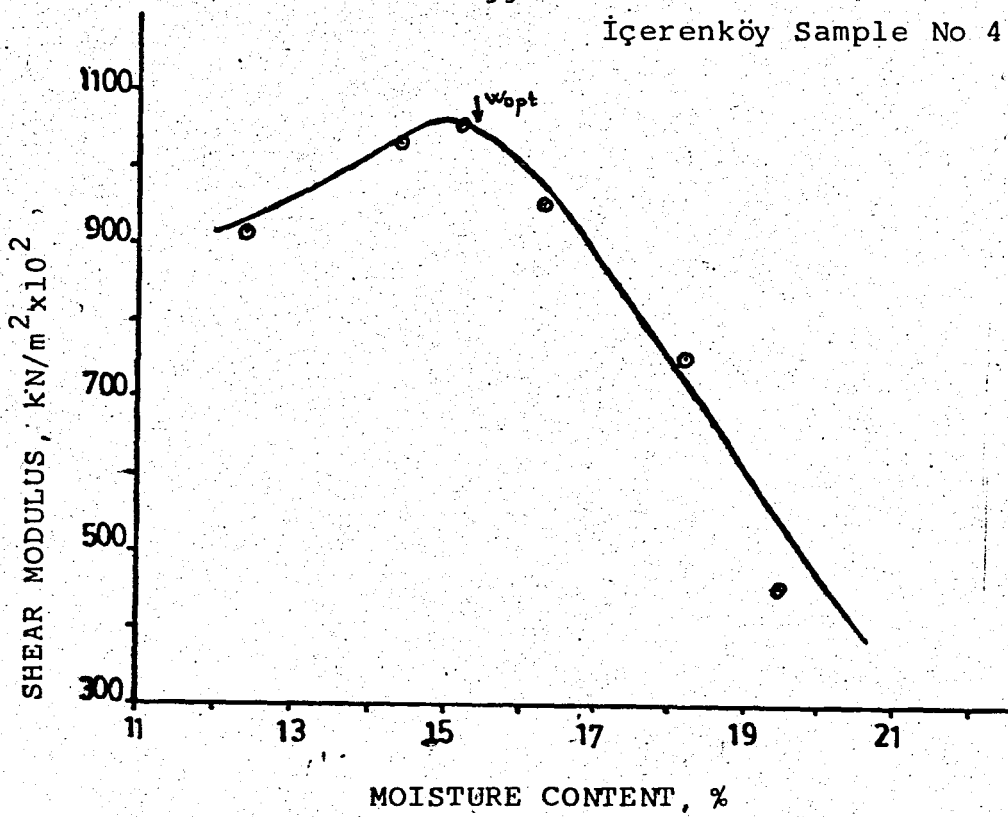İçerenköy Sample 3

İçerenköy Sample No 4

FIG 5.10 Variation of Shear Modulus and Normalized Shear Modulus with Moisture Content for İçerenköy Sample 4
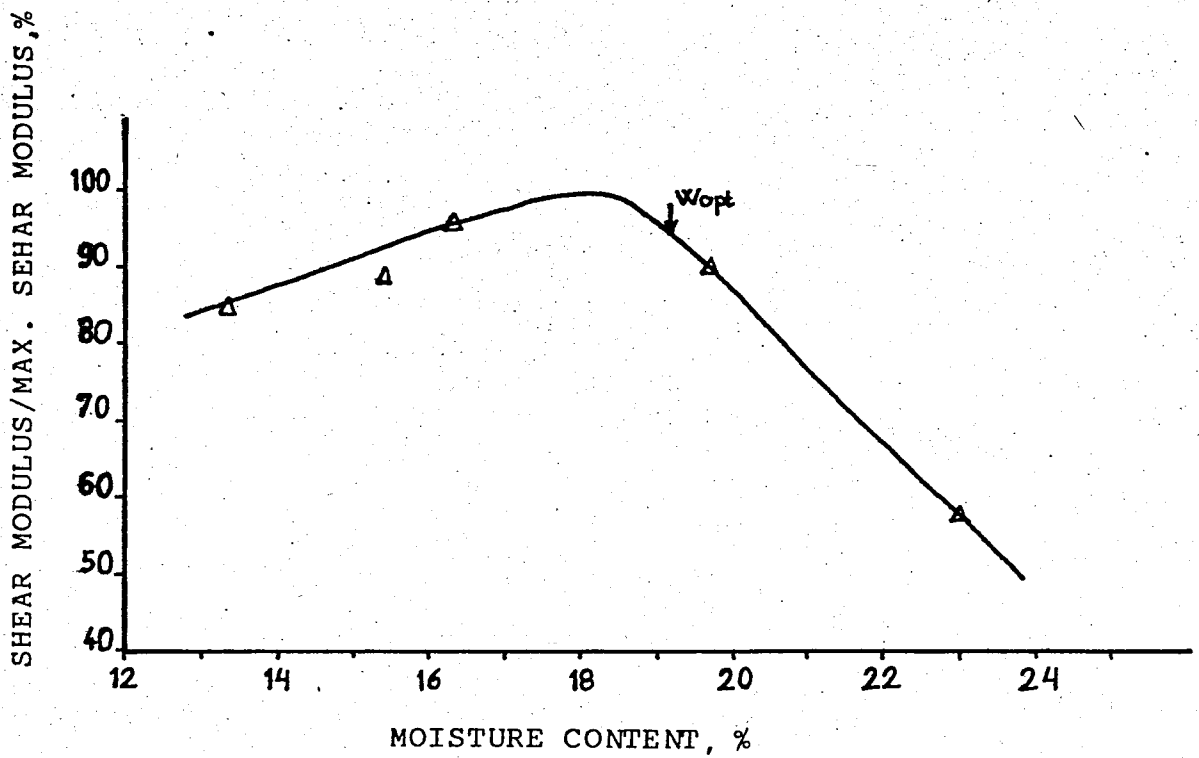
Boğaziçi University Sample
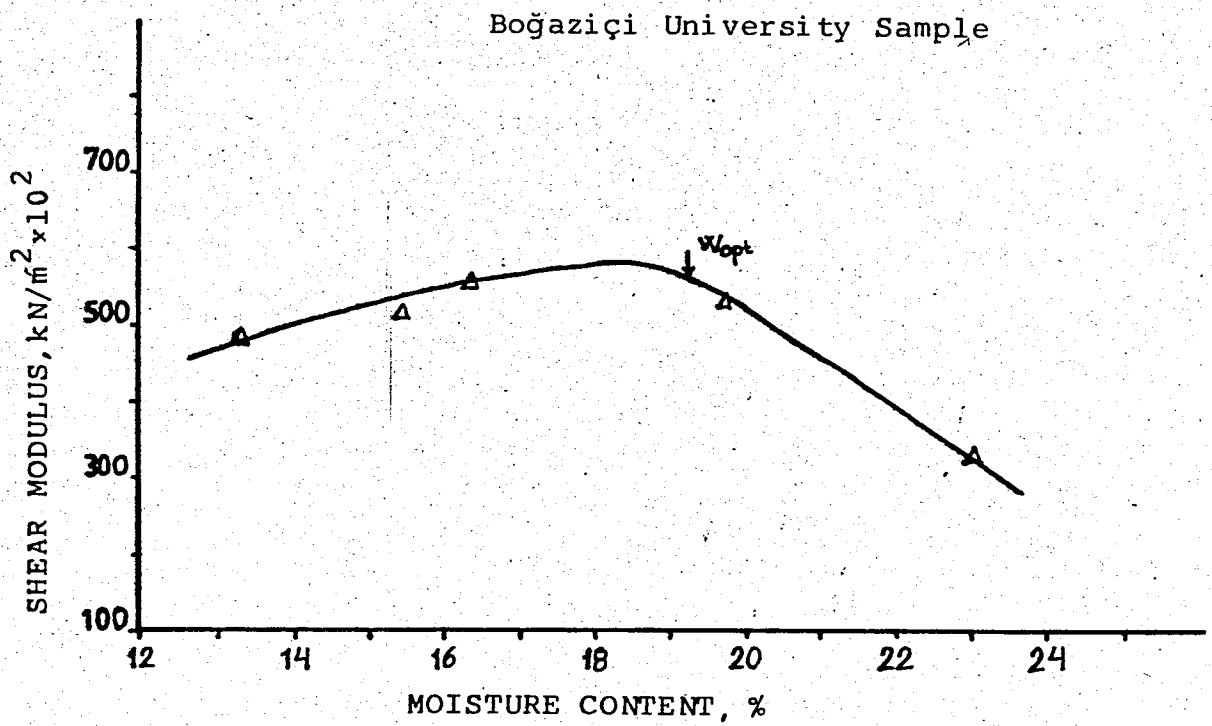
FIG 5.11. Variation of Shear Modulus and Normalized
Shear Modulus with Moisture Content for
Boğaziçi University sample

To illustrate the percent variation of shear modulus, normalized shear modulus versus shear strain amplitude is presented in Fig'.s 5.16 through 5.19 . For sample 1 and 2 up to the strain amplitude 10^{-5} the shear moduli decrease 6% of their maximum value. In the same interval, sample 4 decrease 8% of its maximum shear modulus. Further increase in shear strain amplitude cause to decrease shear modulus rapidly. For samples 1 an 4; when shear strain amplitude reaches to 10^{-4} shear modulus drops to 50% of its maximum value. See Fig's 5.16 and 5.19 . For samples 2 and 3, as shear strain amplitude increase to 10^{-4}, shear modulus decreases to 70% of the maximum values. Shown in Fig's 5.13 and 5.14 . Beyond shear strain amplitude, 10^{-4}, for all samples shear moduli diminish monotonously.

5.5.3 Effect of Vertical Stress on Shear Modulus

One of the important parameters which influence shear modulus is vertical stress. The variation of shear modulus with increasing vertical stress is plotted in Fig's 5.20 through 5.23 . Samples are compacted at their optimum moisture content. For all samples it is observed that shear modulus increases with increasing vertical load. The shape of curves are similar but the rates of change are different.

5.5.4 Comparison of Results

In order to enable a qualitative comparison of the curves Fig 5.24 is prepared. Clay samples which have the same

plasticity index, I_p , gives aproximately the same shear
modulus. Sample 1 and 3 have I_p values of 8.7% and 10.5%,
respectively. Both of these samples have shear moduli about
5.20×10^{-4} KN/m^2 near the optimum moisture content. Sample
2 has an I_p value of 24.2% and a maximum shear modulus about
7×10^{-4} KN/m^2, and sample 4 has I_p value of 16.5%, and maximum
shear modulus 103×10^3 KN/m^2.

The shear moduli obtained by resonant column apparatus
are compared with the shear moduli obtained by the amprical
formula, Eqs., 4.1, which have been developed by Hardin and
Black. The variation of shear mudulus by moisture content
is presented in Fig. 5.25 . The shear strain amplitude for
these curves is around 10^{-4}. Measured versus calculated shear
moduli curves are given in Fig. 5.26 for İçerenköy samples.
Samples 3 and 4 show good correlation, however the others
do not. For sample 1, Eqs. 4.1 yields higher values than
resonant column method, under 0.144 kg/cm^2 vertical load.
Besides, for sample 2, measured shear modulus is 1.5 times
greater than calculated value.

The deviations mainly arise from two factor; (1) Eqs 4.1
is valid for undisturbed soils, contrarily, in this study
samples are compacted. (2) Confining pressure could not be
applied, and, therefore, the value of vertical load is
divided by 3 to obtain mean principal stress, σ_o in Eqs. 4.1,
which will give relatively smaller calculated shear modulus
value.
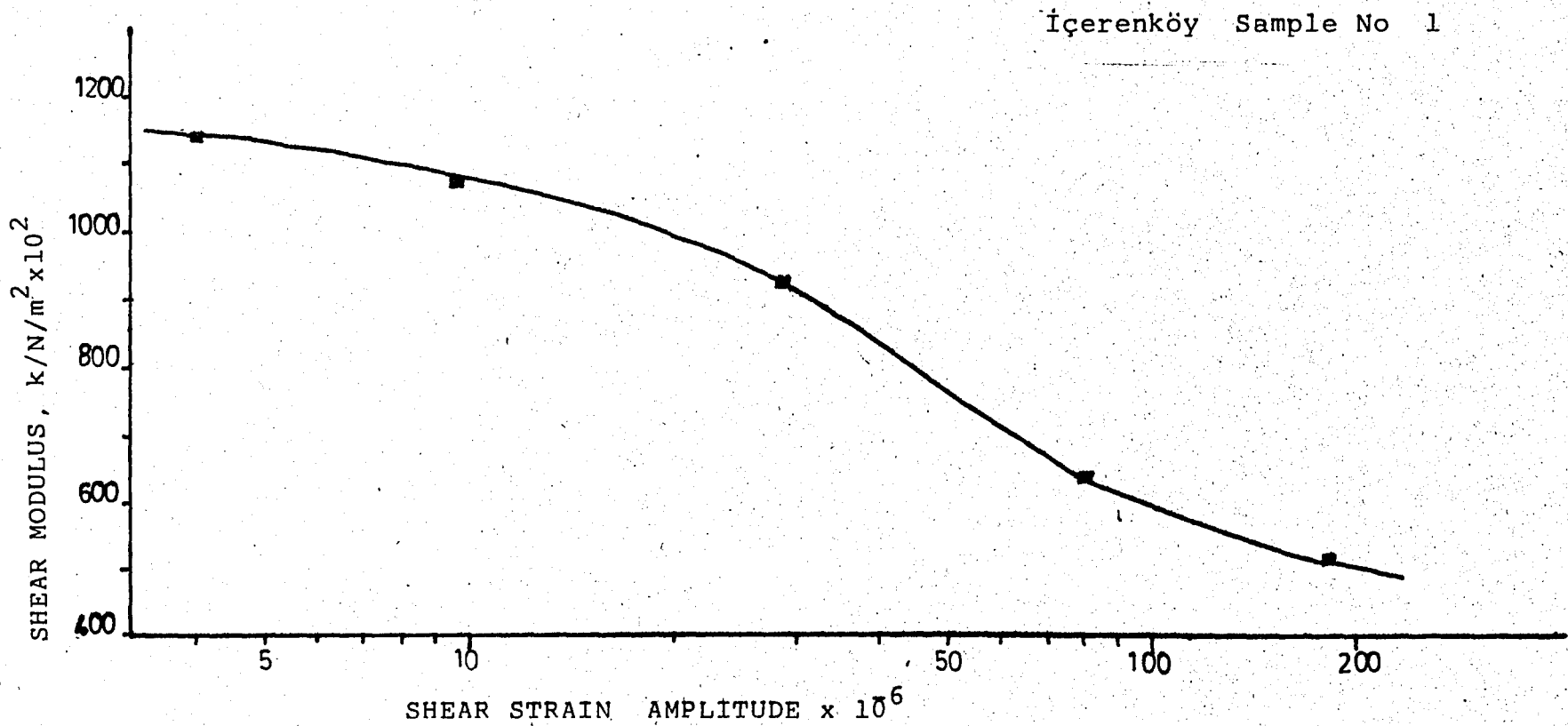
FIG 5.12 Variation of Shear Modulus with Shear Strain Amplitude for
        İçerenköy Sample 1

İçerenköy Sample No 2

Vertical Stress : 0.54 kg/cm^2

w_{opt} : 22. %

I_p : 24.2 %
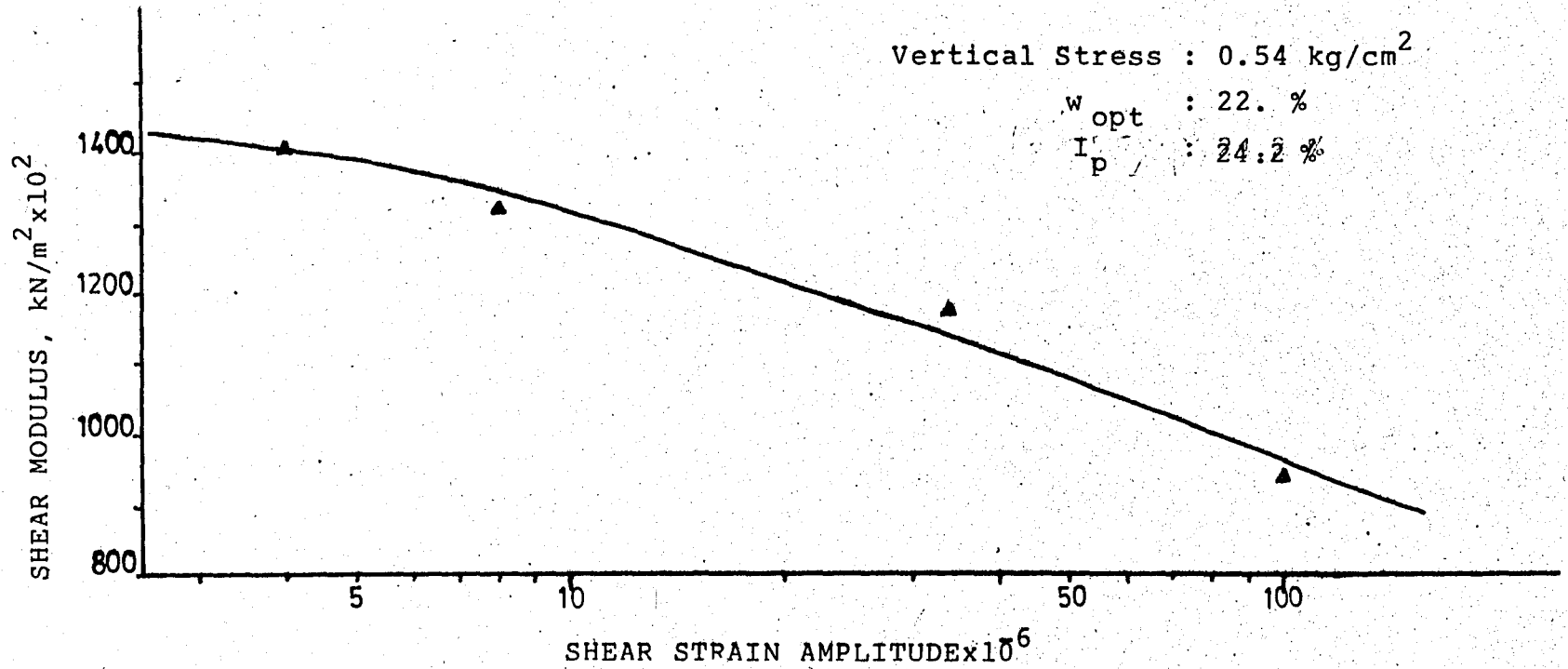
FIG 5.13 Variation of Shear Modulus with Shear Strain Amplitude for İçerenköy Sample 2

İçerenköy Sample No 3

Vertical Stress : 0.54 kg/cm^2

w_{opt} : 13.3 %

I_p : 10.5 %
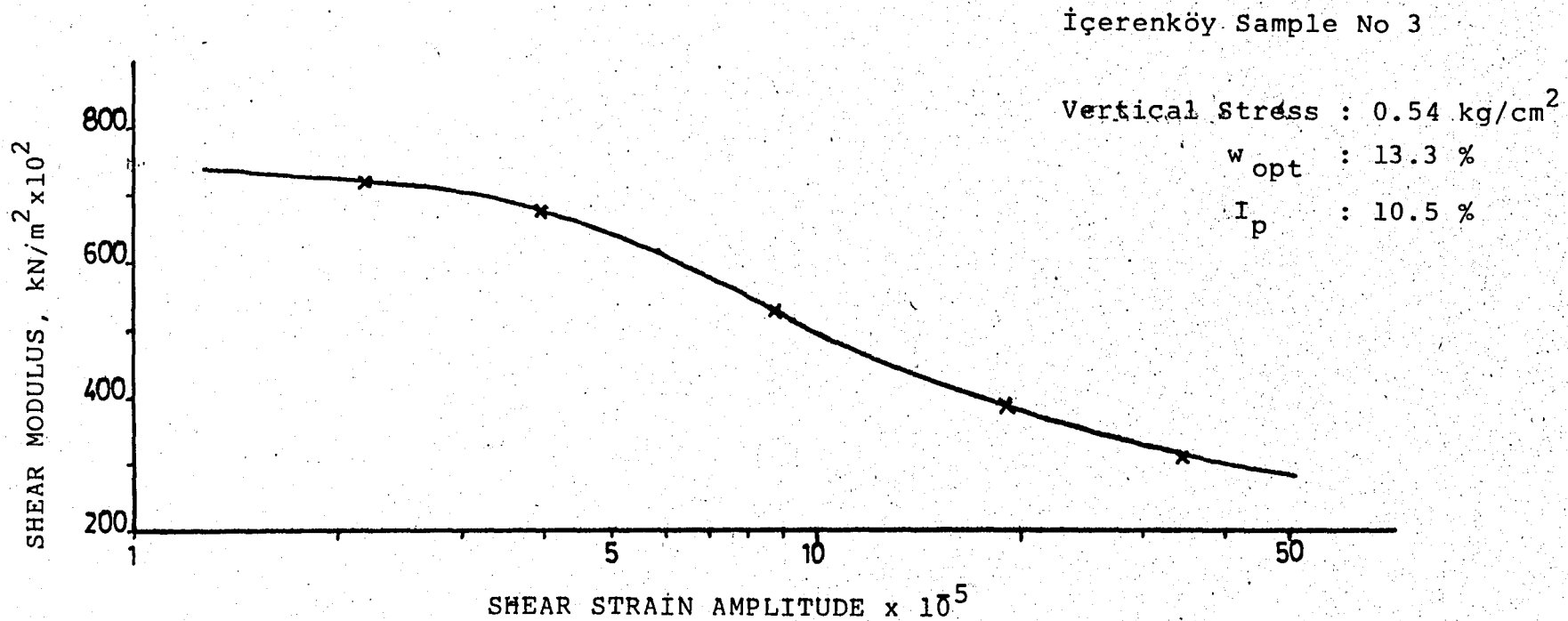
FIG 5.14   Variation of Shear Modulus with Shear Strain Amplitude for
İçerenköy Sample 3

İçerenköy Sample No 4

Vertical Stress : 0.54 kg/cm^2

w_{opt} : 15.4 %

I_p : 16.5 %
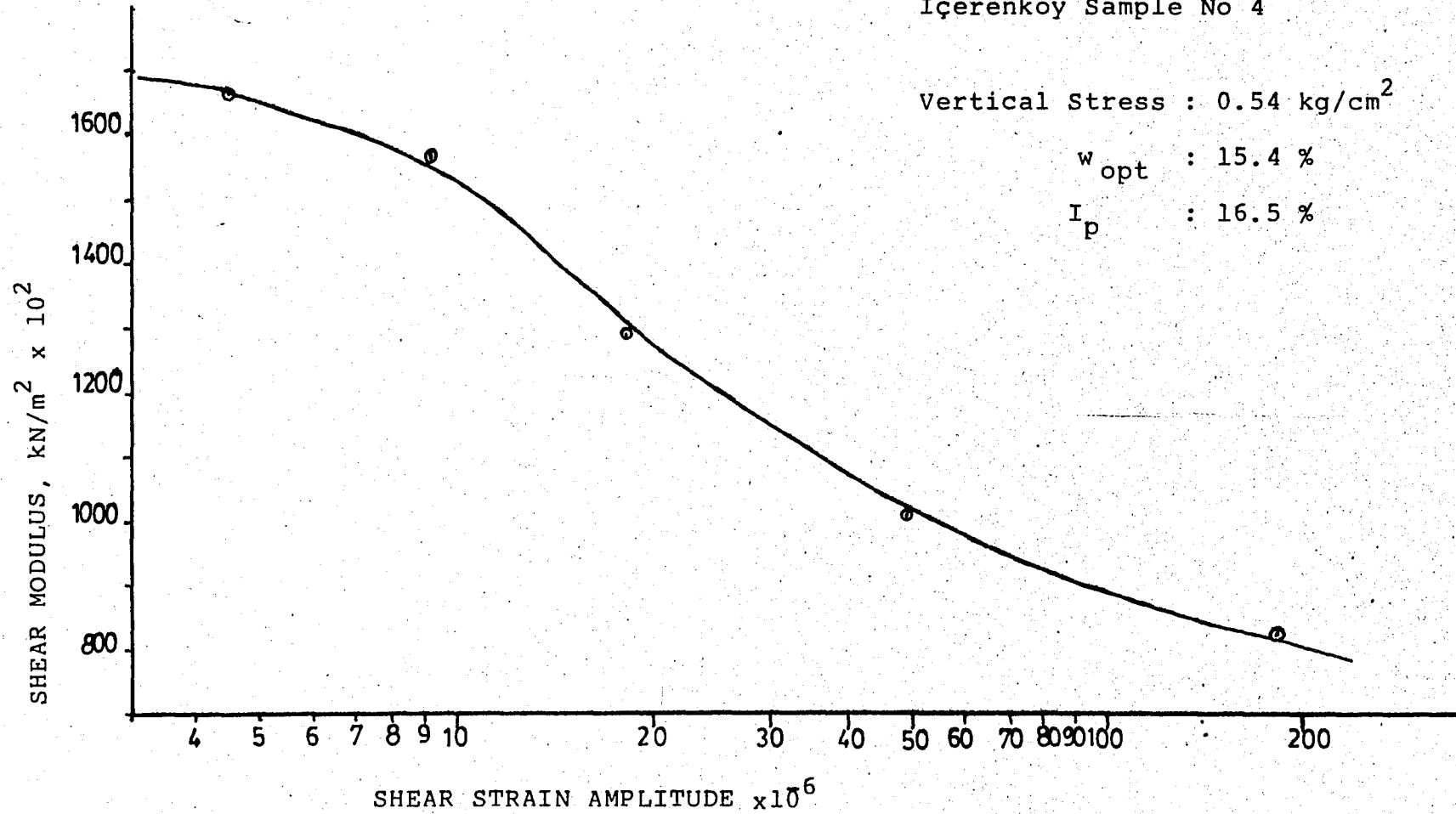
FIG 5.15 Variation of Shear Modulus with Shear Strain Amplitude for İçerenköy Sample 4
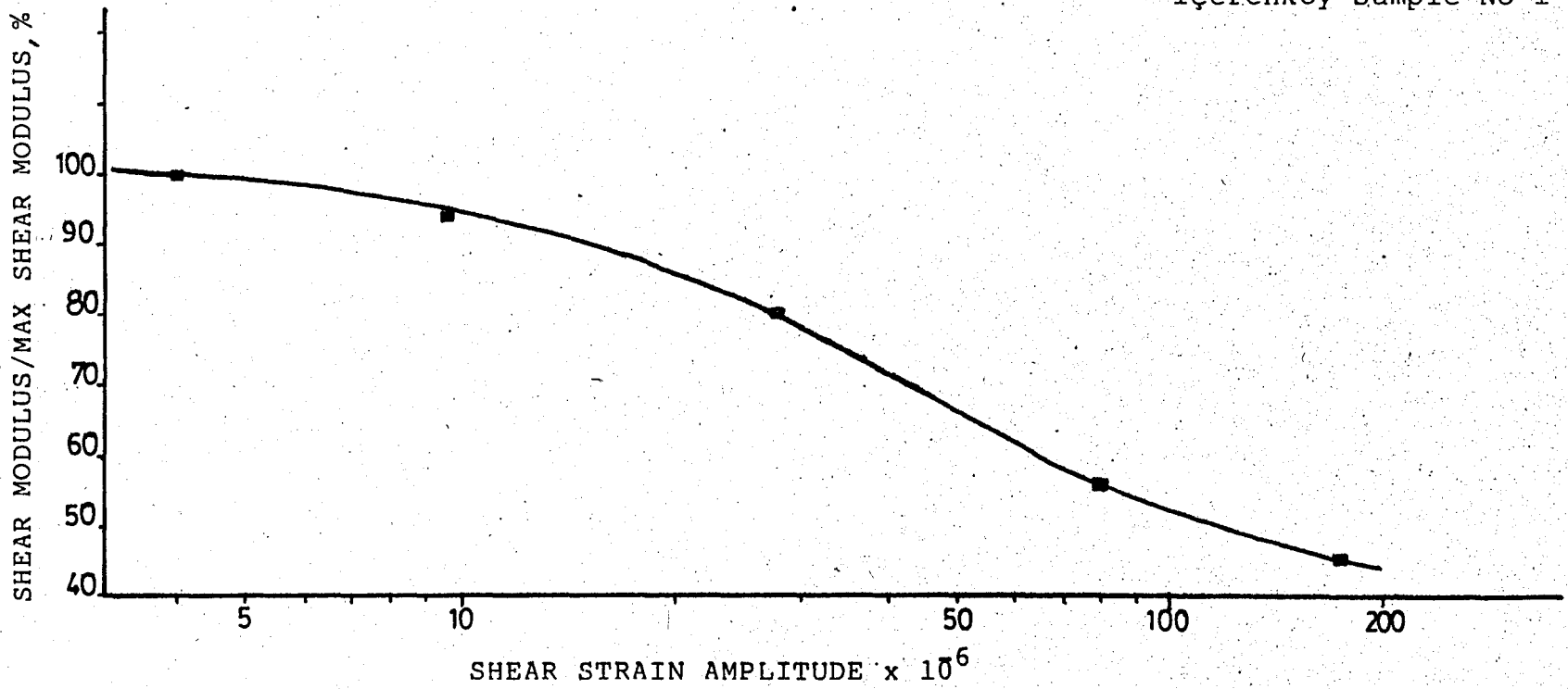
FIG 5.16 Normalized Shear Modulus versus Shear Strain Amplitude for
İçerenköy Sample 1

FIG 5.17 Normalized Shear Modulus versus Shear Strain Amplitude
        İçerenköy Sample 2

İçerenköy sample No 3

SHEAR MODULUS/MAX SHEAR MODULUS , %

SHEAR STRAIN AMPLITUDE x 10^5
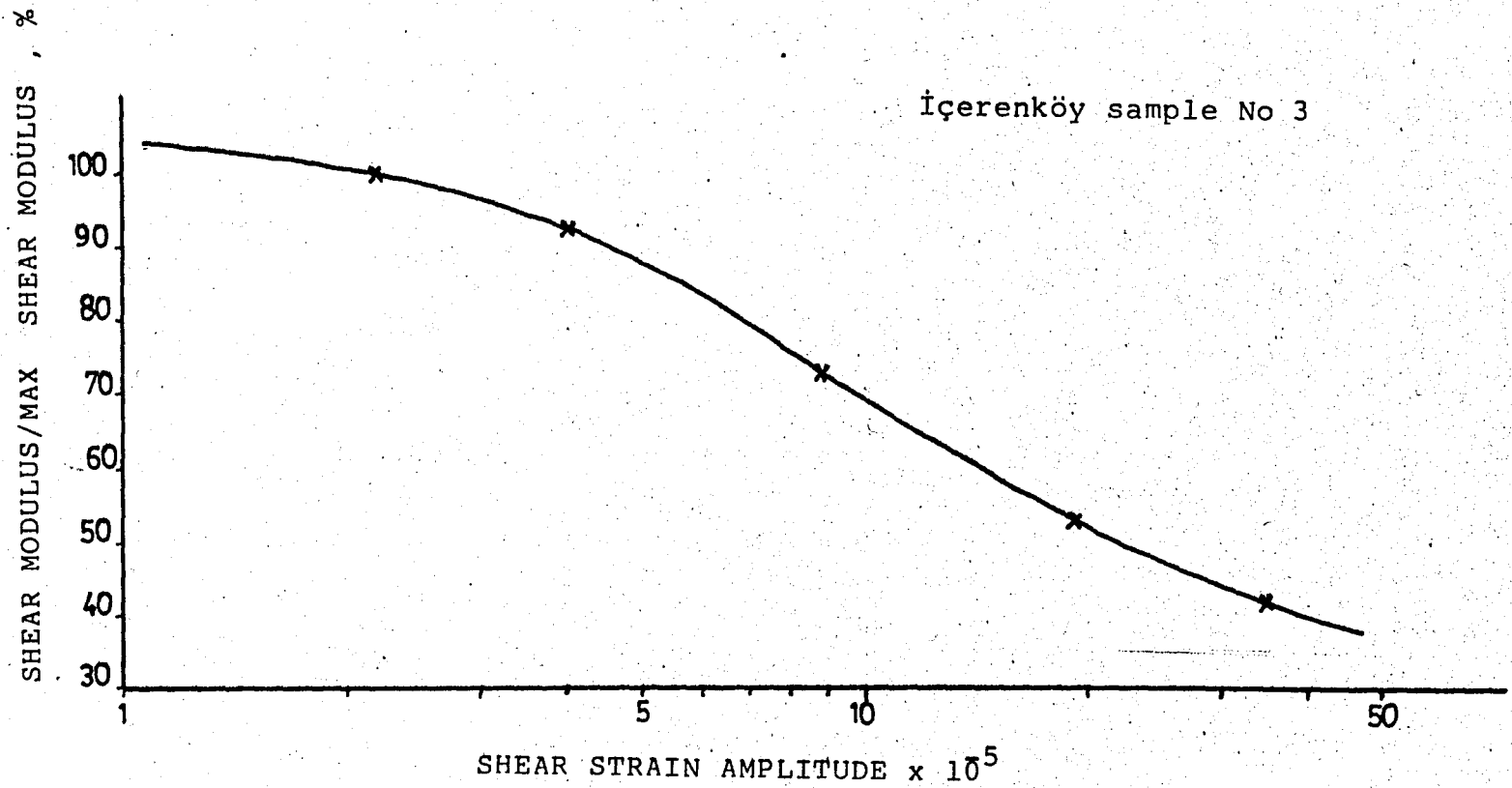
FIG 5.18 Normalized Shear Modulus versus Shear Strain Amplitude
for İçerenköy Sample 3

İçerenköy Sample No 4
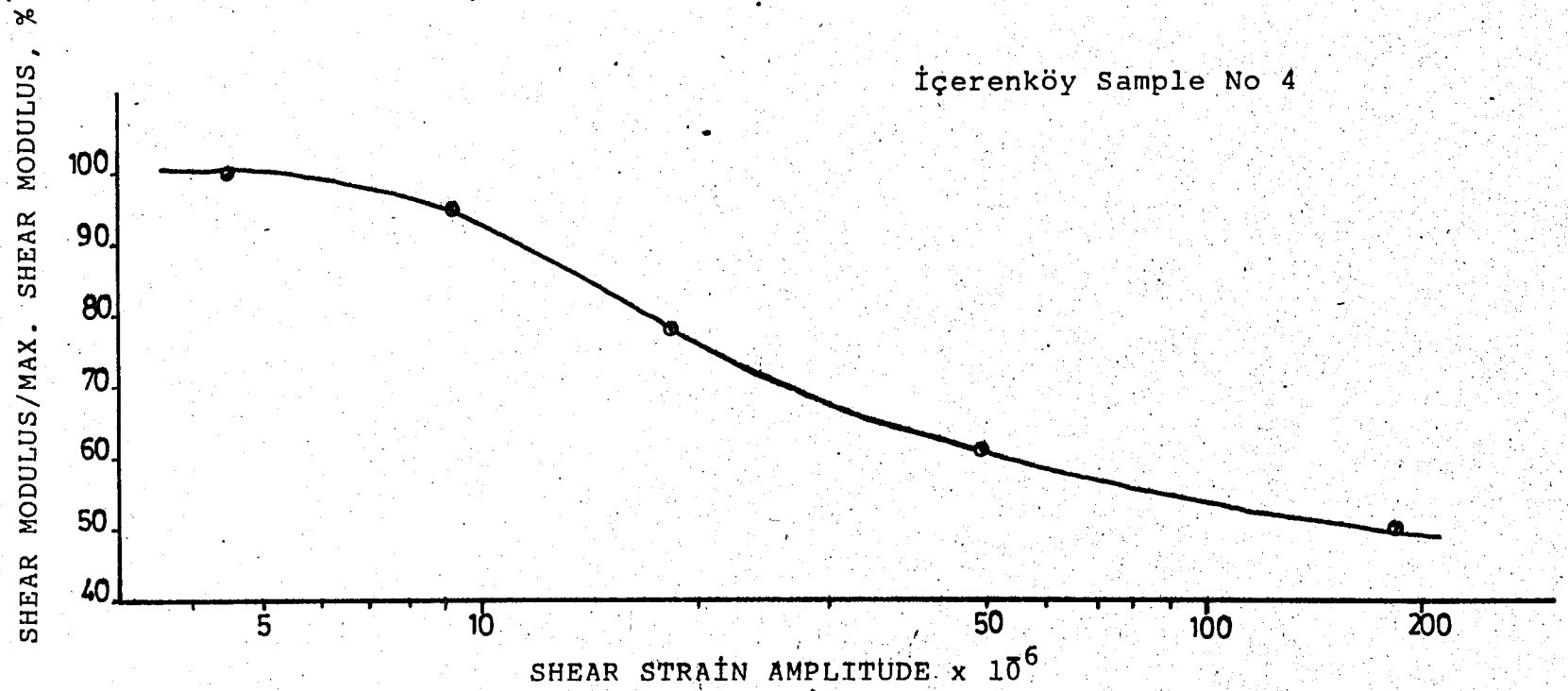
FIG 5.19 Normalized Shear Modulus versus Shear Strain Amplitude for
İçerenköy Sample 4
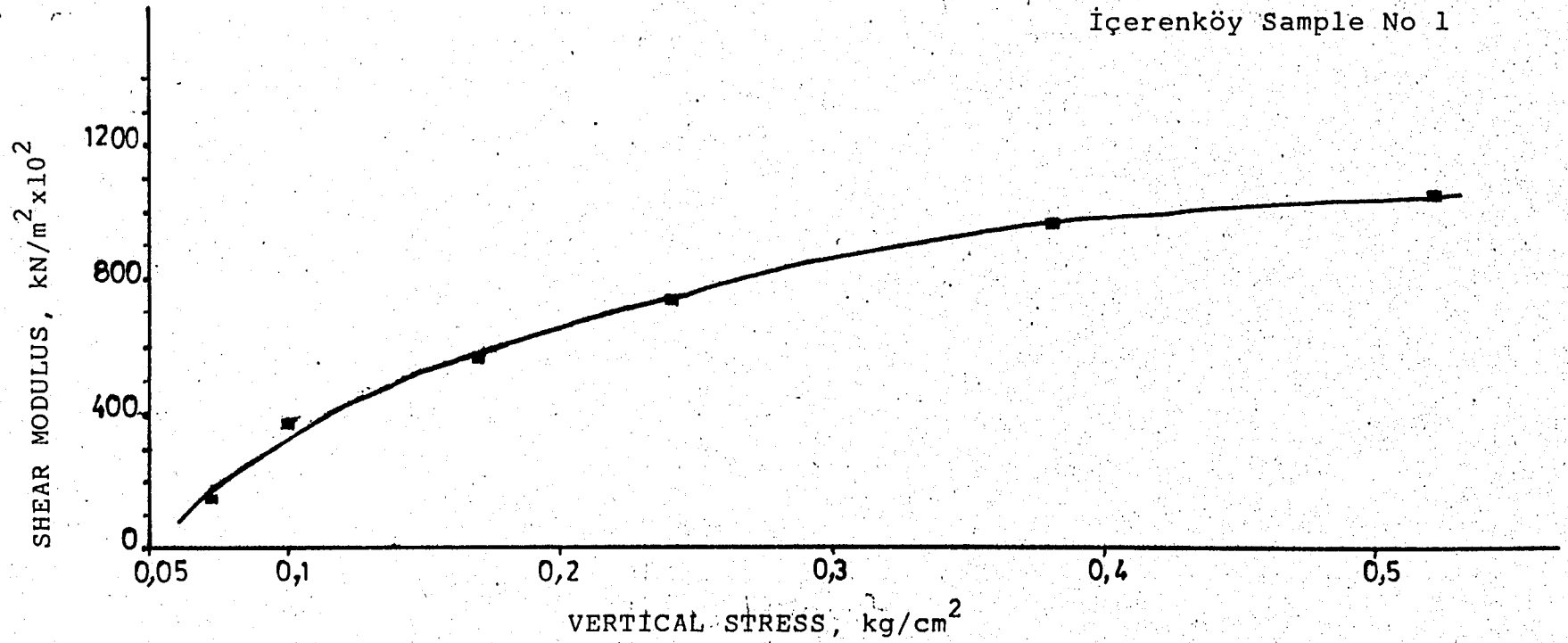
FIG 5.20 Variation of Shear Modulus With Vertical Stress for
İçerenköy Sample 1
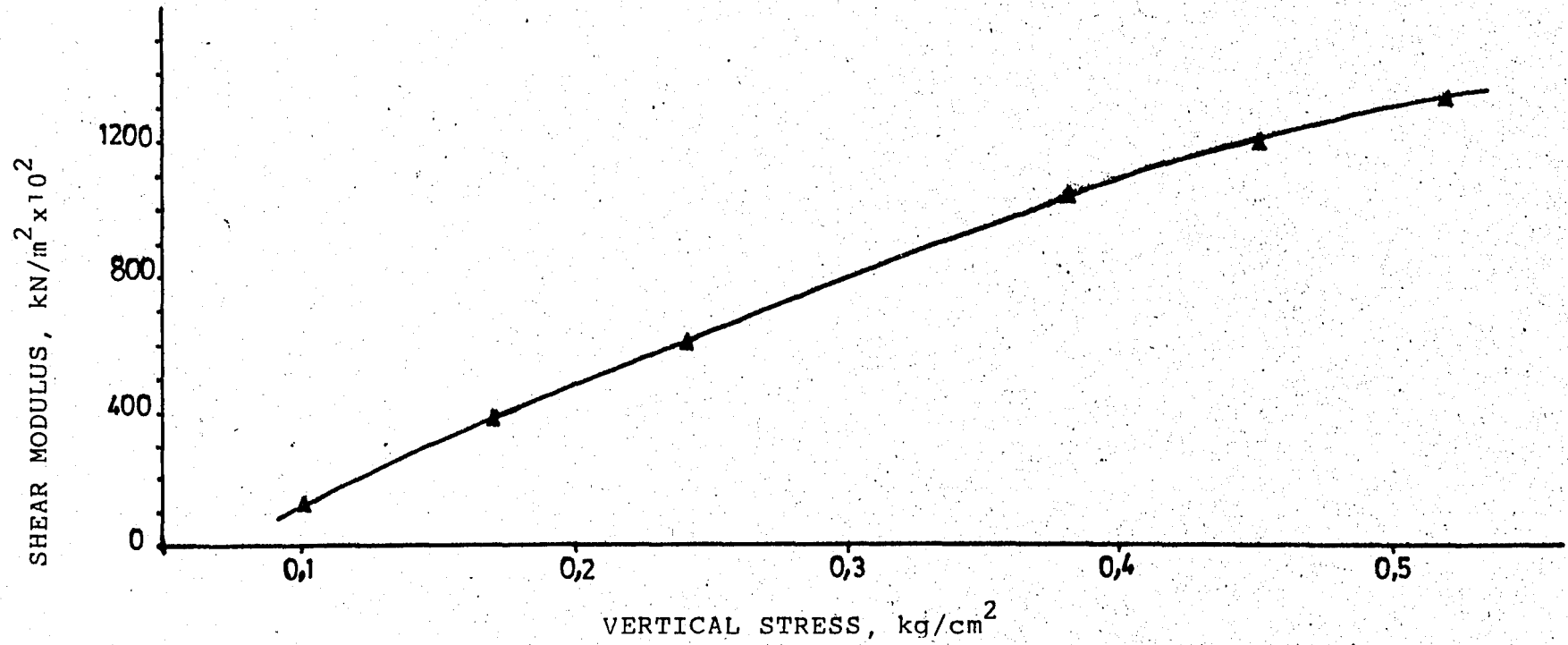
FIG 5.21 Variation of Shear Modulus With Vertical Stress for İçerenköy
          Sample 2
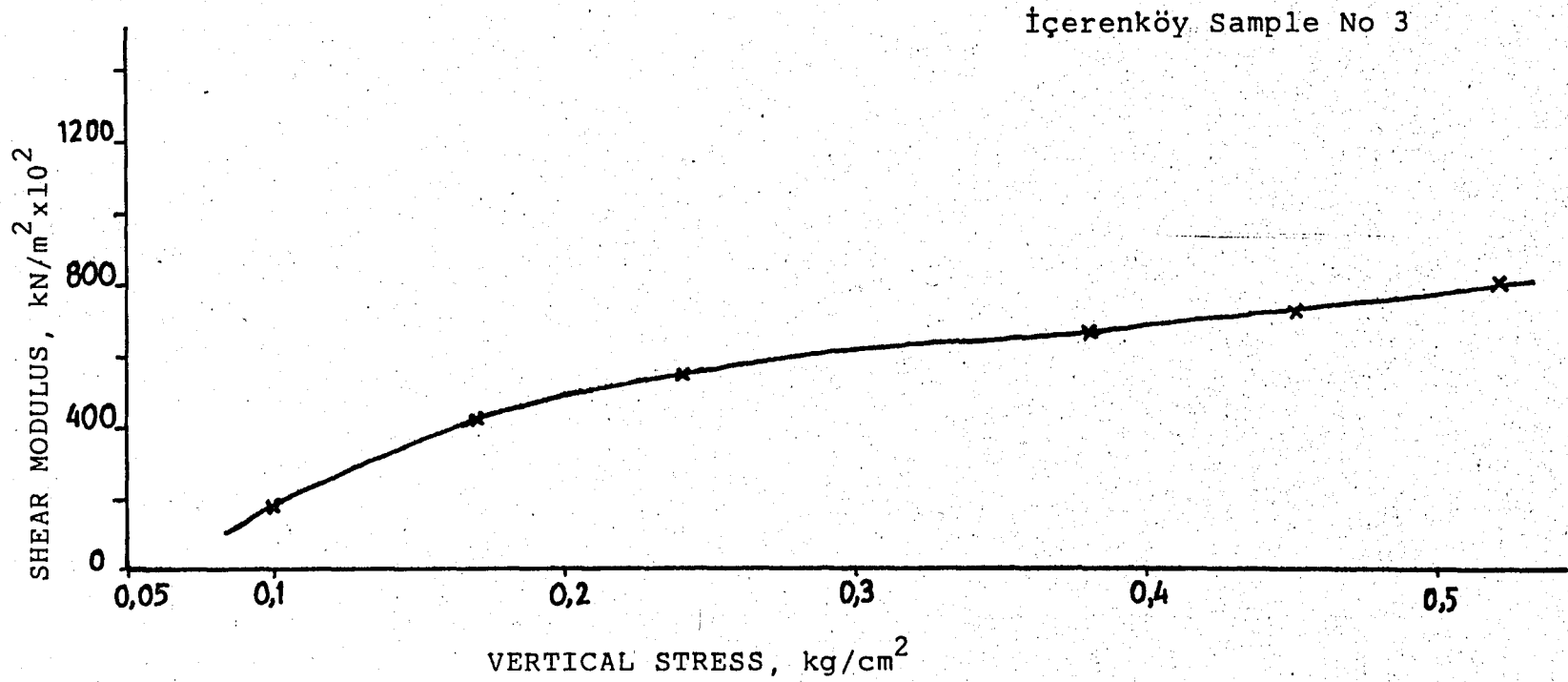
FIG 5.22 Variation of Shear Modulus With Vertical Stress for İçerenköy
           Sample 3

FIG 5:23 Variation of Shear Modulus With Vertical Stress for İçerenköy Sample 4

Axis labels:
- Y-axis: SHEAR MODULUS, $kN/m^2 \times 10^2$ (values: 0, 400, 800, 1200, 1600, 2000)
- X-axis: VERTICAL STRESS, kg/cm^2 (values: 0,05, 0,1, 0,2, 0,3, 0,4, 0,5)

114
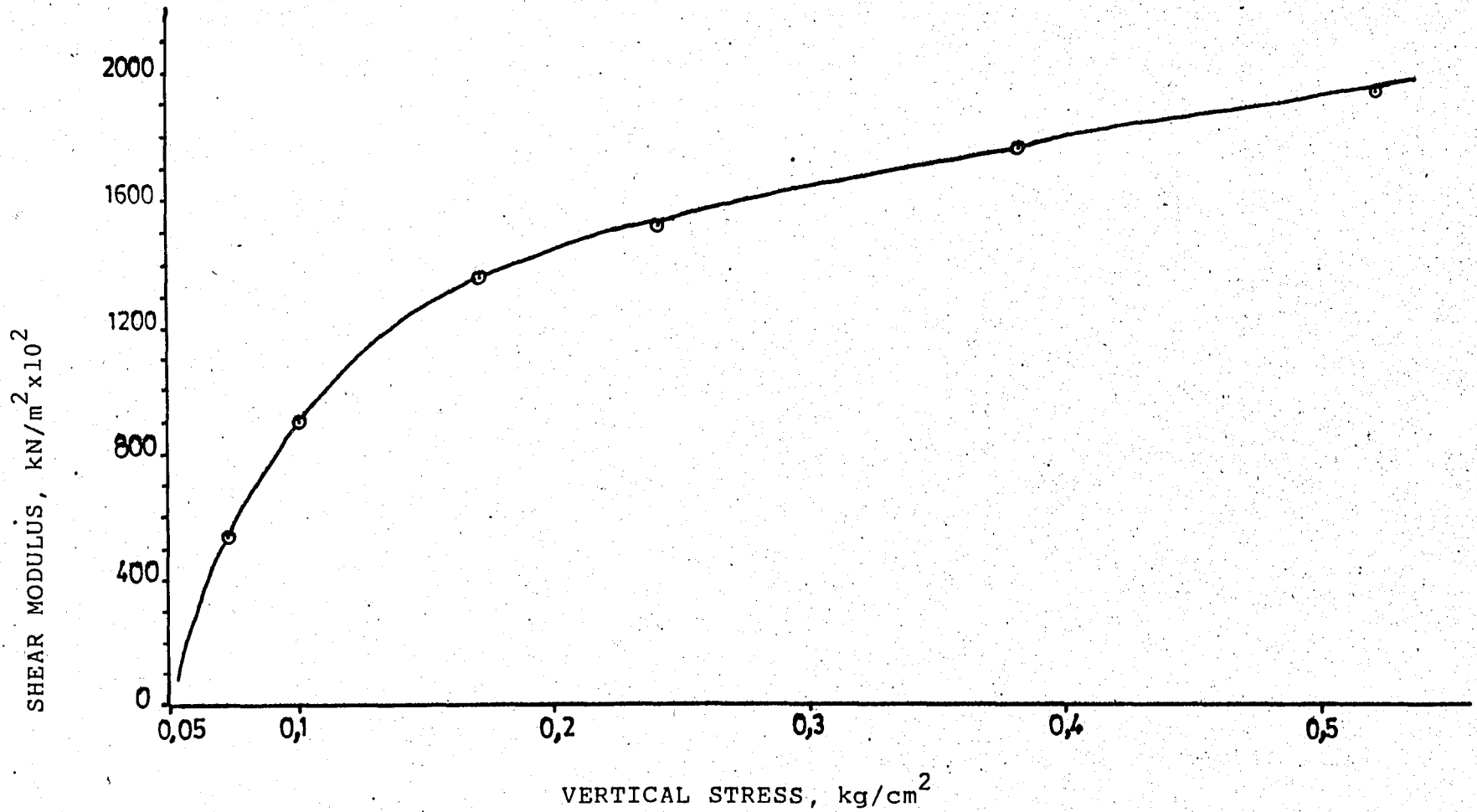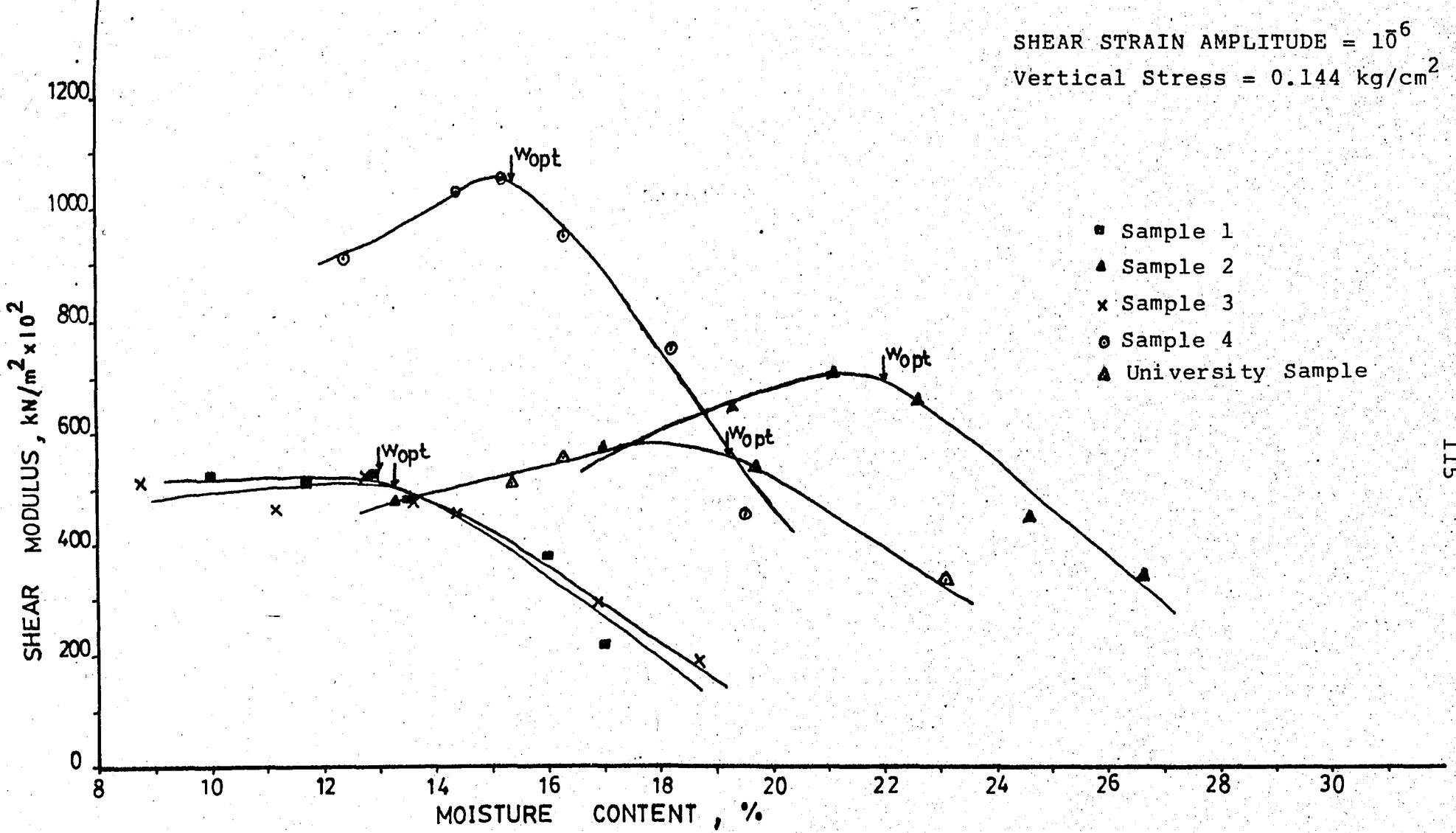
FIG 5.24 Shear Modulus Versus Moisture Content for all Clay Samples Tested
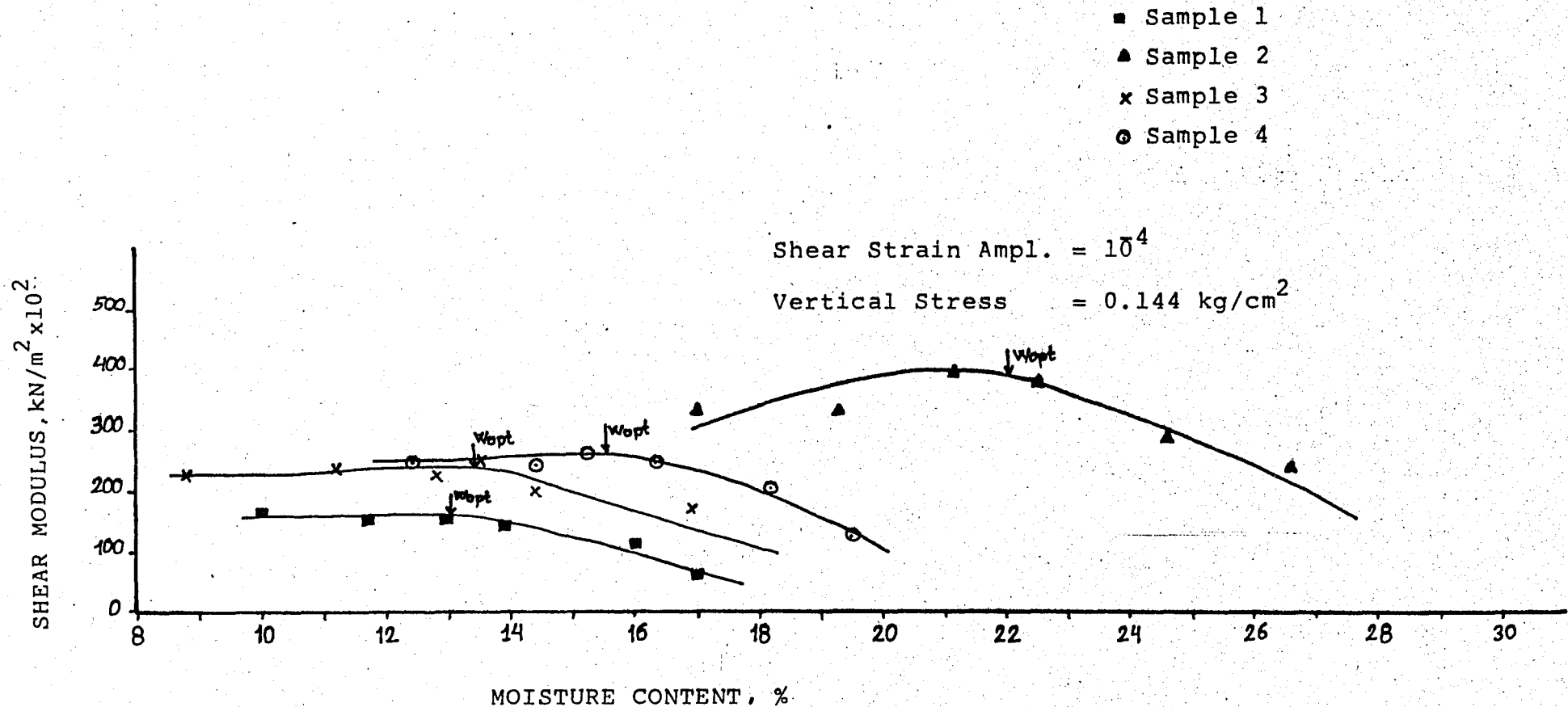
FIG 5.25 Shear Modulus Versus Moisture Content for all Clay Samples Tested
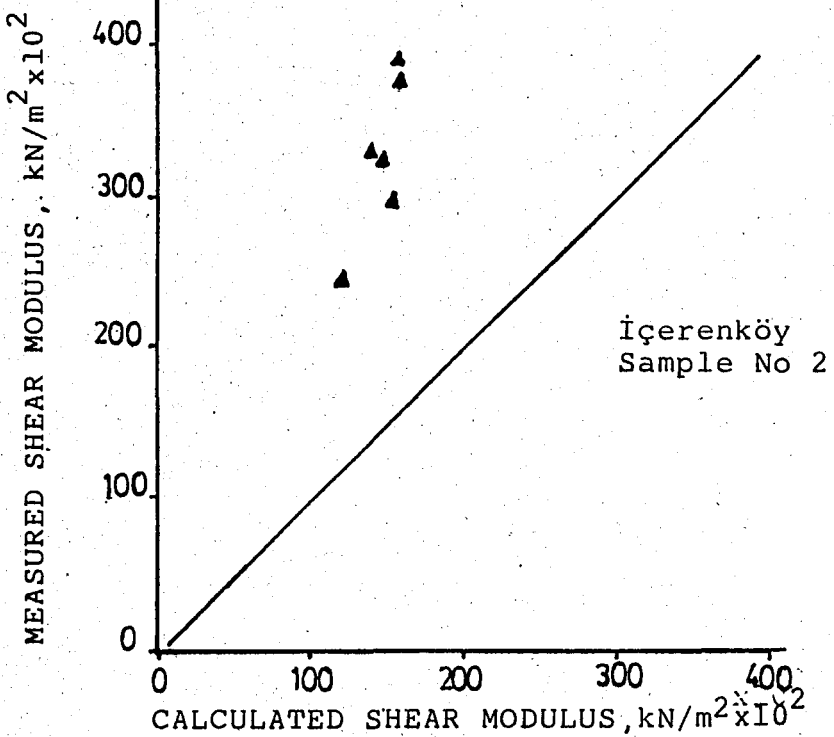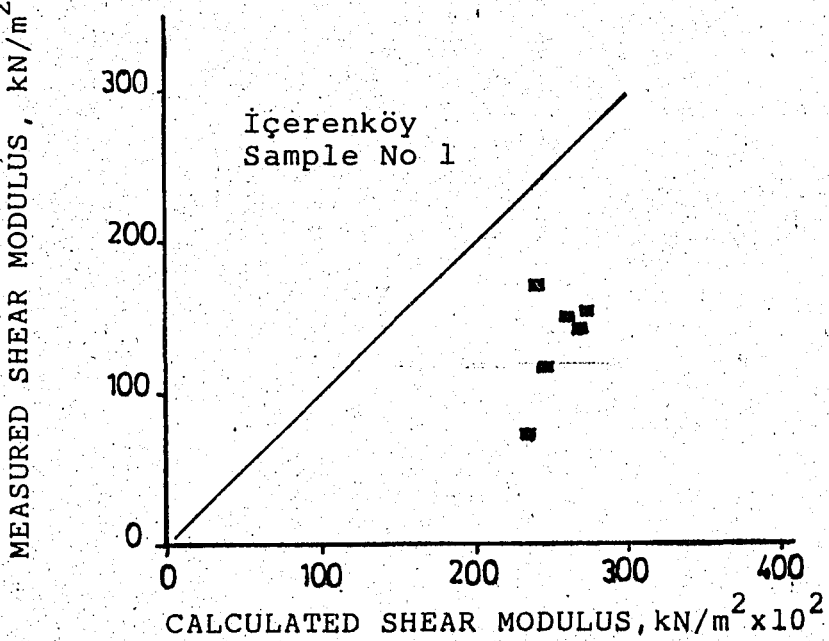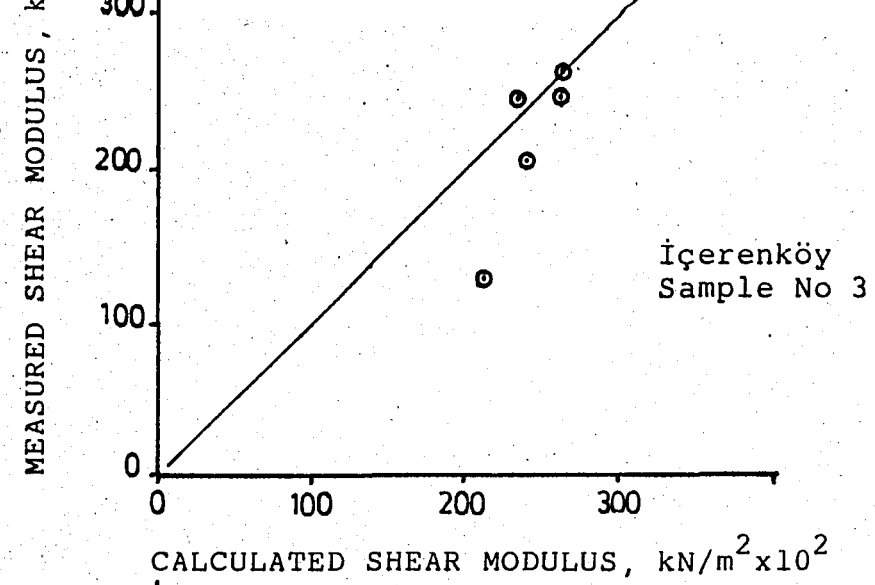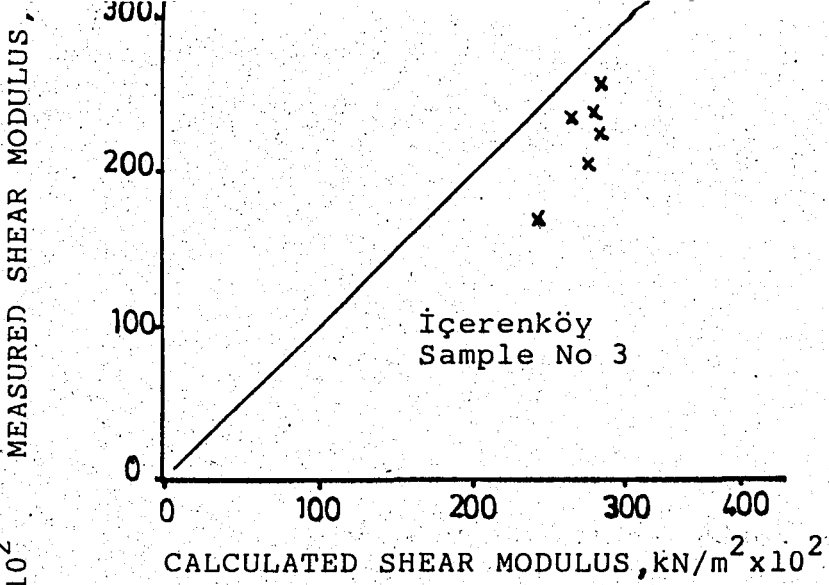
FIG 5.26 Comparison of Calculated and Measured Values of Shear Modulus for İçerenköy Samples

5.6 SUMMARY AND CONCLUSIONS

The determination of the shear modulus by using resonant column method is explained in this chapter. Besides, the variation of shear modulus with moisture content is studied for five samples. The effect of strain amplitude and vertical load on shear modulus are measured and plotted for samples compacted at their optimum moisture content. The change of shear modulus with plasticity index and CBR value is analized. As the result following conclusions are deduced.

1. Maximum shear modulus of samples are attained at values, slightly less than the optimum moisture content.

2. Shear moduli obtained on the dry side of optimum is greater than shear moduli on the wet side.

3. Shear modulus decreases with increasing strain amplitude.

4. Shear modulus increases with increasing vertical load.

CHAPTER 6 DETERMINATION OF DAMPING RATIO BY RESONANT COLUMN METOD

6.1 INTRODUCTION

The energy dissipated by the system is a measure of the damping capacity of the soil. The damping is defined by the shear damping ratio for the soil, D, analogous to the critical viscous damping ratio for a single degree of freedom system, C/C_{cr} . Values of damping by this method correspond to the area of the hysteresis loop stress strain relation divided by 4π times the elastic strain energy stored in the specimen at maximum strain. Both the steady state and the free vibration methods are used to calculate damping ratios.

The damping ratios of specimens, prepared at various moisture contents, are measured and plotted for practical use for each sample. The effects of shear strain amplitude and vertical stress are defined for specimens compacted at their optimum moisture contents.

6.2 MEASUREMENT OF SYSTEM DAMPING RATIO

There are two methods to determine the damping capacity of a soil by resonant column. These methods are the steady state vibration method, and, the free vibration method.

For the steady state vibration method, with the system vibrating at the system resonant frequency, the accelerometer output and torque volts are recorded from the multimeter to

calculate amplitude of vibration at resonance, θ_R, and the current flowing through the coils of the vibration excitation device, C_R.

For the free vibration method, with the system vibrating at the system resonnat frequency power is cut off and the decay curve is recorded for free vibration of the system shown in Fig 6.1.. From the decay curve the logarithmic decrement of the system, δ_s, is computed as follows::

$$\delta_s = \frac{1}{n} \ln \frac{A_1}{A_{n+1}} \qquad (6.1)$$

where; A_1 is the amplitude of vibration for the first cycle after the power is cut off and A_{n+2} is the amplitude for the $(n+1)^{th}$ cycle. Normally n should be less than or equal to 10.

6.3 CALCULATIONS

In this study, both the steady state vibration and the free vibration methods are used to calculate the damping capacity of the soils tested.
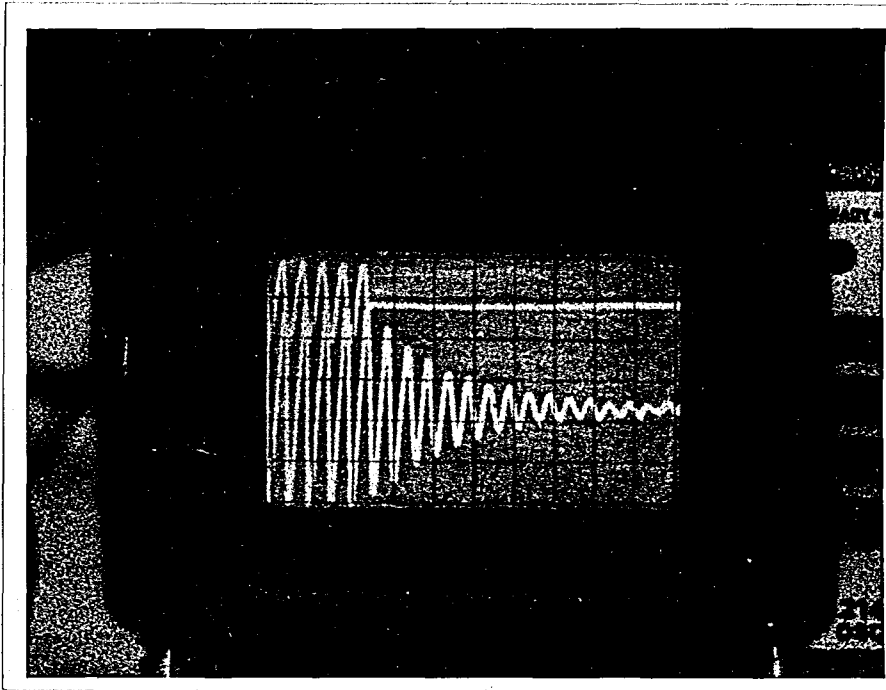
Fig 6.1   Decay Curve of a Sample

A. Steady state Method;

   1. The damping factor, A, is calculated as follows
      by Hardin's equation:

$$A = \frac{1}{4 \pi^2 J f^2} \left[\frac{K_t C_R}{\theta_R} - 2 \pi K_D f \right] \qquad (6.2)$$

   Where; K_t = apparatus torque / current constant,
only one value of it is calculated at the beginning of
test and used for all samples. According to Hardin, to
find torque / current constant, K_t, the apparatus is
excited at frequencies of $(\sqrt{2}/2)$ fo, $\sqrt{2}$fo, and 2fo.
During vibration, at each of these frequencies the current
flowing through the coils, C, and the displacement
amplitude of vibration, θ , are measured. For each
frequency above K_t is calculated as follows;

$$K_t = \frac{\theta K_o}{C M_f} \qquad (Hardin) \qquad (6.3)$$

   M_f is given by Hardin

Frequency	M_f
$(\sqrt{2}/2) f_o$	2
$(\sqrt{2}) f_o$	1
$2f_o$	1/3

K_o = apparatus spring constant = 0.308×10^{-6} g-cm/rad

   (given by the calibration sheet of apparatus)

f_o = 30.21 H_z (given by the calibration sheet of apparatus)

$(\sqrt{2}/2)f_o = 21.36$ H_z $K_t = \dfrac{4.5 \times 10^{-4} \times 308000}{0.0127 \times 2} = 5483$

$\sqrt{2}f_o = 42.7$ H_z $K_t = \dfrac{1.7 \times 10^{-4} \times 308000}{0.0113 \times 1} = 4478$

$2f_o = 60.42$ H_z $K_t = \dfrac{2.3 \times 10^{-4} \times 308000}{0.0106 \times \dfrac{1}{3}} = 4923$

The average value of torque/current constant is calculated as $K_t = 4961$, and used in this study.

K_D = apparatus damping canstant defined by Hardin as follows

$$K_D = \frac{\delta_A}{\pi} \sqrt{K_o \, J_o} \qquad\qquad (6.4)$$

$$K_D = \frac{0.039}{\pi} \sqrt{0.308 \times 10^6 \times 8.02}$$

$$K_D' = 19.5 \text{ gr-cm-sec/rad}$$

where ;

   δ_A = apparatus damping constant, defined by amplitude

   decay method, given in calibration sheet.

J_o = apparatus inertia, = 8.02 g-cm-sec^2

(given in calibration sheet)

C_R = Current flowing through the coils of Hardin oscillator. This value is obtained from torque volts. Torque reading per resistance (10 Ω), in series with coils, will shows the current through the coils in Amperes.

θ_R = amplitude of vibration at the system resonant frequency

$$\theta_R = \frac{(\text{Acc.m VRMS}) (1.414) (386 \text{ in/sec}^2)}{(2500 \text{ mV/g}) (\text{Lever Arm, in}) (4\pi^2)f^2} \qquad (6.5)$$

(given by Hardin)

$$\theta_R \text{ (rad)} = 0.00389 \frac{(\text{Acc.m VRMS})}{f^2}$$

Where ;

f = system resonant frequency

Acc = accelerometer reading in mV RMS

2. The value of R is determined as abscissa corresponding to the value of T as ordinate from Fig. 6.2 .

3. The value of damping ratio, D, is determined as follows ;

$$D = 0.5 \frac{A}{TR} \qquad (6.6)$$
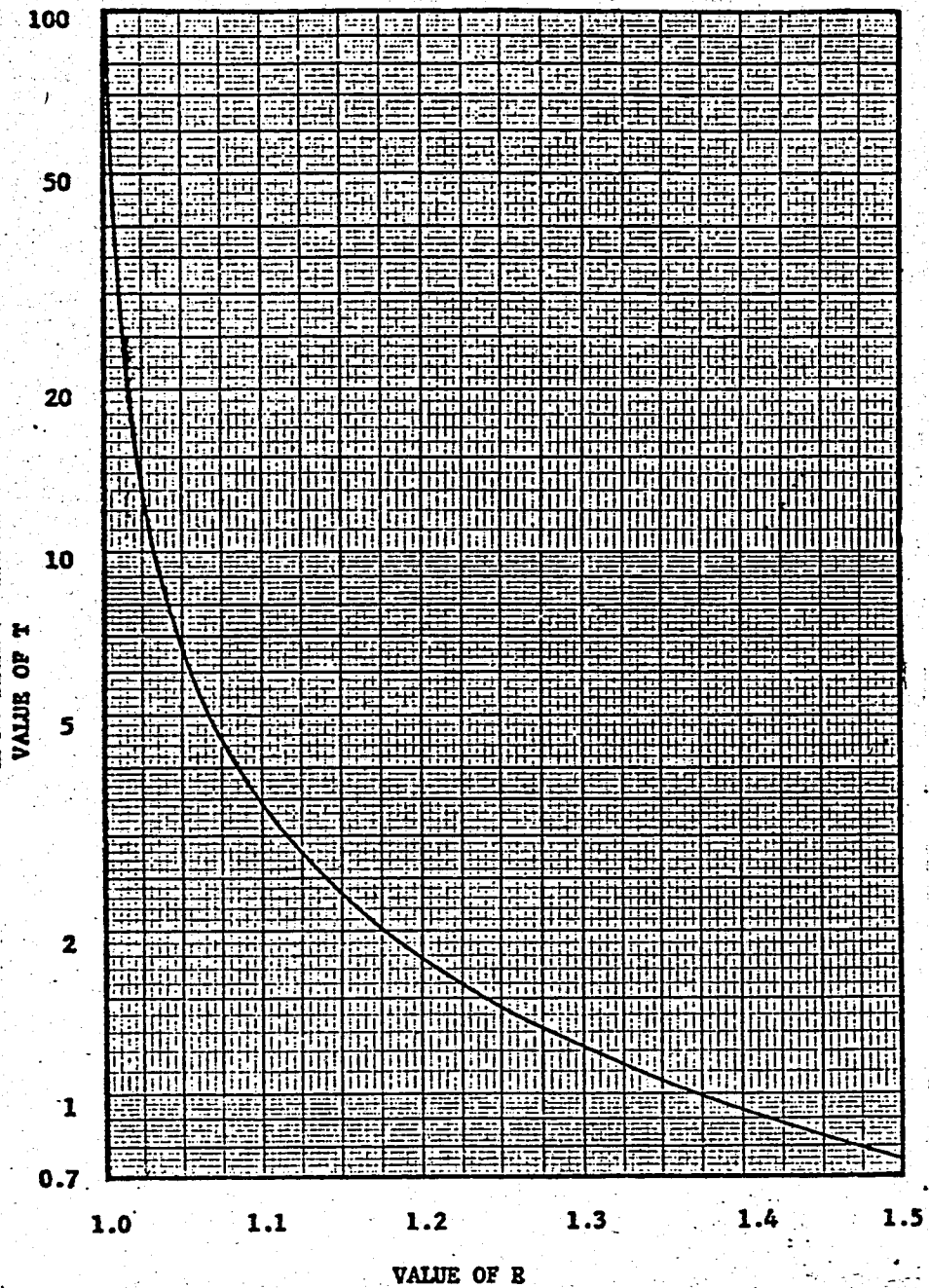
Fig 6.2   System Factor versus R.

(After Hardin)

Using the steady state vibration method the damping ratios of the samples are computed as shown in Tables 6.1 through 6.5 for strain amplitude, 10^{-6} and in Tables 6.6 through 6.9 for strain amplitude, 10^{-4} .

B-Free Vibration Method

1. On the other hand, for the free vibration method of measuring damping the value of the mode shape factor, C_m , is determined as abcissa corresponding to the value of T as ordinate from Fig. 6.3

2. The system energy ratio, S, is computed as follows

$$S = \frac{32\ K_o\ 1}{\pi C_m\ G\ d^4} \tag{6.7}$$

3. The value of the damping ratio, D, is computed as follows

$$D = \frac{1}{2\pi}\left[\delta_S(1+S) - \delta_A\ S\right] \tag{6.8}$$

δ_S = logarithmic decrement of systems was found during testing procedure.

δ_A = logarithmic decrement is given on calibration chart.

Tha values of damping ratios computed by free vibration method are presented on Tables 6.1 through 6.9
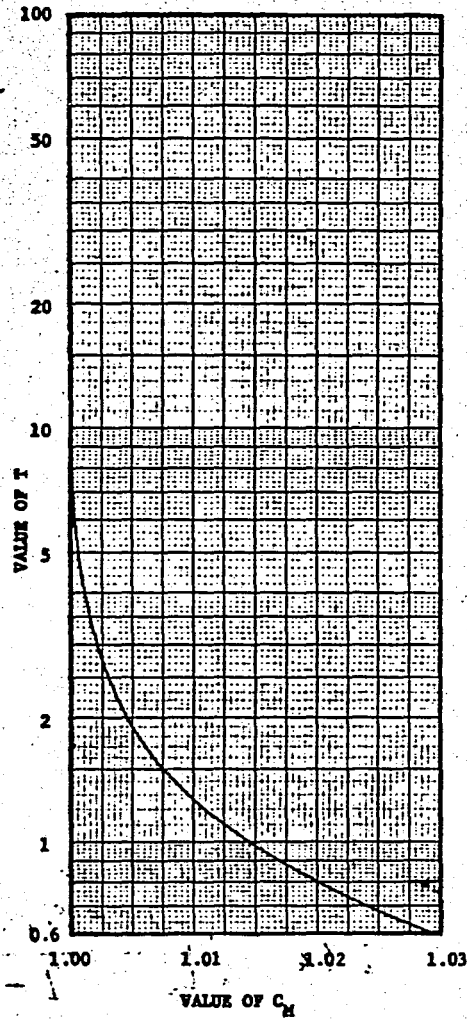
Fig 6.3 System Factor Versus Mode Shape Factor

TABLE 6.1 Damping Ratios for İçerenköy Sample 1

w %	δ_s	S	Cm	% D_{free}	Accl. Rd.	Torq. Rd.	θ_R	C_R	A	R	D steady	Strain Ampl.
10.0	0.336	0.293	1.0	7.4	88	16.5	6.9×10^5	16.5×10^{-4}	3.50	1.010	6.7	1.2×10^{-5}
11.7	0.366	0.304	1.0	7.3	61	18	6×10^5	18×10^{-4}	3.49	1.013	7.2	9×10^{-6}
12.9	0.318	0.293	1.0	6.4	49	15	4.6×10^5	15×10^{-4}	3.59	1.015	7.5	7×10^{-6}
13.5	0.337	0.318	1.0	7.0	48	15	4.86×10^5	15×10^{-4}	4.65	1.015	10.1	7.2×10^{-6}
16.0	0.549	0.405	1.0	12.0	32	10	2.87×10^5	10×10^{-4}	4.70	1.017	11.0	6×10^{-6}
17.0	0.400	0.699	1.0	10.5	24	10	5.3×10^5	10×10^{-4}	3.58	1.020	10.0	6.2×10^{-6}

w : water content, %

δ_s : logarithmic decrement

S : system energy ratio

Cm : mode shape factor

D_{fre} : damping ratio by free vibration method , %

Accl.Rd.: Accelerometer Reading in mV_{RMS}

θ_R : amplitude of vibration

C_R : Current flowing thrangh the coils of hardin asallator , Amper

A : damping factor

D_{steady} : damping natio by steady state method, %

Torq.Rd.: Torque Reading in mV_{RMS}

TABLE 6.2 Damping Ratios for İçerenköy Sample 2

w,%	δ_s	S	Cm	% D_{free}	Accl. Rd.	Torq. Rd.	θ_R	C_R	A	R	D steady	strain amplitude
17.0	0.254	0.270	1.0	5.0	56	13	4.85×10^{-5}	13×10^{-4}	3.12	1.01	5.4	-7.2×10^{-6}
19.3	0.266	0.242	1.0	5.1	73	17	6×10^{-5}	17×10^{-4}	2.91	1.01	5.3	9×10^{-6}
21.1	0.250	0.210	1.0	4.7	70	14	5.3×10^{-5}	14×10^{-4}	2.42	1.01	4.5	8×10^{-6}
22.6	0.327	0.237	1.0	6.3	70	17	5.6×10^{-5}	17×10^{-4}	2.86	1.01	5.6	8.3×10^{-6}
24.6	0.276	0.350	1.0	6.9	70	15	7.6×10^{-5}	15×10^{-4}	2.51	1.015	5.3	1.1×10^{-5}
26.4	0.282	0.446	1.0	6.3	54	10	6.9×10^{-5}	10×10^{-4}	2.70	1.015	5.9	1.04×10^{-5}

TABLE 6.3   Damping Ratios for İçerenköy Sample 3

w %	δ_s	S	Cm	% D_{free}	Accl. Rd.	Torq. Rd.	θ_R	C_R	A	R	D steady	Strain Amp.
8.8	0.305	0.302	1.0	7.4	49.0	11.5	4.3×10^{-5}	11.5×10^{-4}	3.20	1.013	6.54	7×10^{-6}
11.2	0.305	0.334	1.0	6.9	45.0	10.0	4.4×10^{-5}	10×10^{-4}	2.77	1.015	5.80	7×10^{-6}
12.8	0.348	0.294	1.0	7.-	70.0	19.0	6.6×10^{-5}	19×10^{-4}	3.13	1.015	6.60	9.9×10^{-6}
13.45	0.337	0.320	1.0	6.9	56.5	16.0	5.7×10^{-5}	16×10^{-4}	3.27	1.015	7.00	8.5×10^{-6}
14.4	0.366	0.307	1.0	7.5	52.0	16.9	5×10^{-5}	16.9×10^{-4}	3.79	1.015	8.10	7.6×10^{-6}
16.9	0.350	0.526	1.0	8.2	44.0	12.0	6.3×10^{-5}	12×10^{-4}	3.12	1.015	7.70	9×10^{-6}
18.7	0.260	0.864	1.0	8.8	35.0	9.0	6.8×10^{-5}	9×10^{-4}	2.93	1.020	8.70	1×10^{-5}

'TABLE 6.4   Damping Ratios for İçerenköy Sample 4

w %	δ_s	S	Cm	% D_{free}	Accl. Rd.	Torq. Rd.	θ_R	C_R	A	R	% D_{steady}	Strain Amp.
12.4	0.366	0.169	1	6.7	79	25.8	4.8×10^5	25.8×10^4	4.25	1.010	7.2	7.2×10^6
14.4	0.310	0.150	1	5.6	84	25.0	4.5×10^5	25×10^4	3.60	1.010	6.5	$7. \times 10^6$
15.2	0.337	0.146	1	6.0	95	31.1	5×10^5	31×10^4	3.93	1.010	7.2	7.5×10^6
16.3	0.401	0.163	1	7.3	92	34.2	5.3×10^5	34.2×10^4	4.26	1.010	8.4	8×10^6
18.2	0.384	0.206	1	7.5	80	27.0	6.2×10^5	27×10^4	3.83	1.012	7.9	9.2×10^6
19.5	0.400	0.342	1	8.4	42	13.0	4.5×10^5	13×10^4	4.25	1.015	9.3	7×10^6

TABLE 6.5 Damping Ratios for Boğaziçi University Sample

$w, \%$	δ_s	S	Cm	D_{free} %	Accl. Rd.	Torq. Rd.	θ_R	C_R	A	R	D_{steady} %	Strain Ampl.
13.3	0.32	0.32	1.0	6.6	90	25	9.1×10^{-5}	2.5×10^{3}	3.61	1.01	6.9	1.4×10^{-5}
15.4	0.31	0.295	1.0	6.2	85	25	8×10^{-5}	2.5×10^{3}	3.91	1.01	7.1	1.2×10^{-5}
16.3	0.35	0.28	1.0	6.9	94	26	8.4×10^{-5}	2.6×10^{3}	3.49	1.01	6.7	1.3×10^{-5}
19.7	0.41	0.30	1.0	8.3	84	25	7.9×10^{-5}	2.5×10^{3}	3.72	1.01	7.5	1.2×10^{-5}
23.0	0.43	0.47	1.0	9.8	62	22	8.3×10^{-5}	2.2×10^{3}	4.27	1.015	9.6	1.2×10^{-5}

TABLE 6.6 Damping Ratios for İçerenköy Sample 1

w,%	δ_s	S	Cm	% D_{free}	Accl. Rd.	Torq. Rd.	θ_R	C_R	A	R	% D_{steady}	Strain Amp.
10.0	0.69	0.91	1.	23.7	486	324	9.9×10^{-4}	3.24×10^2	8.43	1.015	21	1.4×10^{-4}
11.7	0.82	1.03	1.	25.0	518	280	1.1×10^{-3}	2.8×10^2	6.46	1.020	20	1.6×10^{-4}
12.9	0.80	1.02	1.	25.0	475	250	1×10^{-3}	2.5×10^2	6.14	1.020	19.5	1.49×10^{-4}
13.5	0.87	1.34	1.	28.0	557	290	1.2×10^{-3}	2.9×10^2	5.96	1.022	20	1.7×10^{-4}
16.0	0.65	1.34	1.	26.0	535	280	1.3×10^{-3}	2.8×10^2	5.89	1.025	23	1.9×10^{-4}
17.0	0.63	2.34	1.	32.0	472	240	1.4×10^{-3}	2.4×10^2	5.71	1.036	30	2×10^{-4}

TABLE 6.7 Damping Ratios for İçerenköy Sample 2

w,%	δ_s	S	Cm	% D_{free}	Accl. Rd.	Torq. Rd.	θ_R	C_R	A	R	% D_{steady}	Strain Ampl.
17.0	0.52	0.46	1.	11.8	532	220	7.1×10^{-4}	2.2×10^{-2}	5.83	1.01	11.5	1.06×10^{-4}
19.3	0.55	0.47	1.	12.6	510	240	6.8×10^{-4}	2.4×10^{-2}	5.8	1.015	12.8	1.01×10^{-4}
21.1	0.51	0.39	1.	11.0	657	280	7.6×10^{-4}	2.8×10^{-2}	5.34	1.015	11.4	1.1×10^{-4}
22.6	0.60	0.41	1.	13.0	635	370	7.6×10^{-4}	3.7×10^{-2}	7.1	1.015	15.8	1.13×10^{-4}
24.6	0.64	0.52	1.	15.2	528	280	7.6×10^{-4}	2.8×10^{-2}	6.4	1.015	15.0	1.13×10^{-4}
26.4	0.58	0.63	1.	15.0	617	210	1×10^{-4}	2.1×10^{-2}	4.8	1.015	16.0	1.4×10^{-4}

TABLE 6.8 Damping Ratios for İçerenköy Sample 3

w %	δ_s	S	Cm	% D_{free}	Accl. Rd.	Torq. Rd.	θ_R	C_R	A	R	% D_{steady}	Strain Ampl.
8.8	0.64	0.67	1.	16.7	426	180	7.2×10^{-4}	1.8×10^{2}	5.04	1.015	13	1.08×10^{-4}
11.2	0.57	0.65	1.	14.6	496	175	8.2×10^{-4}	1.75×10^{2}	4.15	1.015	11	1.2×10^{-4}
12.8	0.55	0.69	1.	14.4	412	175	7.1×10^{-4}	1.75×10^{2}	4.89	1.017	13	1.06×10^{-4}
13.45	0.61	0.61	1.	15.3	491	230	7.8×10^{-4}	2.3×10^{2}	5.42	1.015	14	1.16×10^{-4}
14.4	0.67	0.76	1.	18.0	417	170	7.5×10^{-4}	1.7×10^{2}	4.56	1.020	16	1.12×10^{-4}
16.9	0.68	0.91	1.	20.0	383	150	7.7×10^{-4}	1.5×10^{2}	4.10	1.020	17	1.15×10^{-4}

TABLE 6.9 Damping Ratios for İçerenköy Sample 4

w %	δ_s	S	Cm	% D_{free}	Accl. Rd.	Torq. Rd.	θ_R	C_R	A	R	% D_{steady}	Strain Ampl.
12.4	0.44	0.63	1.0	11.0	802	340	1.3×10^3	3.4×10^{-2}	5.29	1.014	12.2	1.9×10^{-2}
14.4	–	–	–	–	–	–	–	–	–	–	–	–
15.2	0.50	0.58	1.0	12.2	899	340	1.4×10^3	3.4×10^{-2}	4.5	1.014	11.5	2×10^{-4}
16.3	0.52	0.62	1.0	13.0	806	410	1.3×10^3	4.1×10^{-2}	5.77	1.016	15.7	1.9×10^{-4}
18.2	0.60	0.71	1.0	15.8	848	390	1.5×10^3	3.9×10^{-2}	5.22	1.020	16.5	2.2×10^{-4}
19.5	0.63	0.80	1.0	17.6	691	350	1.6×10^3	3.5×10^{-2}	5.84	1.025	18.0	2.3×10^{-2}

6.4 TEST RESULTS

6.4.1 Effect of Moisture Content on Damping

The variation of damping ratios with moisture content
are presented in Fig's 6.4 through, 6.8 . Steady State method
and free vibration method yield similar results.

On the dry side of optimum, damping ratio either
decreases or stays constant with increasing moisture content
and it reaches its minimum value at the maximum dry density,
or optimum moisture content. Further increase of moisture
content causes in a gradual increase in damping. It is interesting
that, the sape of curves obtained for damping is exactly
opposite to those with shear modulus, where the shear modulus
shows a little change up to the optimum moisture content,
but decreases gradually beyond the optimum moisture content.

6.4.2 Effect of Shear Strain Amplitude on Damping

Fig's 6.9 through 6.12 show the effect of shear strain
amplitude on damping. The samples tested are compacted at
optimum moisture content. It is observed that ; damping increases
with increasing shear strain amplitude. These curves are again
opposite to the shear modulus versus the shear strain amplitude
curves. At the small shear strain amplitudes damping ratio
is lower and increases with increasing shear strain amplitude.
In the $10^{-5} - 10^{-4}$ strain interval, for sample 4, the damping
ratio approximately daubles itself as shown in Fig. 6.12,

.In the same interval, damping gains 1.5 fold of its initial value for smaple 2, as shown in Fig. 6.10 . The other samples show similar results.

6.4.3 Effect of Vertical Stress on Damping

The change of damping with vertical stress is studied for four samples. Fig.'s 6.13 through 6.16 show the effect of vertical stress on damping. Under very small vertical stress, damping has higher values. A small amount of increase in vertical stress causes an important decrease in damping. For sample 1, in Fig. 6.13, damping ratio is 12% under 0.10 kg/cm^2 vertical stress. When the vertical stress reaches to 0.5 kg/cm^2, the damping ratio drops to 6% . Other samples represent similar results shown in Fig'.s 6.14 through 6.16 .

6.5 CONCLUSIONS

Fig 6.17 and Fig 6.18 show the variation of damping ratio by moisture content for free vibration and steady state vibration methods, respectively, for all samples tested. Tests are performed under a constant strain amplitude of 10^{-6}, and under a constant vertical stress of 0.144 kg/cm^2 . For strain amplitude, 10^{-4} , the variation of damping by moisture content is also shown in Fig 6.19 .

Depending on the test results following conclusions can be deduced.

1. Both the steady state vibration method and free

İçerenköy Sample No 1

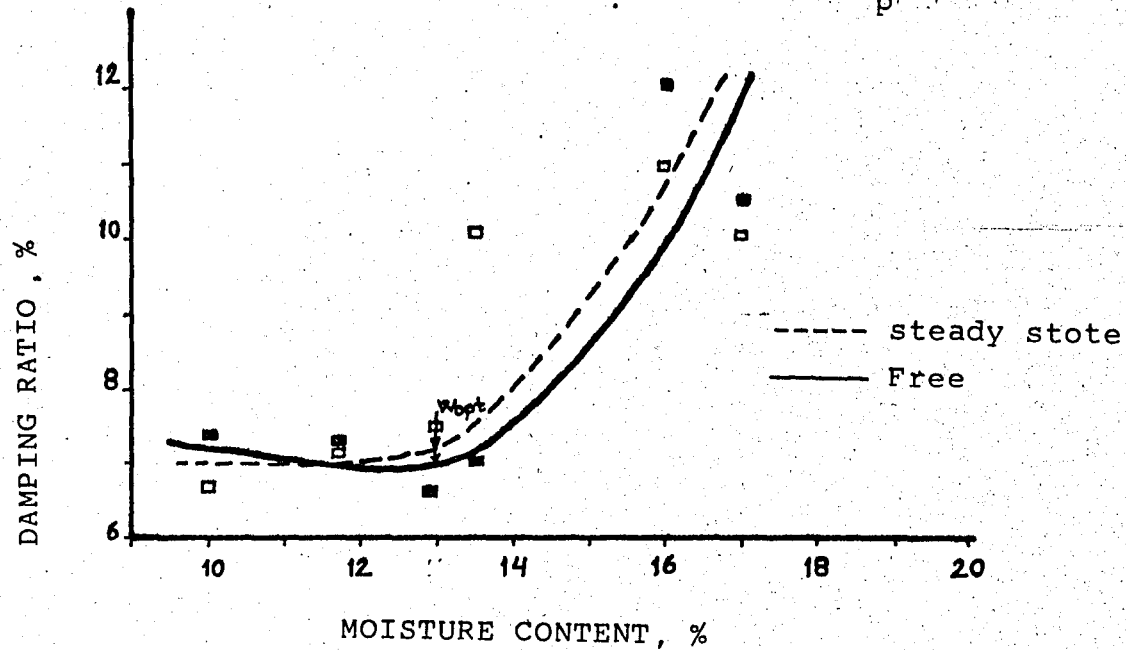Vertical Stress : 0.144 kg/cm^2

w_{opt} : 13. %

I_p : 8.7 %

---- steady stote

—— Free

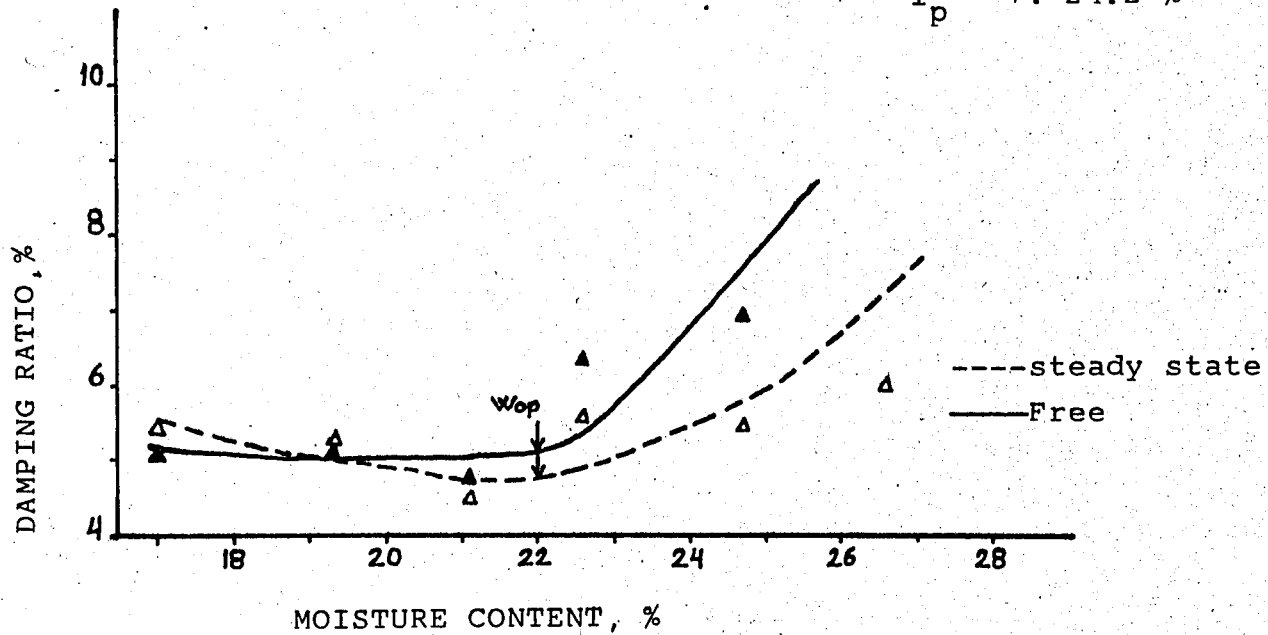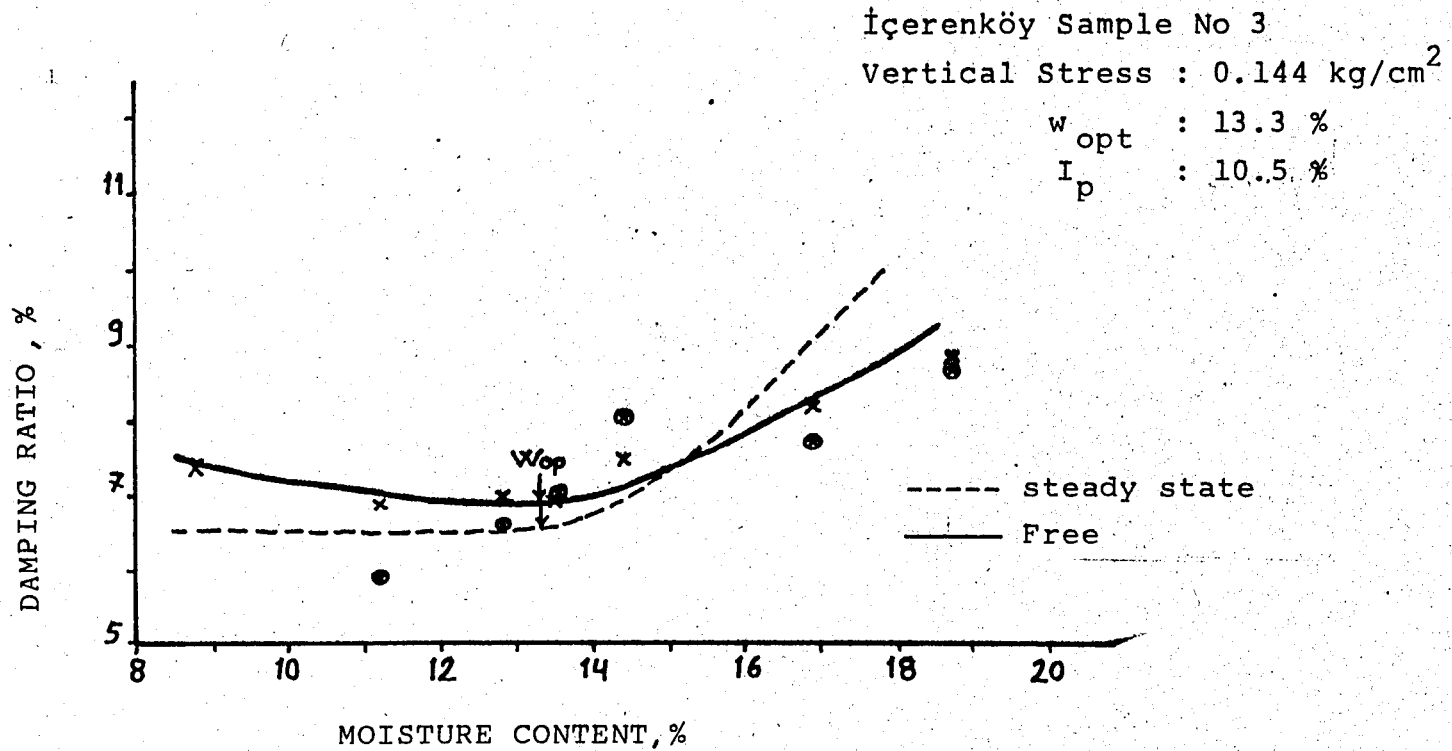FIG 6.4 Damping Ratio Versus Moisture Content for
İçerenköy Sample 1

FIG 6.5 Damping Ratio Versus Moisture Content For
İçerenköy Sample 2

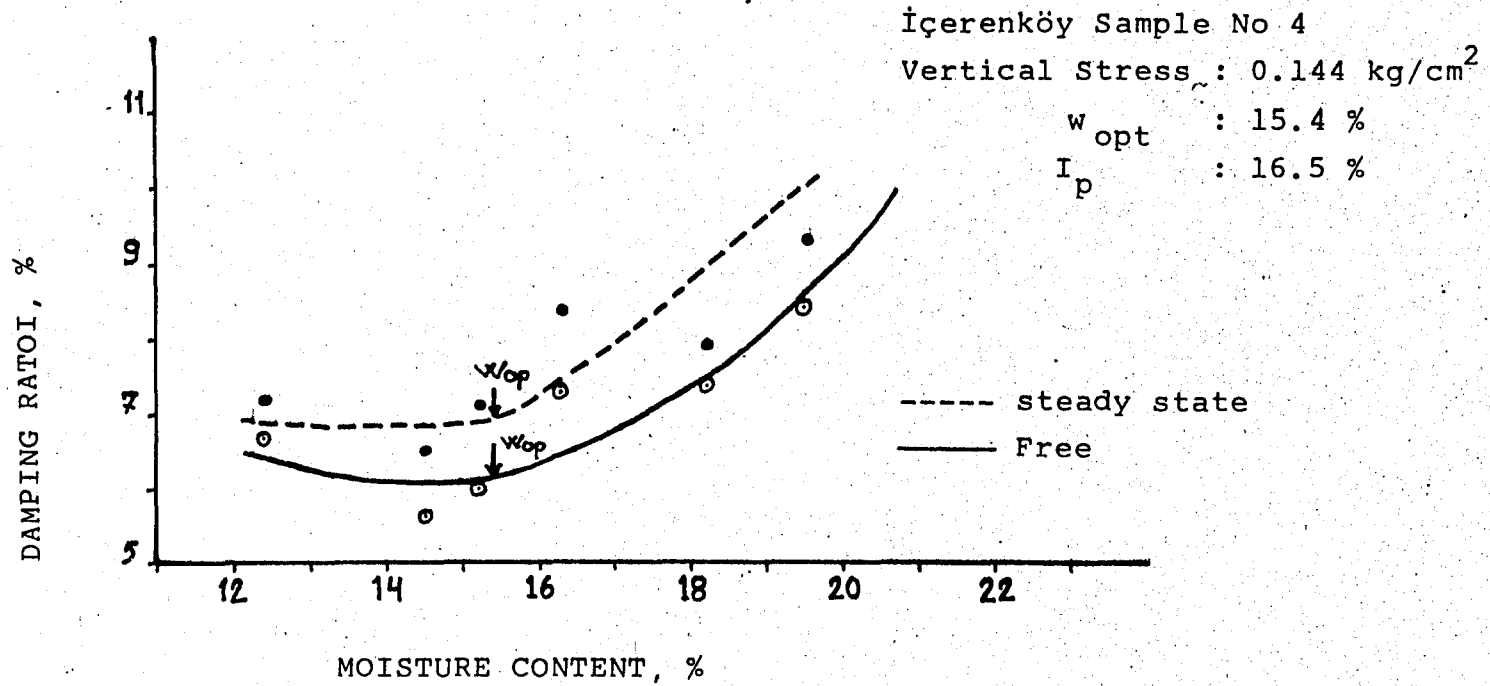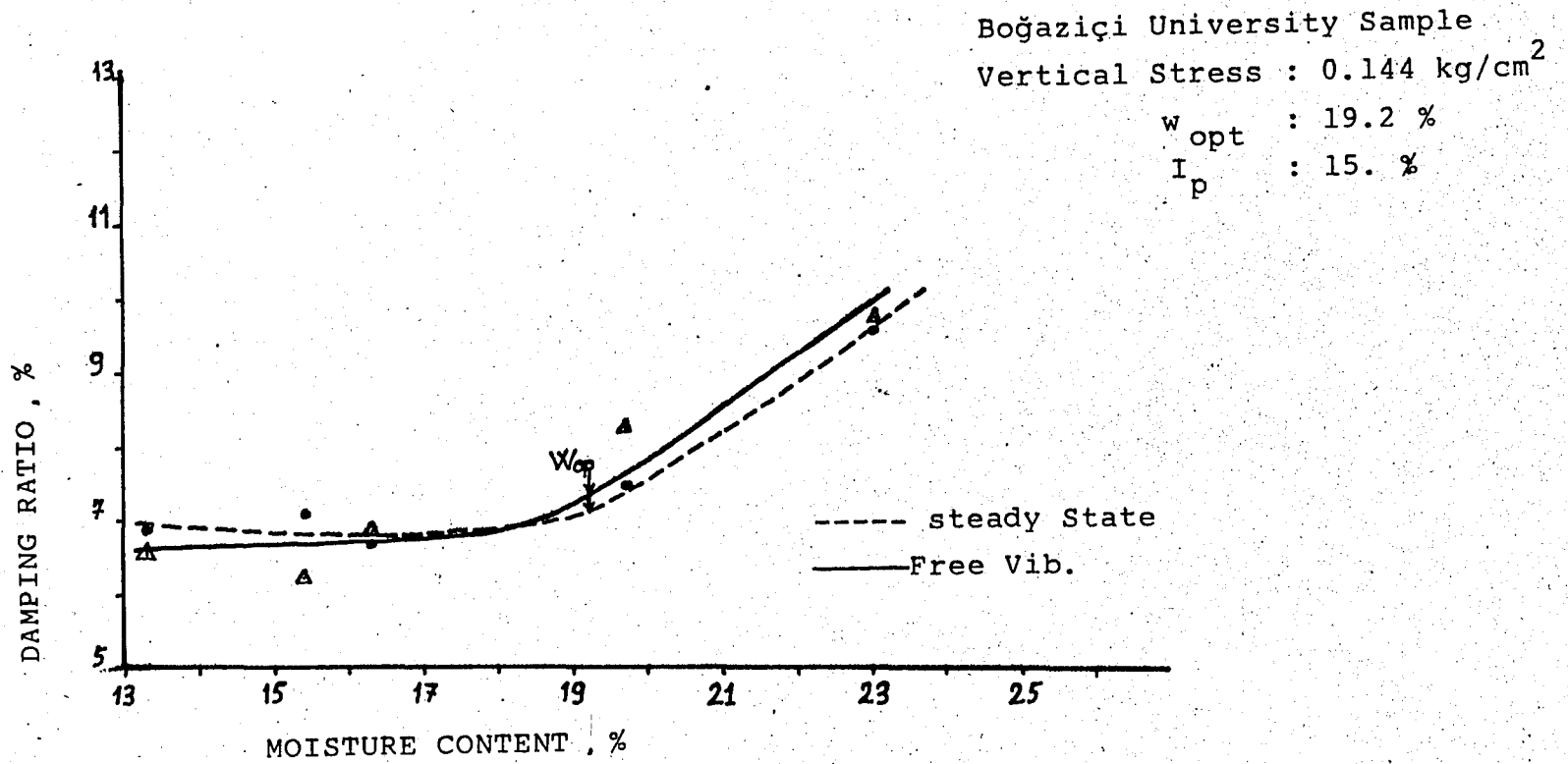İçerenköy Sample No 3

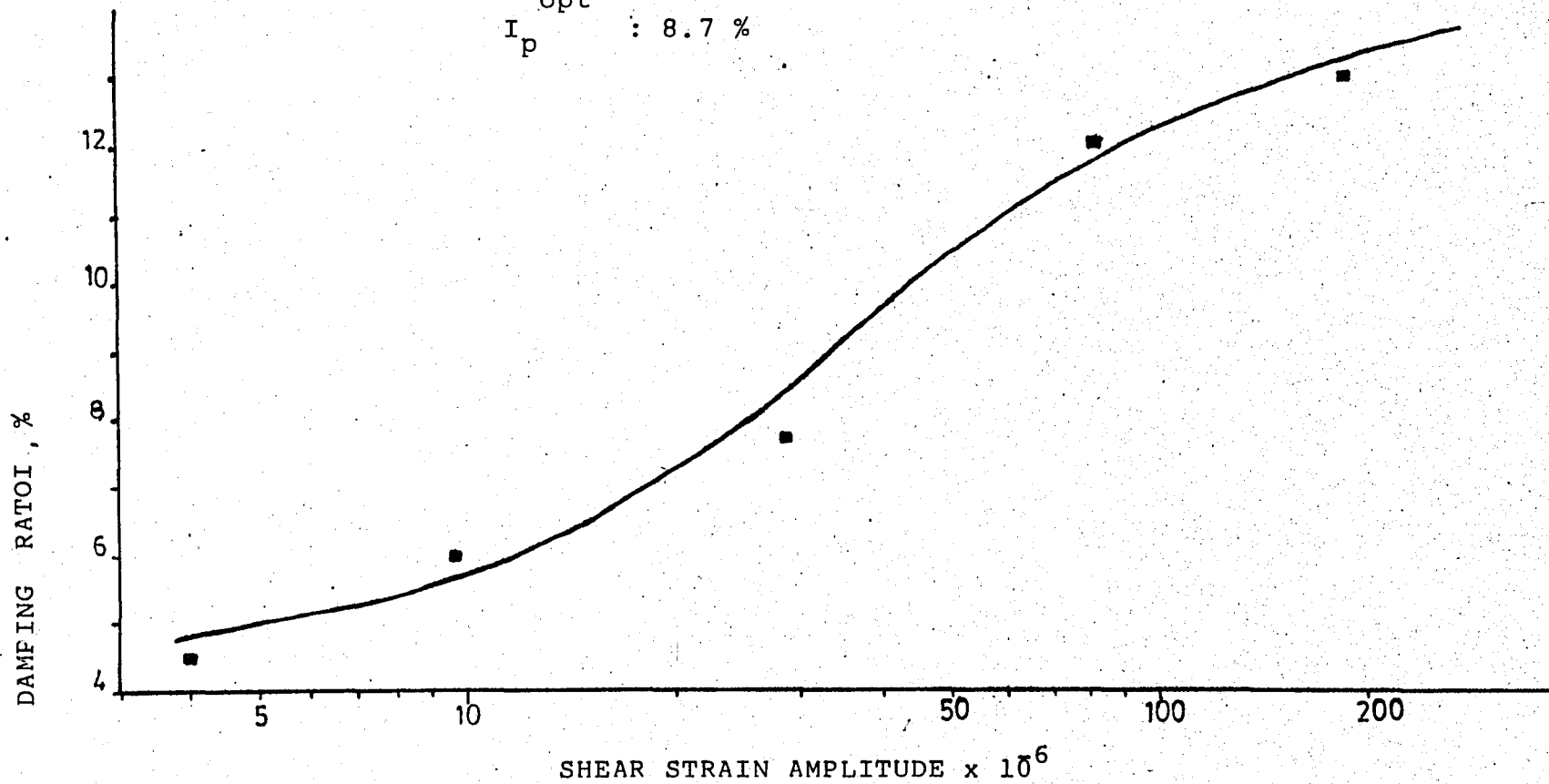Vertical Stress : 0.144 kg/cm^2

w_{opt} : 13.3 %

I_p : 10.5 %

----- steady state

——— Free

FIG 6.6 Damping Ratio Versus Moisture Content for İçerenköy
Sample 3

FIG 6.7 Damping Ratio Versus Moisture Content for
       İçerenköy Sample 4

FIG 6.8 Damping Ratio Versus Moisture Content for
Boğaziçi University Sample

İçerenköy Sample No 1

vertical Stress : 0.54 kg/cm^2

w_{opt} : 18 %

I_p : 8.7 %

FIG 6.9 Damping Ratio Versus Shear Strain Amplitude for İçerenköy Sample 1

144

İçerenköy Sample No 2

Vertical Stress : 0.54 kg/cm^2
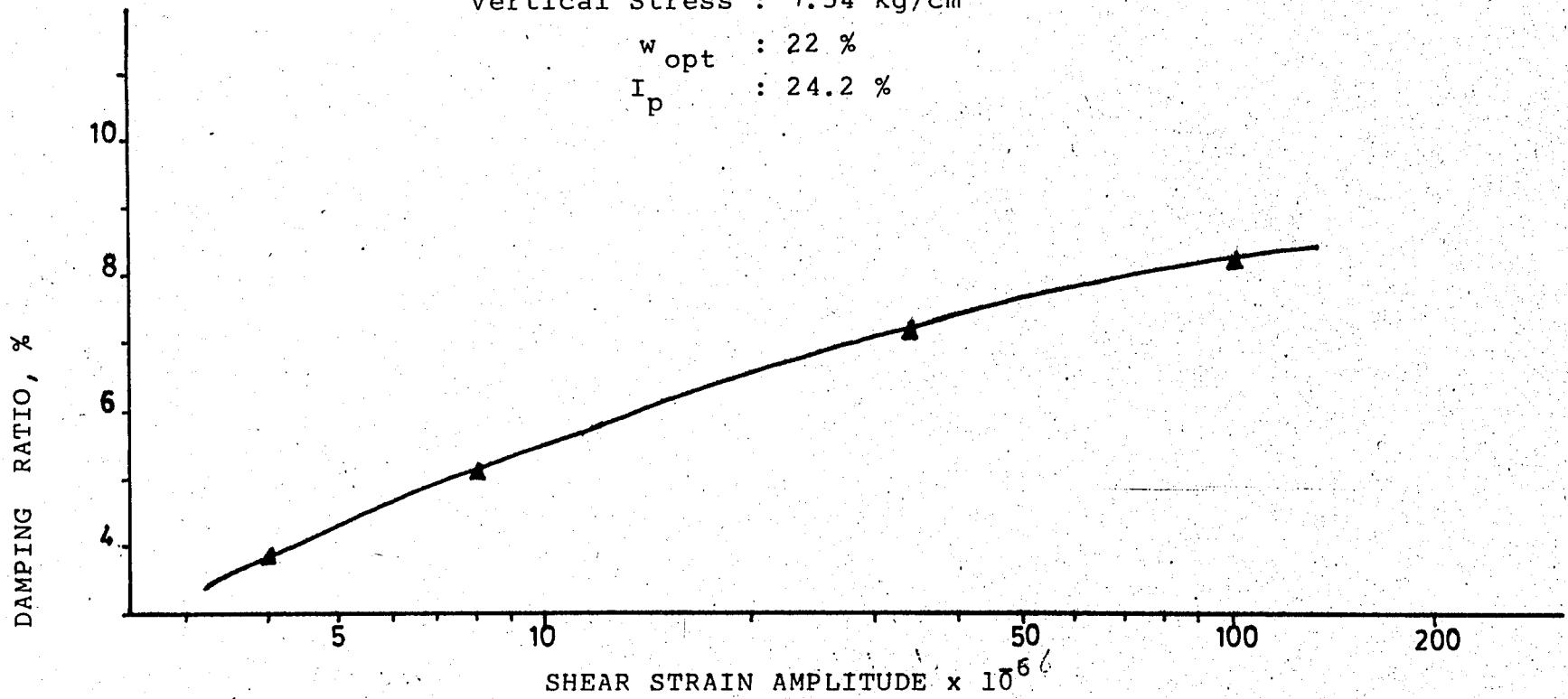
w_{opt} : 22 %

I_p : 24.2 %

DAMPING RATIO, %

SHEAR STRAIN AMPLITUDE x 10^6

FIG 6.10 Damping Ratio Versus Shear Strain Amplitude For İçerenköy Sample 2

İçerenköy Sample No 3
Vertical Stress : 0.54 kg/cm^2
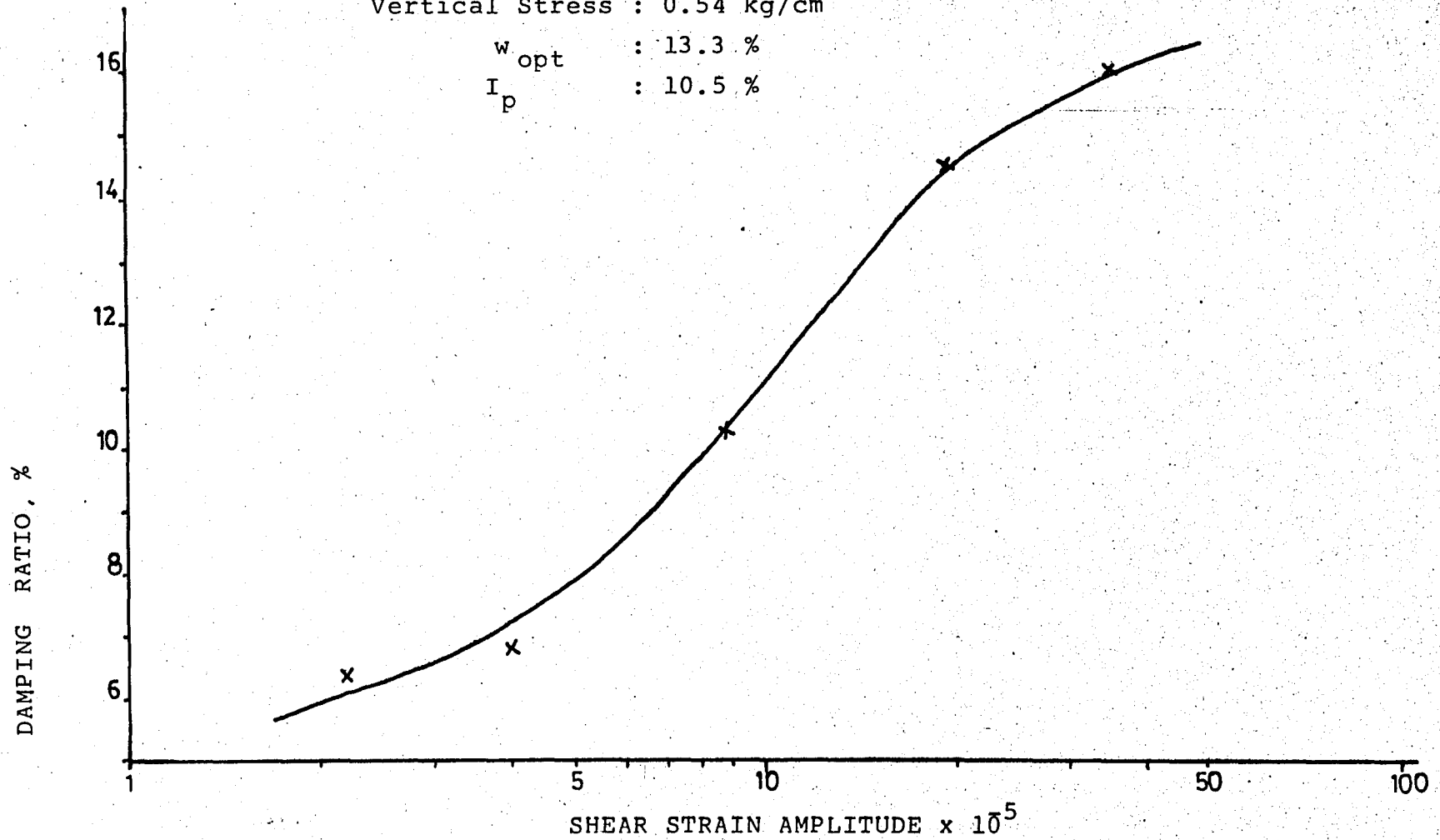w_{opt} : 13.3 %
I_p : 10.5 %

DAMPING RATIO, %

SHEAR STRAIN AMPLITUDE x 10^5

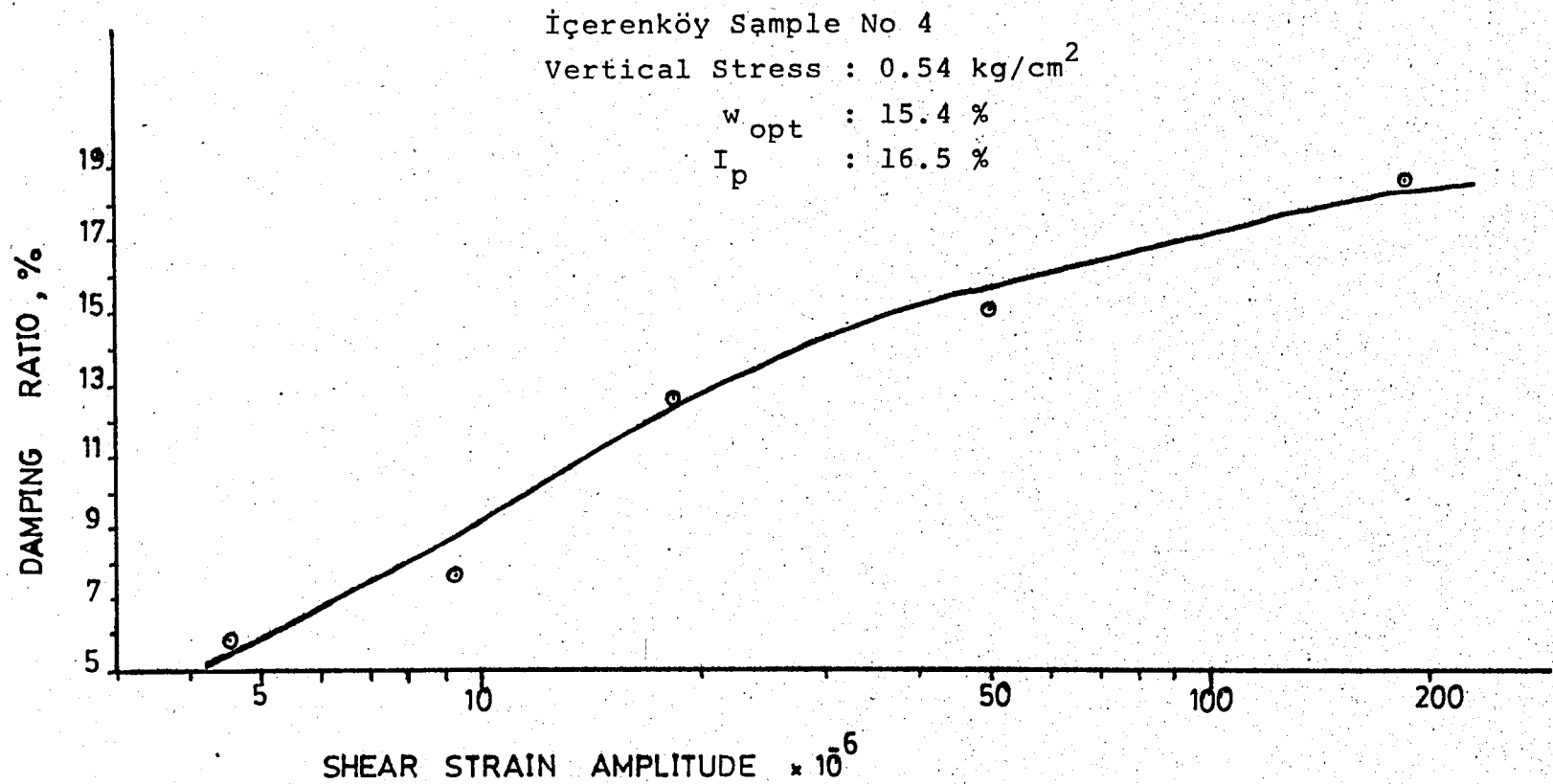FIG 6.11   Damping Ratio Versus Shear Strain Amplitude for İçerenköy Sample 3

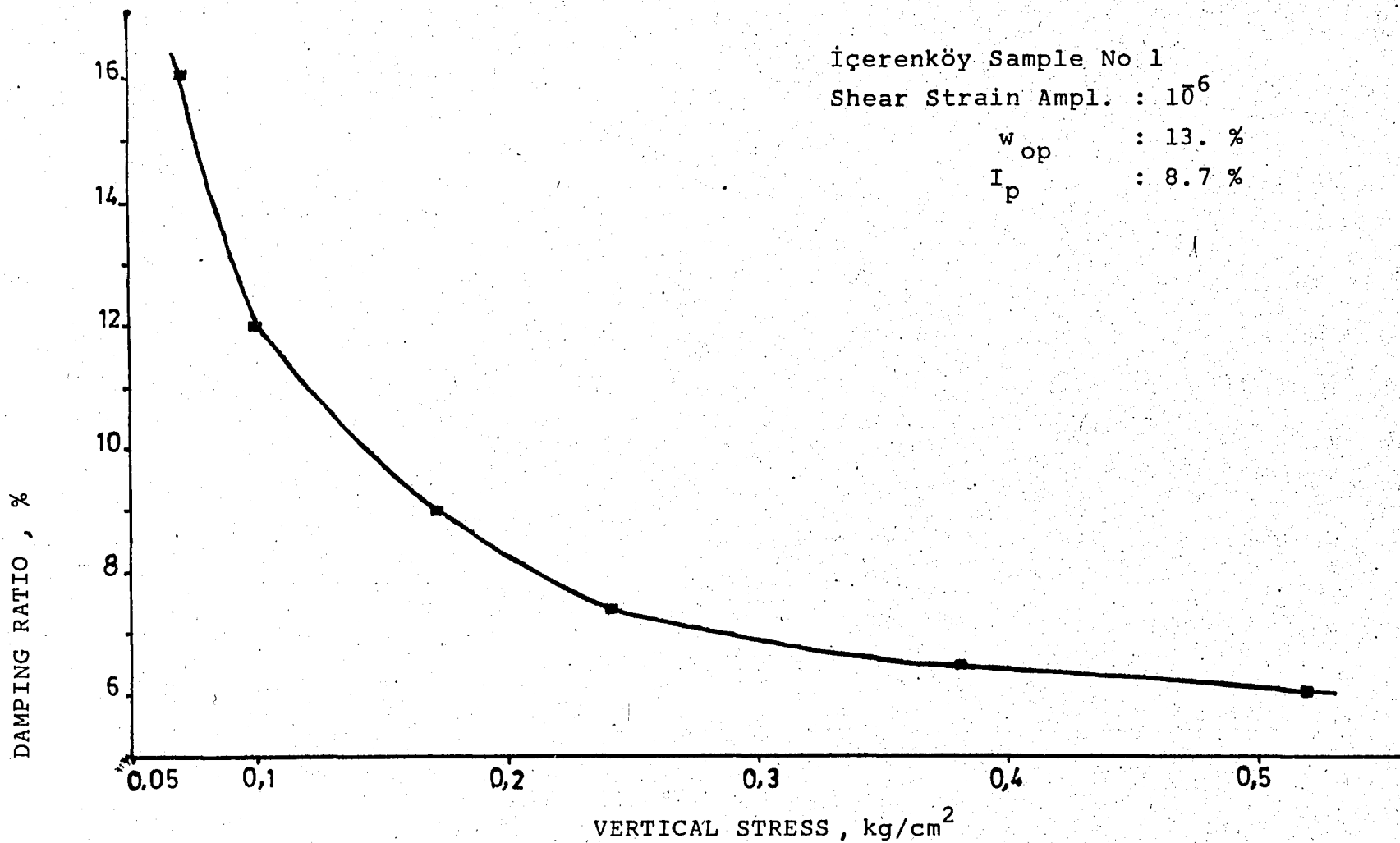FIG 6.12 Damping Ratio Versus Shear Strain Amplitude for İçerenköy Sample 4

FIG 6.13 Damping Ratio Versus Vertical Stress for İçerenköy Sample 1

İçerenköy Sample No 2

Shear Strain Ampl. : 10^6

w_{opt} : 22 %

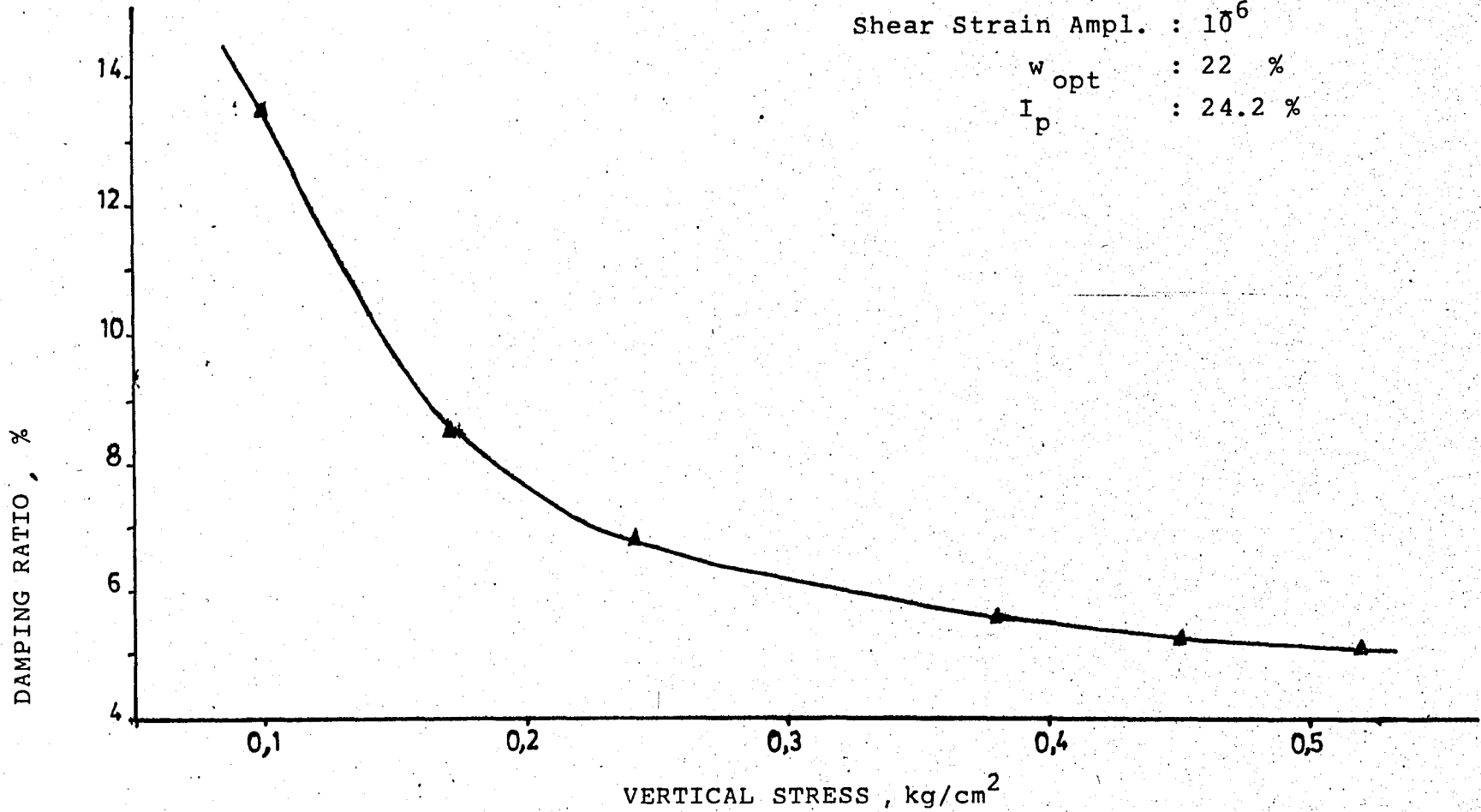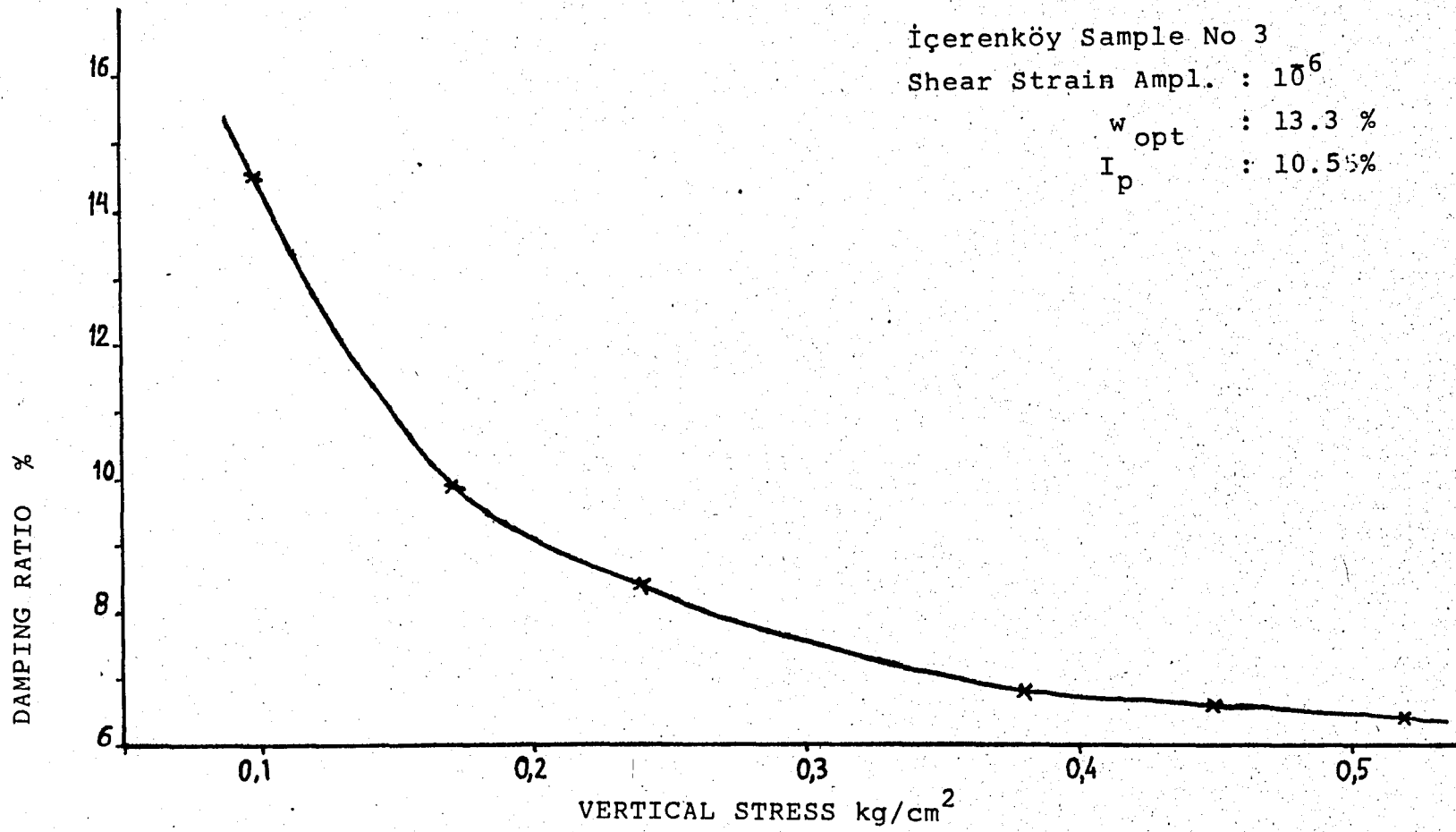I_p : 24.2 %

DAMPING RATIO , %

VERTICAL STRESS , kg/cm^2

FIG 6.14   Damping Ratio Versus Vertical Stress for İçerenköy Sample 2

FIG   6.15   Damping Ratio Versus Vertical Stress for İçerenköy Sample 3

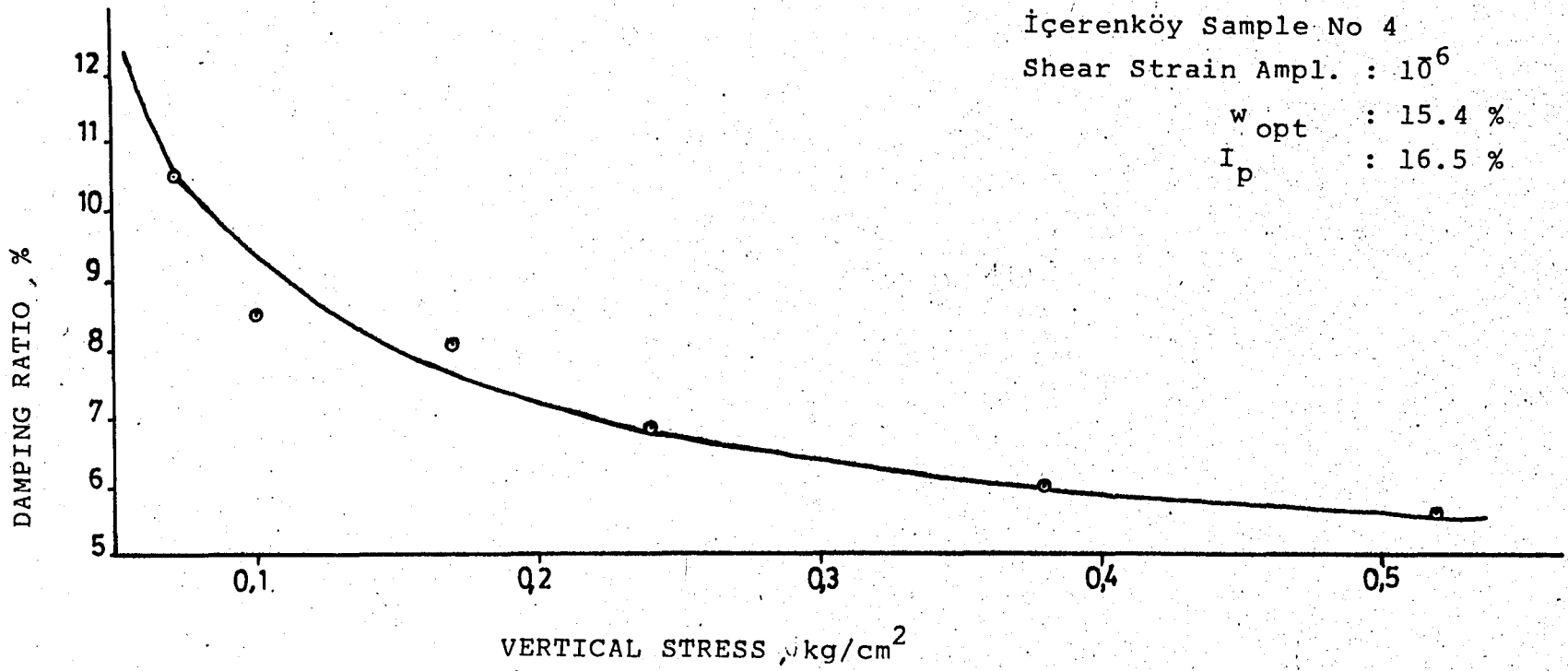İçerenköy Sample No 4

Shear Strain Ampl. : 10^{6}

w_{opt} : 15.4 %

I_{p} : 16.5 %

VERTICAL STRESS , kg/cm^2

FIG 6.16 Damping Ratio Versus Vertical Stress for İçerenköy Sample 4

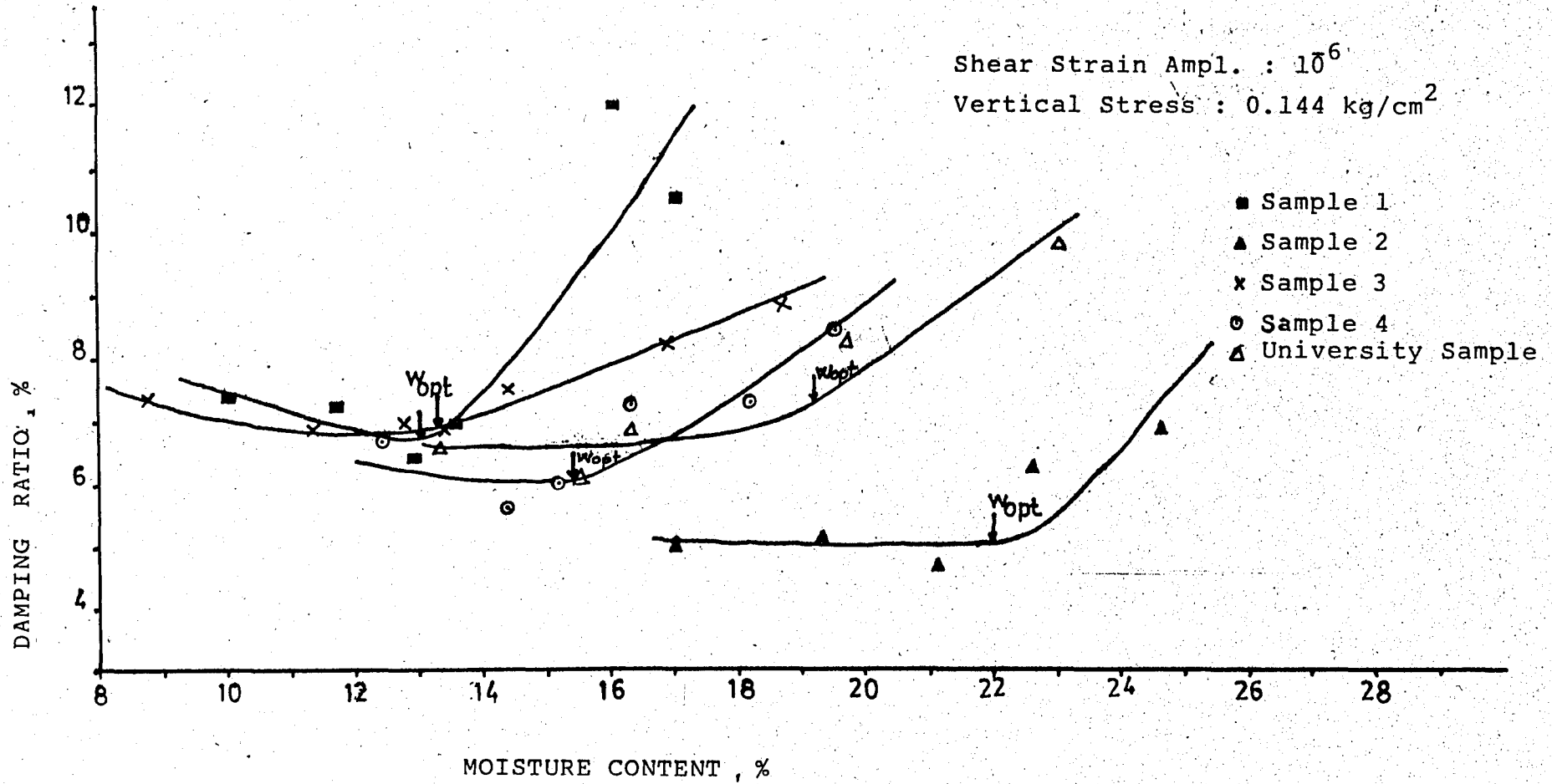FIG   6.17 · Damping Ratio Versus Moisture Content for Samples for the Free Vibration Method
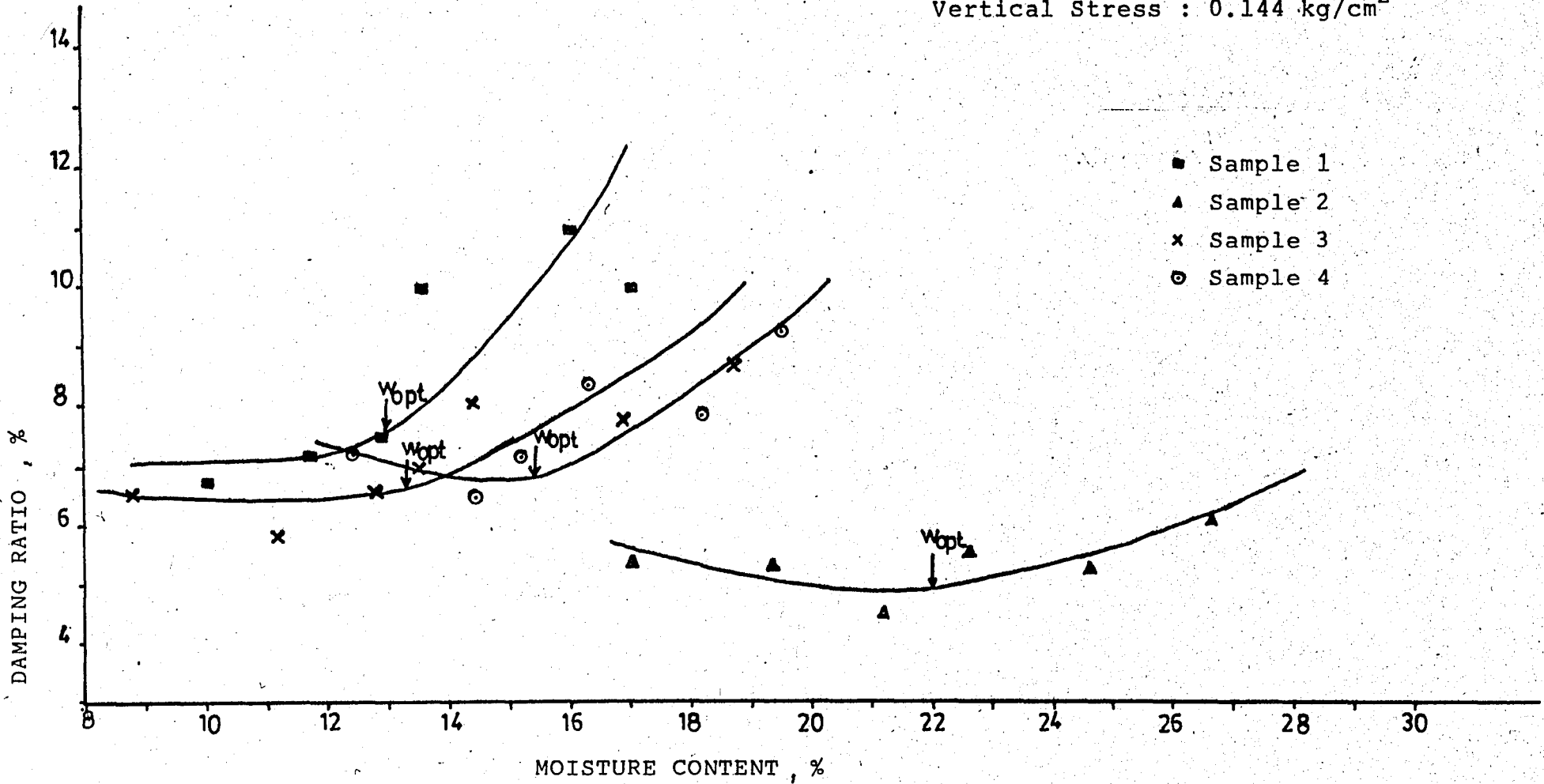
FIG 6.18 Damping Ratio Versus Moisture Content for Samples for Steady State Method.

FREE VIBRATION METHOD
Shear Strain Ampl. : 10^{-4}
Vertical Stress : 0.144 kg/cm^2

■ sample 1
▲ sample 2
✗ sample 3
⊙ sample 4
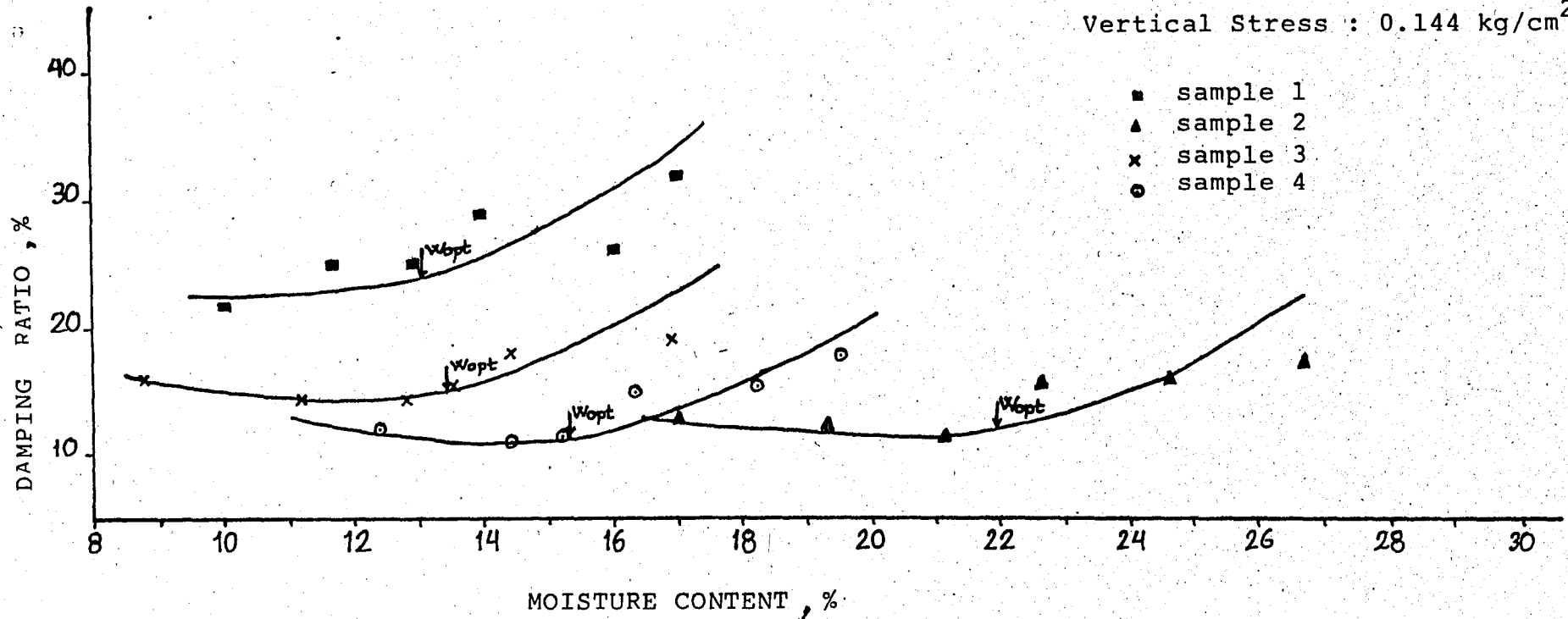
FIG 6.19 Damping Ratio Versus Moisture Content For İçerenköy Samples for the Strain Amplitude, 10^{-4}

154

vibration method determines similar results.

   2.   Up to the optimum moisture content, it may be assumed that damping ratio remains constant. Beyond the optimum moisture content, a gradual increase is observed in damping ratio.

   3.   Damping ratio increases with increasing shear strain amplitude

   4.   Damping ratio decreases with increasing vertical stress.

CHAPTER 7. SUMMARY AND CONCLUSIONS

In this study, five cohesive soil samples are tested and analized. The index properties W_L, W_P, and I_P are determined. In addition, the compaction properties, wop, and, γdry ; and CBR value are initially obtained. Then, using Hardin type resonant column apparatus and related supplementary equipment, the resonant frequency, f, vibration ampilitude, θ_R, current passing through the coils, C_R, are measured, and, free vibration decay curves are obtained for each specimen, of each type soil. Using the chart given by Hardin, the strain amplitude is determined. Then, using formulas given, the shear modulus G, and damping ratio, D, are computed for each specimen. The results of experiments are tabulated and plotted for prectical use in chapters 5 and 6.

From previous studies, and the results of tests conducted in this study, the following conclusions are deduced.

1. The electrical forces acting between clay particles are most responsible for soil strength in compacted clays.

2. According to the generally accepted concept and theory of the structures and strength characteristics of compacted clays, when a clay specimen is compacted on the dry side of optimum, a flocculated structure is formed and the edge-to-face contact between soil particles provides high shear strength resistance to load, thus the values of shear modulus are higher ; when compacted on wet side of optimum, the specimen has a disperesd structure, resulting in lower

shear strength resistance so the shear modulus obtained is lower.

3. Variation of damping ratio with moisture content is practically negligible up to the optimum moisture content. Beyond optimum moisture content, an increase in moisture results in a gradual increase in damping ratio. The shape of curves obtained for damping is opposite to those for shear modulus.

4. For undisturbed, remolded and compacted clays, as shear strain amplitude increases ; shear moduli decrease, however damping ratio increases.

5. For cohesive soils, as void ratio decrease, shear modulus increase, however damping ratio decrease.

6. During secondary consolidation of clays shear modulus continues to increase, with a smaller increasing rate.

7. For cohesive soils the shear modulus decreases with the increasing numben of cycles, but damping ratio ramains constant.

8. In general, additives increase both the shear modulus and damping ratio of soils.

9. Shear modulus reaches its maximum value just before the optimum moisture content.

10. Damping ratio drops to its minimum value around the optimum moisture content.

11. Shear modulus increases with vertical stress, however, damping ratio decreases.

REFERENCES

CHAE, Y.S., and CHIANG, J.C., "Dynamic Properties of Lime and LFA Treated soils", Earthquake Engineering and soil Dynamics, ASCE, Vol. 1, 1978 pp. 308-323 .

CHEONG Au, W., and CHAE, Y.S., "DYnamic SHear Modulus of Treated Expansive Soils", Journal of the Geotechnical Engineering Division, ASCE, Vol. 106, No.GT3, March 1980, pp. 255-274 .

DRNEVICH, V.P., and MASSARSCH, K.R., "Sample Disturbence and Stress Strein Behavior", Journal of the Geotechnical Engineering Division, ASCE, Vol. 105, No GT9, September, 1979, pp. 1001-1016 .

DURGUNOĞLU, H.T., Denizcilik Bankası T.A.O. İçerenköy Gümrüklü Sahada Prefabrika Sundurma İnşaatı Geoteknic Raporu, 1983 .

FISCHER, J.A., and KOUTSOFTOS, D.C., "Dynamic Properties of Two Marine Clays", Journal of the Geotechnical Engineering Division, ASCE, Vol. 106, No GT6, June, 1980, pp. 645-657 .

HARDIN, B.O., and MUSIC, J., "Apparatus for Vibration During the Triaxial Test", STP392, Symposium on Instrumentation and Apparatus for Soils and Rocks American. Society for Testing and Materials, 1965 .

HARDIN, B.O., and BLACK, W.L., "Vibration Modulus of Normally
Consoludated Clay", ASCE, Vol. 94, No SM2, March, 1968,
pp. 353-369 .

HARDIN, B.O., and DRNEVICH, V.P., "SHear Modulus and Damping
in Soils: Measurements and Parameter Effects", Journal
of the Soil Mechanics and Foundations Divisions, ASCE,
Vol. 98, No SM6, June, 1972, pp. 603-624 .

HARDIN, B.O., and RDNEVICH V.P., "Shear Modulus and Damping
in Soils: Design Equations and curves", ASCE, Vol. 98,
No SM7, July, 1972, pp. 667-692 .

HARDIN, B.O., "The Nature of Stress-Strain Behavior for soils",
Earthquake Engineering and Soil Dynamics, ASCE, Vol.1,
1978, pp. 3-90 .

HUMPHRIES, W.K., and WAHLS, H. E., "Stress History Effects
on Dynamic Modulus of Clay", Journal of the Soil
Mechanics and Foundations Division, ASCE, Vol. 94,
No SM2, March, 1968, pp. 371-390 .

LAMBE, T.W., "The STructure of Compacted Clay", Journal of
the Soil Mechanics and Foundations Divisions, ASCE,
May, 1958, Vol. 84 .

LEONARDS, G.A., Foundation Engineering Mc. GRAW-HILL BOOK
COMPANY, INC, 1962 .

MARCUSON, W.F., and WAHLS, H.E., "Time Effects on Dynamic
Shear Modulus of Clays", Journal of the Soil Mechanics

Division, ASCE, Vol. 98, No SM12, December, 1972, pp. 1359-
1373.

MARCUSEN, W.F., and CURRO, J.R., "Field and Laboratory
Determination of Soil Moduli", Journal of the Geotechnical
Engineering Division, ASCE, Vol. 107, No GT10, October,
1980, pp. 1269-1292 .

ÖZTURAN, T "A Study on Stress-Strain and Voume Change Properties
of Compacted Clay", Thesis for the Degree of Maister
of Science. February, 1977 .

RICHART, F.E. Jr., Hall, J.R., Jr., and Woods, R.D., "Behavior
of DYnamically Loaded Soils", Vibrations of Soils and
Foundations, Prentice. Hall, Inc., Englewood Cliffs,
N.J. 1970, pp. 140-160 .

WOODS, R.D., "Measurement of Dynamic Soil Properties", Earthquake
Engineering and Soil Dynamics, ASCE, Vol. 1, 1978,
pp. 91-178 .

YOSHIMI- Y., and RICHART, F.E., "Soil Dynamics and Its Applicatio
to Foundation Engineering", Proceedings of the Ninth
International Conference on Soil Mechanics and Foundation
Engineering. Volume 2, 1977, TOKYO .